Review

Yuan Zhou*, Deepam Maurya, Yongke Yan, Gopalan Srinivasan, Eckhard Quandt and Shashank Priya

Self-Biased Magnetoelectric Composites: An Overview and Future Perspectives

DOI 10.1515/ehs-2015-0003

Abstract: Self-biased magnetoelectric (ME) composites, defined as materials that enable large ME coupling under external AC magnetic field in the absence of DC magnetic field, are an interesting, challenging and practical field of research. In comparison to the conventional ME composites, eliminating the need of DC magnetic bias provides great potential towards device miniaturization and development of components for electronics and medical applications. In this review, the current state-of-the-art of the different self-biased structures, their working mechanisms, as well as their main characteristics are summarized. Further, the nature and requirement of the self-biased magnetoelectric response is discussed with respect to the specific applications. Lastly, the remaining challenges as well as future perspective of this research field are discussed.

Keywords: self-biased, magnetoelectric, energy harvesting

Introduction

Multiferroic and Magnetoelectric Materials

Multiferroic (MF) magnetoelectric (ME) materials have attracted great interest due to their technological importance in various applications including magnetic field sensors, filters, transformers, information storage devices and energy harvesters. In general, ferroic materials including ferroelectric, ferromagnetic, and ferroelastic materials exhibit hysteretic behavior between physical parameters (magnetization M, polarization P, strain $\boldsymbol{\varepsilon}$) and their conjugate external stimuli (magnetic field H, electric field E, external stress $\boldsymbol{\sigma}$) (Eerenstein, Mathur, and Scott 2006). The term "multiferroic" is used for the materials that possess more than one ferroic order in a single phase (Schmid 1994). The multiferroic coupling allows tuning of two or more physical parameters under external stimuli as shown in Figure 1. Out of various interesting possibilities, one of the most appealing properties of the multiferroics is the magnetoelectric coupling, which results in magnetoelectricity. It is a product property of piezoelectricity and magnetoelasticity, where a large variation in electric polarization P can be obtained under external magnetic field H (direct ME effect) or a change in magnetization M can be obtained by applying electric field E (converse ME effect), given as (Wang, Liu, and Ren 2009; Ma et al. 2011a):

$$\Delta P = \alpha \Delta H \quad or \quad \Delta E = \alpha_E \Delta H \text{ (direct ME effect)} \qquad [1]$$

$$\Delta M = \alpha \Delta E \text{ (converse ME effect)} \qquad [2]$$

The ME coupling is reported in several single phase compounds, such as $BiFeO_3$, Cr_2O_3, and $YMnO_3$ at room temperature (Fiebig 2005; Prellier, Singh, and Murugavel 2005; Spaldin and Fiebig 2005). In these single-phase ME materials, the upper limit for ME susceptibility can be given as (Brown, Hornreich, and Shtrikman 1968):

$$\alpha_{ij}^2 < (\kappa_{ii}^e \chi_{jj}^m) \qquad [3]$$

where κ^e and χ^m are the electric and magnetic susceptibilities, respectively. Unfortunately, most of the single-phase materials possess either low permittivity or low permeability at room temperature leading to a low ME coupling that hinders their practical application. Several researchers have investigated single phase ME materials

***Corresponding author: Yuan Zhou,** Bio-inspired Materials and Devices Laboratory (BMDL), Center for Energy Harvesting Materials and Systems (CEHMS), Virginia Tech, Blacksburg, VA 24061, USA, E-mail: yzhou6@vt.edu
Deepam Maurya, Yongke Yan, Bio-inspired Materials and Devices Laboratory (BMDL), Center for Energy Harvesting Materials and Systems (CEHMS), Virginia Tech, Blacksburg, VA 24061, USA
Gopalan Srinivasan, Physics Department, Oakland University, Rochester, MI 48409, USA
Eckhard Quandt, Inorganic Functional Materials, Institute for Materials Science, Kiel University, Kiel 24143, Germany
Shashank Priya, Bio-inspired Materials and Devices Laboratory (BMDL), Center for Energy Harvesting Materials and Systems (CEHMS), Virginia Tech, Blacksburg, VA 24061, USA, E-mail: spriya@vt.edu

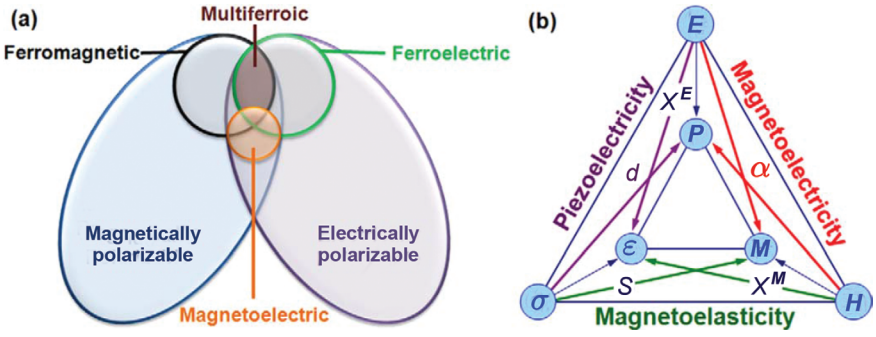

Figure 1: (a) Relationship between ferroic materials. Notice that only small group of materials are both multiferroic and magnetoelectric. (b) Heckman diagram illustrating the physical relationships present in commonly occurring materials and principle for design of new materials (Eerenstein, Mathur, and Scott 2006; Martin et al. 2008).

and have proposed alternative strategies to overcome the fundamental problem related with the filling of electronic states (Hill 2000; Wang, Liu, and Ren 2009). Hill summarized that in all of the conventional ferroelectric perovskite the transition metal (TM) ions, such as Ti^{4+} and Ta^{5+} occupying the B-sites has an empty *d* shell to allow the formation of a partial covalent bond with the surrounding oxygen anions, whereas magnetism arises from unpaired electrons in the *d* or *f* shell of TM ions at the B-site, such as Cr^{3+}, Mn^{3+}, Fe^{3+}. The difference in filling of the TM ion *d*-shells at the B-site makes these two ordered states mutually incompatible. To solve this paradox, efforts have been made to search for ferroelectricity intrinsically generated by special spin orders. This not only enables an effective combination of the two orders but also their spontaneous mutual control (Wang, Liu, and Ren 2009).

Alternatively, a class of artificial multiferroic ME materials in the form of piezoelectric and magnetostrictive composites has drawn significant interest in order to enhance the ME coupling (Nan et al. 2008; Srinivasan 2010a). In ME composites, the magnetic-field-induced strain (magnetostriction) in magnetostrictive phase is transferred to piezoelectric component through elastic coupling, which consequently generates electrical charges and vice-versa. The magnetoelectric coupling can be given as (Nan et al. 2008):

$$\frac{\partial P}{\partial H} = \alpha_{ME} = k_c q e \qquad [4]$$

where

$$q = \frac{\partial S}{\partial H} \text{ and } e = \frac{\partial P}{\partial S} \qquad [5]$$

where k_c is coupling factor ($0 \le k_c \le 1$) between the consecutive phases (Nan 1993), α_{ME} is the ME coefficient of the composite, *S* is the strain, *q* and *e* are piezomagnetic and piezoelectric coefficients, respectively. This coupling is tightly related to the intrinsic properties of each constituents and the effectiveness of elastic coupling between the two phases. Therefore, a high piezoelectric coefficient, *e*, a high piezomagnetic coefficient, *q*, and good coupling factor (large k_c) will result in large ME coefficient α_{ME}. Efforts have been made to enhance the ME voltage coefficient through various materials combination and configurations.

Development of Self-Biased ME Composites

In general, under a constant applied AC magnetic field (H_{ac}), the ME coupling coefficient (α_{ME}) shows a peak in its response to varying DC magnetic bias field, as shown in Figure 2. The peak is caused by the dependence of α_{ME} on piezomagnetic coefficient ($q = d\lambda/dH$, λ: magnetostriction) with respect to DC magnetic field, delineating the requirement of optimizing the magnitude of DC magnetic bias (H_{opt}) to obtain the maximum ME voltage output. One needs to use a permanent magnet or a solenoid to provide the external H_{bias}, which in turn results in problem of large device size, electromagnetic interference and potentially additional noise sources. Thus, a novel architecture is needed where one can achieve ME coupling with large tunability in the absence of a DC magnetic field. This will allow the development of on-chip devices utilizing magnetoelectric phenomena such as energy harvesters, AC magnetic field sensors and high frequency circuit components.

In order to address the requirement for DC magnetic sources, efforts to reduce H_{bias} have been emphasized. Researchers were able to tune the magnitude of optimum DC bias ranging from 6.8 kOe to 5 Oe by optimizing the composition and geometry of magnetostrictive phase (Srinivasan 2010b; Nan et al. 2008; Dong et al. 2006).

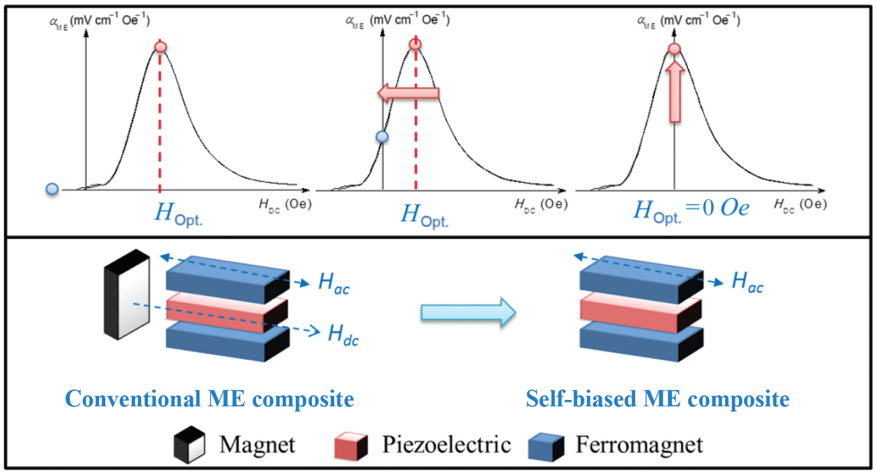

Figure 2: Schematic diagrams depicting the comparison between conventional and self-biased ME composites.

However, the requirement for the DC magnetic bias has been still hindering their implementation in miniaturized devices. Therefore, magnetoelectric composites with large non-zero α_{ME} in the absence of DC magnetic field, namely with "Self-biased ME effect", have been developed in various configurations using different strategies. Figure 2 illustrates a comparison between the conventional ME composites and self-biased ME (SME) composites. The self-biased effect could be an effective answer to this issue.

The highlights in the development of self-biased magnetoelectric composites can be summarized in Figure 3.

Self-biased ME effect was observed by Srinivasan et al. (2002) where they found hysteresis and remanence of α_{ME} as a function of H_{bias} in co-fired LSMO-PZT laminates (Srinivasan et al. 2002). Similar behavior was also found in other laminates (Laletin et al. 2005). However, this phenomenon did not attract much attention in the following decade were most of the efforts were focused on optimizing materials, structures and working mode to enhance the ME voltage coefficient and sensitivity (Nan et al. 2008; Zhai et al. 2008).

In 2010, Mandal et al. demonstrated a compositionally graded ferrites/PZT (PZT: $Pb(Zr,Ti)O_3$) laminate structure which produced non-zero ME voltage at zero DC magnetic bias (Mandal et al. 2010). They first correlated this non-zero ME behavior with the presence of flexural deformation and grading induced out-of-plane internal magnetic field in the ferrite. Subsequently, Yang et al. presented a methodology that conventional ME laminate composites can possess self-biased ME response by changing vibration mode through electrical connections (Yang et al. 2010). Soon after that, Srinivasan et al. systematically investigated the hysteresis and remanence in magnetoelectric effects in functionally graded magnetostrictive-piezoelectric layered composites. They further proposed a theoretical model for the self-biased graded composites (Mandal et al. 2011; Sreenivasulu et al. 2011; Laletin et al. 2012). Yang et al. analytically studied the lead-free based self-biased laminates and proposed an electrically controlled core-free magnetic flux control devices by using the self-biased converse magnetoelectric effect (Yang et al. 2010; Yang, Ahn, et al. 2011; Yang, Cho, et al. 2011). Alternative approaches have been suggested for the case of thin films that rely on the angular dependence of exchange bias field from a multicomponent magnetic system to provide a non-zero piezomagnetic coefficient at zero bias (Lage et al. 2012, 2014; Onuta et al. 2011). This phenomenon is quite promising for various applications including magnetic field sensors and energy harvesting systems. The focus of these studies was mainly on

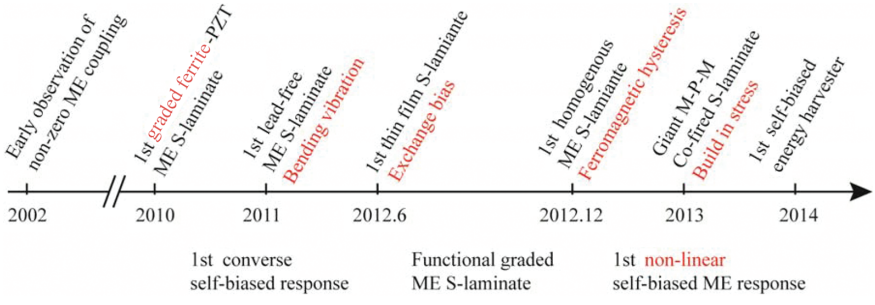

Figure 3: Milestones for the development of self-biased magnetoelectric composites.

understanding the nature of self-biased effect from multi-component magnetic systems.

Subsequently, self-biased magnetoelectric composites with homogenous magnetostrictive phase were developed. Yuan et al. demonstrated a simple Ni/PZT bilayer laminate structure that exhibits tunable self-bias phenomenon with single phase magnetic material (Zhou et al. 2012). In this study, fundamental understanding of the role of domain structure and demagnetization field of magnetic materials toward self-biased effect was provided. The self-biased response was found to be related with the nature of magnetic phase and hence could be controlled by variation in demagnetization state and the resultant differential magnetic flux distribution. Subsequently, Yan et al. successfully co-fired a self-biased composite NCZF/Ag/PMN-PT/Ag/NCZF (NCZF: nickel copper zinc ferrite; PMN-PT: Pb$(Mg_{1/3}Nb_{2/3})_3$-$PbTiO_3$) with homogeneous magnetic phase (Yan, Zhou, and Priya 2013). Co-fired structure provides the opportunity of interfacial engineering to obtain the optimum strain transfer from two phases with a giant self-biased response $> 1V\ cm^{-1}\ Oe^{-1}$. The self-bias response in the co-fired laminates was explained by the low field magnetostriction hysteresis and the built-in stress from the internal electrode during co-firing process. Further, by considering the non-linear magnetic properties of the ferromagnetic phase, the self-biased phenomenon could be observed in conventional ME composites when measured in non-linear region (Shen et al. 2013).

These observations provide us the insight that the self-biased effect could not only be observed in ME composites with complex multicomponent magnetic system, but can also be realized in simple composites with homogenous magnetostrictive phase. Five main types of self-biased magnetoelectric composites have been investigated both experimentally and theoretically: (a) functionally graded FM based SME; (b) exchange bias mediated SME; (c) magnetostriction hysteresis based SME; (d) built-in stress mediated SME; and (e) non-linear SME.

The goal of this review is to summarize the above mentioned composite systems exhibiting self-biased magnetoelectric effects. We will begin with a brief overview of the development of the conventional ME composites (Section 2), including some of the state-of-art research achievements in this area in the past decade. Section 3 describes the five main types of self-biased ME composites and their main characteristics, working principle, magnitude, advantages and limitations. Further, various potential applications related to unique response of different self-biased composites are discussed. Finally, the review concludes with some significant achievements and future perspective of self-biased ME composites.

Conventional Magnetoelectric Composites

Since the first observation of magnetoelectric effect in single phase Cr_2O_3 (Buchel'nikov, Romanov, and Shavrov 1998; Folen, Rado, and Stalder 1961), the development of magnetoelectric materials has been pursued for last several decades. Specifically, the investigations on generating magnetoelectric coupling at room temperature through product property of piezoelectric materials and magnetostrictive materials in a composite configuration have drawn much attention. There are many milestones along the development of ME composites, which have been well reviewed by Fiebig (2005), Priya et al. (2007), Ramesh and Spaldin (2007), Nan et al. (2008) and Srinivasan (2010b). Here, we mainly survey some important developments with respect to conventional magnetoelectric composites.

In early 70s, Boomgard et al. synthesized the first ME composites consisting of $BaTiO_3$ and $CoFe_2O_4$ using unidirectional solidification process which demonstrated a much higher ME response than that of single phase multiferroics with the magnitude of 0.13 V cm^{-1} Oe^{-1} (Suchtelen 1972; Vandenbo et al. 1974; Vandenboomgaard, Vanrun, and Vansuchtelen 1976; Vandenboomgaard and Born 1978). Subsequently, combinations of a variety of two-phase materials have been investigated. However, none of these efforts were able to push the ME coupling coefficient beyond the strength of –0.1 V cm^{-1} Oe^{-1}, although the corresponding theoretical calculation predicts a much higher response on the order of 1 V cm^{-1} Oe^{-1}. It was not until 2001, when Ryu et al. reported the fabrication of ME composites from a PZT ceramic disc sandwiched between Terfenol-D discs using Ag epoxy in a laminated configuration (Figure 4(a)) This configuration not only preserved the physical properties of each constituents but also provided the highest ME voltage coefficient up to 4.68 V cm^{-1} Oe^{-1} at that time (Jungho et al. 2001). This work provided a new path for fabrication of ME composites through simple epoxy bonding technique.

Continuing the research on ME laminated composites, a series of studies considering materials selection (all ceramics, ceramic-metal, polymer-metal), phase connectivity (0–3, 2–2, 1–3), geometry effect (thickness ratio, length ratio), synthesis method (bonding, co-fired, thin/thick film) and operation modes (L-T/T-L, T-T, L-L) have been conducted both experimentally and theoretically.

In the development of bulk ME composites, longitudinal mode laminates have been under intensive study due to their high ME voltage coefficient. Specifically, epoxy bonded Metglas/piezofiber multi-push-pull structure working under L-L mode (longitudinally magnetized

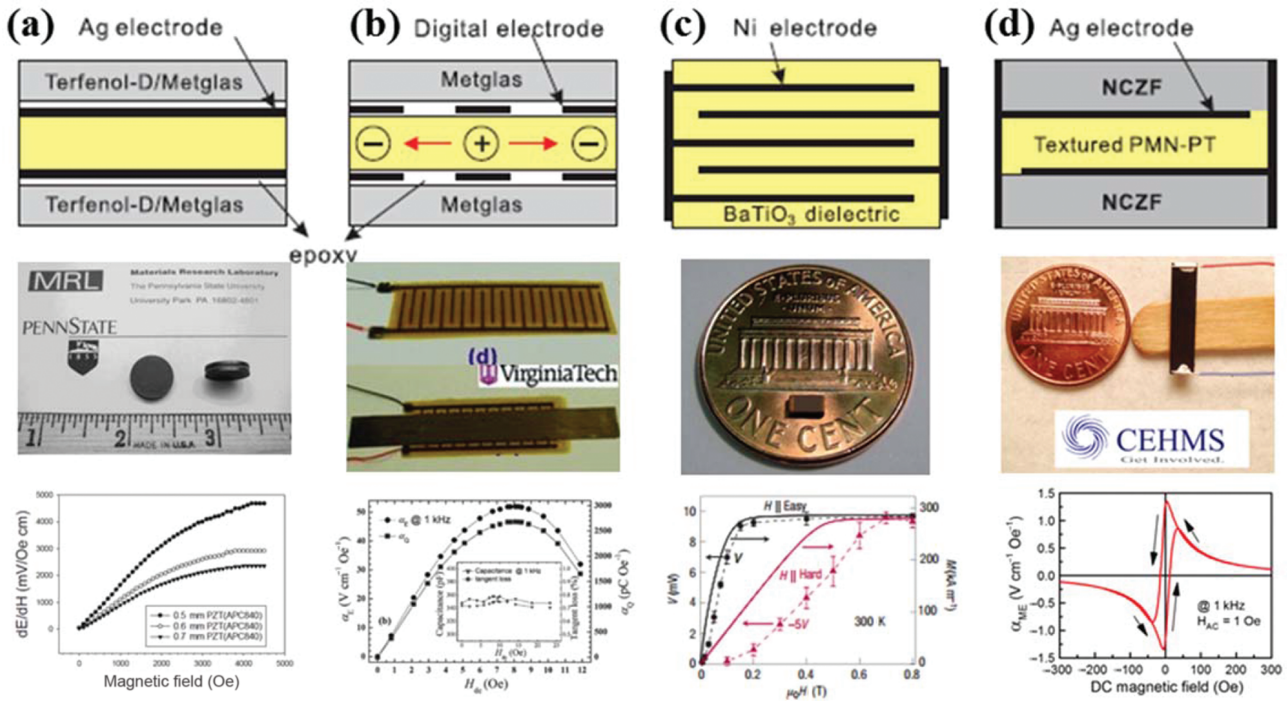

Figure 4: Development of bulk ME composite structures. (a) L-T mode epoxy bonded ME laminate (Jungho et al. 2001); (b) L-L mode epoxy bonded ME composite, (c) co-fired Ni-BTO layered ME composite (Israel, Mathur, and Scott 2008); (d) co-fired NCZF-PMNPT-NCZF trilayer ME laminate (Yan, Zhou, and Priya 2013).

and longitudinal poled) showed a gigantic ME voltage coupling coefficient up to 52 V cm^{-1} Oe^{-1} with high magnetic field detection sensitivity on the order of 10 pT at 1 Hz (Figure 4(b)). The large ME coupling was attributed to several factors including: (1) utilization of L-L mode, where the longitudinally poled piezoelectric provides more efficient stress transfer ($d_{33} > 2d_{31}$ since Poisson's ratio is smaller than 0.5); (2) the large q_{11} value and high permeability of Metglas, (3) high g_{33} value of the 1D piezofiber layer. Thus, the ME voltage coefficient of this L-L mode structure is nearly an order of magnitude higher than those of L-T type ME laminates.

Considering the mechanical coupling, direct bonding of the consecutive constituents through co-firing techniques has been developed. One of the ultra-low cost multilayer ME composites consists of alternate $BaTiO_3$ thin layers and Ni electrodes (Figure 4(c)), which possess a low α_{ME} of 7.1 mV cm^{-1} Oe^{-1} (Israel, Mathur, and Scott 2008). This structure is commonly utilized for multilayer capacitors and is thus widely available. Further, by selecting materials with large magnetostriction (NCZF) and high piezoelectric coefficient (textured PMN-PT), a giant α_{ME} of –1.3 V cm^{-1} Oe^{-1} was obtained in NCZF/PMN-PT/NCZF layered structure through low temperature co-firing ceramics (LTCC) process, as shown in Figure 4(d) (Yan, Zhou, and Priya 2013). This result is so far the largest ME response in all bulk ceramic ME composites with extremely low cost processing method based upon LTCC techniques.

In the development of ME nanostructures, nanocomposite thin films with various material combination and connectivity have been reported synthesized via either physical deposition [pulsed laser deposition (PLD), sputtering] or chemical deposition (sol-gel spin coating). Zheng et al. reported the vertical heterostructures consisting of magnetic spinel pillars ($CoFe_2O_4$) vertically embedded into ferroelectric films ($BaTiO_3$) through a self-assembled process on $SrTiO_3$ substrate using PLD (Zheng et al. 2004) as shown in Figure 5(a). Motivated by their work, tremendous investigations on 0–3 and 2–2 heterostructure have been performed. Although excellent ferroelectric and ferromagnetic properties can be obtained in these nanostructures, it is quite challenging to quantify the ME coupling due to high leakage current of the ferromagnetic pillars. On the other hand, a finite ME voltage coefficient was observed in 0–3 and 2–2 nanocomposites due to the large in-plane strain from the film-on-substrate structure and built-in residual stress arising from the lattice/thermal mismatch of consecutive constituents. In addressing these issues, a number of nanocomposite films were synthesized and characterized. Among them, two cases are worth mentioning. For 0–3

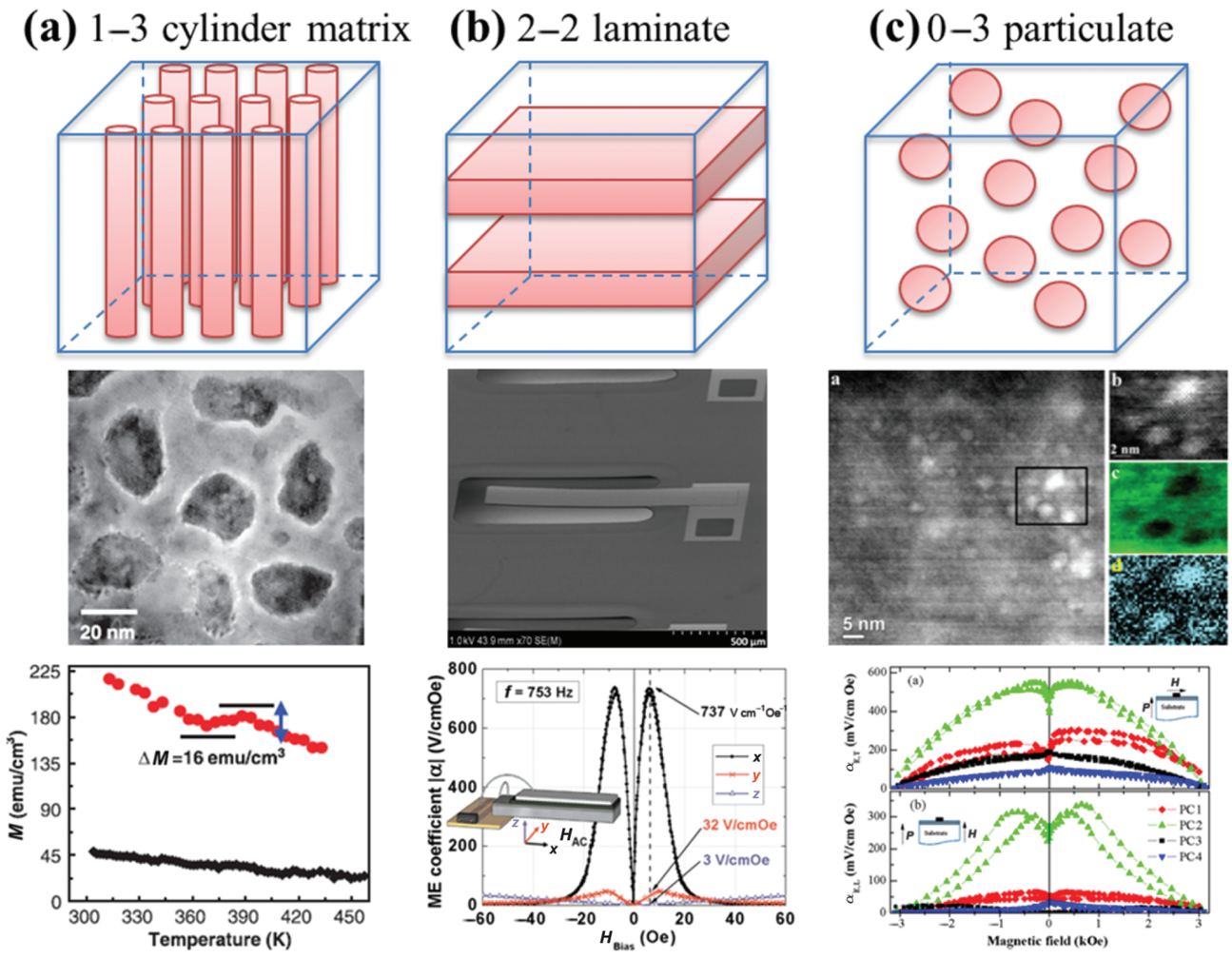

Figure 5: Development of ME nanostructures with different phase connectivity: (a) 1–3 cylinder matrix (Zheng et al. 2004); (b) 2–2 layered laminate (Onuta et al. 2011; Greve et al. 2010) and (c) 0–3 particulate ME thin film (McDannald et al. 2013).

type particulate films (Figure 5(c)), by dispersing magnetic nanoparticles ($CoFe_2O_4$) with optimized concentration (0.1% molar concentration) in PZT matrix, the spin coated nanocomposites thin film exhibited high transverse α_{ME}, of the order of 0.55 V cm^{-1} Oe^{-1} at $H_{dc} = 453$ Oe at 1 kHz, in comparison to that of prior work on 0–3 type nanostructured films (McDannald et al. 2013). This was attributed to the enhanced contact surface area from the well dispersed nano-scale magnetic particles and coherent interface between the constituents. For the 2–2 type horizontal thin film heterostructures in air, the highest reported ME coefficient of magnitude 737 V cm^{-1} Oe^{-1} at resonance frequency of 753 Hz and 3.1 V cm^{-1} Oe^{-1} at 100 Hz was observed in a FeCoSiB(1.75 μm)/AlN(1.8 μm)/Si(140 μm) multilayer cantilever structure, as shown in Figure 5(b) (Greve et al. 2010). By considering the air damping, the influence of vacuum on ME sensor was investigated resulting in a giant ME coefficient of 20 kV cm^{-1} Oe^{-1} at 152 Hz (Kirchhof et al. 2013). The high ME coupling coefficient was related to several reasons including (1) high Q factor of thick AlN film; (2) good geometrical configuration with longitudinal-type cantilever configuration 20 × 2 mm; and (3) giant magnetostriction of $\lambda_s = 158$ ppm in the annealed magnetic layer.

In summary, the development of conventional magnetoelectric composites can be explained on the basis of synthesis-structure-behavior parameters as listed in Table 1. Some parameters are associated with the material itself (physical properties, anisotropy, and geometry), while others originate from the consecutive constituent interface coupling (connectivity, bonding) or the measurement conditions (operation mode, frequency dependence and magnetic field dependence). Understanding of these parameters is of utmost importance for the integration of ME composites with functional devices.

Table 1: Controlling parameters and behavior in development of magnetoelectric composites.

Design factors	Features	Challenges	Realization
Materials	Piezoelectric Magnetostrictive	α_{ME}	Appropriate combination
Connectivity	1–3	High leakage current	0–3 or 2–2
Synthesis	Epoxy bonding	Low coupling	Co-firing Thin/thick film deposition
Characterization	Operation mode	Stress transfer	(L-L) > (L-T/T-L) > (T-T)
	ME vs f_{ac}	High f_r, narrow peak	Geometry effect
	ME vs H_{dc}	Need for H_{bias}	Self-biased ME

Self-Biased Magnetoelectric Coupling in Composites

There are several types of self-biased magnetoelectric systems that have been reported since the discovery of the zero-biased ME coupling in functionally graded laminates. Each system possesses characteristic interaction. In this review, the self-biased ME composites are categorized into five groups according to their working mechanism:

(a) Functionally graded FM based SME;
(b) Exchange bias mediated SME;
(c) Magnetostriction hysteresis based SME;
(d) Built-in stress mediated SME;
(e) Non-linear SME.

Information on these composites covering the ME response, working principle, design factors, advantages and limitations will be provided here.

Functionally Graded Ferromagnetic Effect

Magnetization-Graded ME-Laminates

As discussed in the previous section there are several ways to improve the magnetoelectric response of a composite. Out of these various approaches, the selection of high performance materials for improving the ME response has been the primary focus in most of the studies. The ferroelectric and ferromagnetic materials used in ME composites exhibit a symmetric hysteresis loop such as in polarization versus applied electric field (*P-E*) or magnetization versus applied magnetic field (*M-H*) measurements. A product property is then obtained in the form of polarization variation under an applied magnetic field (*P-H*) or conversely a magnetization variation under an applied electric field (*M-E*).

Recently, investigations on compositionally graded ferroelectrics have demonstrated hysteresis loop translation along the polarization axis due to the gradient polarization induced internal potential (Schubring et al. 1992; Ban, Alpay, and Mantese 2003). Figure 6 shows a schematic of the three separate cases for the creation of internal potentials in semiconductor, ferroelectric and ferromagnetic materials systems (Mantese et al. 2005), namely functionally graded materials (FGM). Such structures have given rise to a new class of transcapacitive ferroelectric devices (Transpacitors) viewed to be the dielectric equivalent of semiconductor junction devices, having potential applications in infrared detection, actuation, and energy storage. The similar concept was extended to the graded ferromagnetic systems (Mantese et al. 2005; Sudakar et al. 2007). A compositionally-graded Ni-Zn ferrite (Mantese et al. 2005) or hexagonal ferrite (Sudakar et al. 2007), with a spatial variation in saturation magnetization, had an internal magnetostatic potential, namely built-in magnetic bias along the gradient direction. Magnetization-graded structures can also be realized by subjecting a homogeneous ferromagnetic material to either temperature or stress gradients. However, these *extrinsic* magnetization-graded constructs differ from their compositionally graded counterparts since the internal magnetic fields of the extrinsic devices vanish once the external stress or temperature gradients are relaxed or removed. In the study in Ref. 46 magnetization graded samples of nickel zinc ferrite was synthesized by obtaining a linear variation in the zinc concentration along the length of the sample, leading to a corresponding linear variation in *M*. The presence of a small "built-in" magnetic field H_{int} of 30–44 Oe aligned along the magnetization-gradient is revealed as a shift in the magnetic inflection point of the ferromagnetic resonance signal; the shift coming from an alignment of the

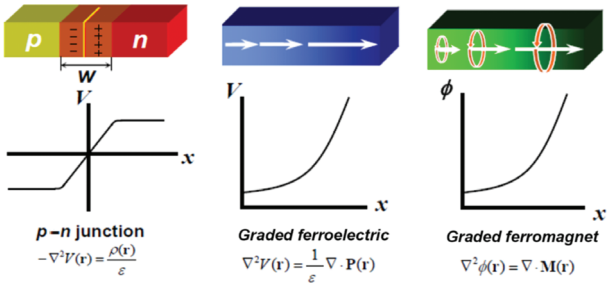

Figure 6: Internal potentials of semiconductors, ferroelectrics, and ferromagnetics created by gradients in charge density, polarization, and magnetization, respectively (Mantese et al. 2005).

external field either parallel or antiparallel to the internal field. Similarly, an internal field of same magnitude was measured by low-frequency AC susceptibility measurements in compositionally graded hexagonal ferrites (Sudakar et al. 2007). Further, considering the similarity of other ferroic system, one was able to provide a quantitative theoretical analysis readily expandable to other graded ferroic system with proper modifications. Thus, investigations on functionally graded ferroics offer opportunities for discovery of novel phenomena and devices.

Considering the unique properties of the above mentioned functionally graded materials, Petrov and Srinivasan et al. proposed a model for ME interactions in a functionally graded ferroelectric-ferromagnetic bilayer structure (Petrov and Srinivasan 2008). In their study, a model focused on a bilayer of graded nickel zinc ferrite (NZFO) and lead zirconate titanate (PZT) with grading axis perpendicular to its plane under both free-standing condition and clamped condition (bilayer on $SrTiO_3$ substrate) was presented. The theoretical calculations predicted an enhancement in ME coupling in the graded structure as compared to the homogenous bilayer in both low frequency and resonance frequency condition. The magnitude of ME coupling coefficient was further correlated with the grading strength and direction. The theory predicted an enhancement of 50-60% in the ME coefficient due to grading as compared to homogenous bilayers. This approach suggested a promising path for manipulating the ME coupling in a composite.

However, this idea did not attract much attention until 2010, when Mandal et al. experimentally demonstrated the compositionally graded NZFO in a bilayer ME composite with PZT (Mandal et al. 2010). The grading induced bending moment counteracted with the flexural deformation due to structural asymmetry strengthening the ME coupling significantly. These experimental results were comparable to the previous theoretical calculation (Petrov and Srinivasan 2008). Further, a strong ME coupling at zero-bias field (self-biasing) and a zero ME coupling at a certain bias (zero-crossing) were observed by replacing homogenous composition with graded ferrites, as shown in Figure 7 (Mandal et al. 2010). Considering the built-in bias arising from magnetization graded structure, the self-biased α_{ME} was explained by assuming a torque. This torque was considered to be generated from the interaction between the out-of-plane H_{int} and the applied in-plane AC magnetic field (H_{ac}). With the increase in the in-plane DC magnetic

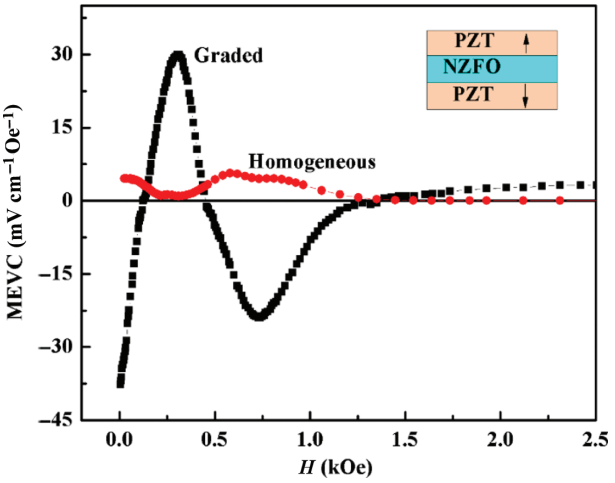

Figure 7: ME voltage coefficient (MEVC) as a function of DC magnetic field for trilayer PZT/NZFO/PZT composites with graded or homogenous NZFO (Mandal et al. 2010).

field (H_{dc}), the value of torque was found to decrease, shifting the net internal magnetic field towards the direction of $H_{dc.}$ and finally vanishing (zero-crossing) when it is parallel to the H_{dc}.

Keeping the magnetization-graded structure as basis, but in a more efficient and cost-effective experimental approach, Mandal and Sreenivasulu et al. further investigated a magnetostriction-stepped ferromagnetic layer consisting of Ni and Metglas with negative and positive magnetostriction, respectively (Mandal et al. 2011; Sreenivasulu et al. 2011). Interestingly, they demonstrated the appearance of built-in magnetization and the resultant zero-biased ME coupling by using the ferromagnetic biphase with stepped saturation magnetization instead of a compositionally graded magnetic phase. The self-biased ME coefficient has been found to be sensitive to the gradient direction and ferromagnetic layer thickness, as shown in Figure 8. In this work, gradient direction was considered as the direction of varying magnitude of q away from the PZT-ferrite interface. For positive grading, the magnitude of q should increase away from the interface and vice-versa. The physical mechanism behind this self-biased effect was further attributed to the induced torque rising from the interacted H_{int} and H_{ac}. Interestingly, a unique MEVC hysteresis loop (Figure 8) was observed in the static transverse magnetic field measurement of ME coefficient. This behavior was further attributed to the domain rearrangement arising due to the interaction of built-in magnetization under applied transverse DC magnetic field. Theoretical calculation of

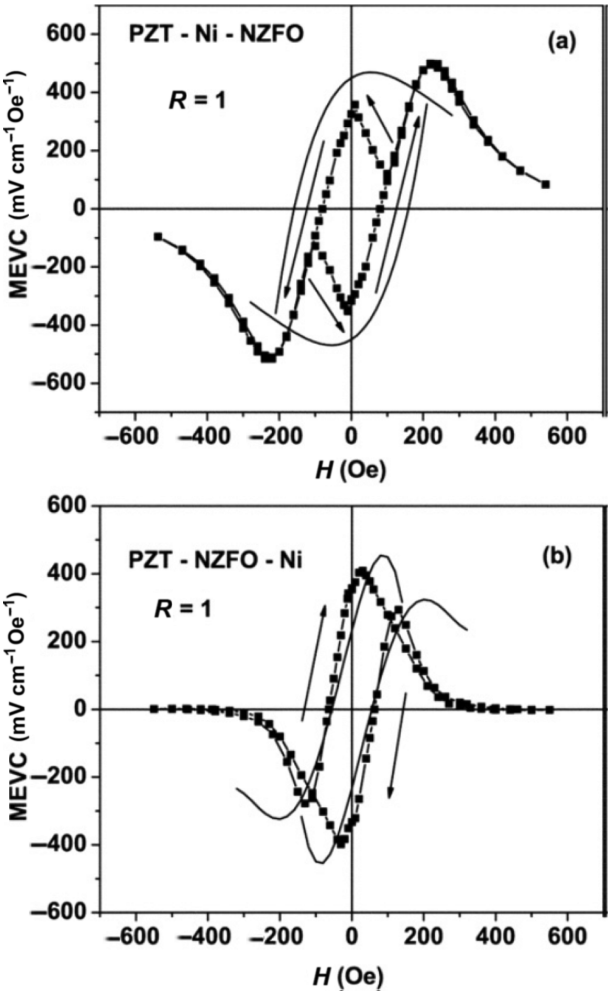

Figure 8: Theoretical (line) and experimental (line + symbol) ME voltage coefficient (MEVC) vs H for (a) PZT-Ni-NZFO and (b) PZT-NZFO-Ni samples with NZFO ferrite-to-Ni thickness ratio $R = 1$ (Laletin et al. 2012).

the self-biased ME properties for functionally-graded ferromagnetic/ferroelectric bilayer under low frequency and bending resonance was also provided in their study (Mandal et al. 2011; Sreenivasulu et al. 2011).

Further, in order to understand the unique hysteresis and self-biased ME response in ME composites with functionally graded ferroic phases, Laletin et al. provided a systematic study on the control of the hysteresis and remanent magnetoelectric coupling in functionally stepped NZFO/Ni-PZT layered composites (Laletin et al. 2012). Differences in ME response from the homogenous ME composites in α_{ME} vs H was attributed to variation of q with H_{dc}. Significant changes including a pronounced hysteresis with a large self-biased α_{ME} was observed and demonstrated to be sensitive with the grading direction and ferrite-to-Ni thickness ratio. A progressive (monotonous) enhancement in maximum α_{ME} occurred as the ferrite-to-Ni thickness ratio was increased in grading direction, as shown in Figure 9. In similar fashion, the peak value of α_{ME} with positive grading was found to be higher than that of negative one. What was more interesting in this study was the observation of unusual trend/shape of the hysteresis loop depending on magnetic layer sequence and thickness ratio (Figure 9). The loop was counterclockwise under low field region when the composite has positive grading (PZT-Ni-NZFO) while clockwise at higher field range with negative grading. In both condition, the loop was found to tilt toward the H axis with larger H_{bias} for the peak position of α_{ME}. These experimental results were found to be in good agreement with theoretical calculations. The origin of this unique hysteretic behavior was attributed to the grading induced built-in field at the interface and its strain redistribution (depending on sequence and thickness of magnetic layers).

These interesting results inspired further research on functionally graded ME composites on the magnetostrictive-stepped structure. The effect of grading was further studied with various combinations of other ferromagnetic materials. Researchers have used Ni, $SmFe_2$ (Smfenol), $NiFe_2O_4$ (NFO) and $Ni_{0.7}Zn_{0.3}Fe_2O_4$ (NZFO) as negative piezomagnetic coefficient (q) phase and Metglas, Ni-Fe alloy, Permendur, Terfenol-D (TD), Fe-Co alloy, FeCuNbSiB (FCNSB) alloy as positive q phase. The main characteristics of the developed functional-ferromagnetic-graded ME composites are shown in Table 2 in order of composite configuration. In addition to the asymmetric piezoelectric/graded-ferromagnetic (P-M_1-M_2) laminates, piezoelectric layer laminated between two graded-ferromagnetic layers (M_2-M_1-P-M_1-M_2) in a symmetric configuration has also been studied. For comparison, homogenous ME composites with piezoelectric/ferromagnetic (P-M) and ferromagnetic/piezoelectric/ferromagnetic (M-P-M) configurations were also provided. Other structures like semicircular composite (Hong et al. 2013), piezoelectric cantilever with graded-ferromagnetic tip mass have also been reported (Zhang et al. 2013).

From the results provided in Table 2, several interesting factors can be noticed: (a) The ferromagnetic-graded laminates resulted in a giant ME effect under zero-magnetic bias and an enhancement in ME coefficient under a magnetic bias field; (b) The self-biased ME coupling arises due to transverse magnetization that originates from grading in magnetization. This mechanism is effective in both

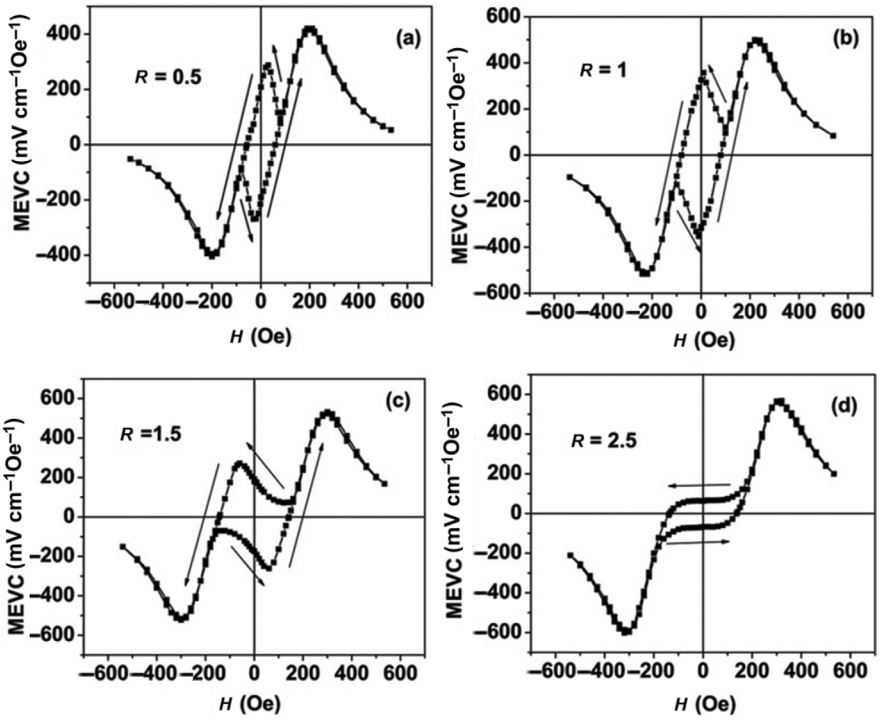

Figure 9: PZT-Ni-NZFO graded composites, results are for samples with ferrite-to-Ni thickness ratio R in the range of 0.5–2.5. (a) R = 0.5, (b) R = 1, (c) R = 1.5, (d) R = 2.5. The arrows indicate the direction of *H* variation (Laletin et al. 2012).

Table 2: Comparison of the homogenous and functionally graded magnetoelectric composites.

P	Constitution				ME coupling ($V\ cm^{-1}\ Oe^{-1}$) (kHz)			H-field (Oe)		References
	M_1	M_2	t_{m1}/t_{m2}	g	a_{H0}	a_{max}	f_{ac}	H_c	H_{opt}	
(a) P-M asymmetry laminates										
PZT	NZFO				0	0.065	0.03	0	200	Mandal et al. (2010)
PZT	Ni				0.16	0.23	0.03		75	Mandal et al. (2010)
PZT	Ni				0	0.31	0.02	0	150	Laletin et al. (2012)
PZT	Ni-Fe				0	19.86	168.4	0	200	Chen et al. (2012)
PZT	Samfenol				39.5	48	119.7	200	272	Zhang et al. (2013)
(b) P-M_1-M_2 asymmetry laminates										
PZT	NZFO	NFO	1	N	−0.03	0.06	0.03	38	114	Mandal et al. (2010)
PZT	NFO	NZFO	1	P	−0.09	0.16	0.03	90	179	Mandal et al. (2010)
PZT	Metglas	Ni	0.47	N	−1.71	2.1	0.03	3	9	Mandal et al. (2011)
PZT	Ni	Metglas	2.1	P	−1.69	3.5	0.03	6	11	Mandal et al. (2011)
PZT	Ni	Ni-Fe	1	P	0	0.78	0.03	0	50	Mandal et al. (2011)
PZT	Ni	Permendur	1	P	0.4	0.93	0.03		40	Mandal et al. (2011)
PZT	NZFO	Ni	0.5	N	0.28	0.28	0.02	70	0	Laletin et al. (2012)
PZT	Ni	NZFO	2	P	0.22	0.42	0.02	70	220	Laletin et al. (2012)
PZT	Ni-Fe	FCNSB	20	N	27.4	37.4	168.4	30	67	Chen et al. (2012)
PZT	Ni	Fe-Co	1	P	0.06	0.085	1		240	Hong et al. (2013)
PZT	Ni	FCNSB	4.4	P	49.5	51.4	0.35	10	4	Lu et al. (2014)
(c) M-P-M symmetry laminates										
PZT	Terfenol-D (TD)				0	0.97	1	0	650	Chen et al. (2013)
PZT	Ni				10	35	f_r		320	Lu et al. (2013)
(d) M_2-M_1-P-M_1-M_2 symmetry laminates										
PZT	Ni-Fe	FCNSB	20	N	42.12	53.8	164.8	40	100	Chen et al. (2012)
PZT	TD	FCNSB		N	0.27	1	1	60	600	Chen et al. (2013)
PZT	Ni	FCNSB	10	P	86	99.6	f_r	100	25	Lu et al. (2013)
PZT	Ni	FCNSB	10	P	89.2	100	193.3	100	25	Lu et al. (2014)
PMNPT	TD	Samfenol		N	13.75	61.87	97.5		235	Zhang et al. (2014)

asymmetric and symmetric functionally-graded ME composites; (c) Thickness ratio between magnetization-graded ferromagnetic phases plays an important role towards tuning the magnitude of both self-biased, peak ME coupling coefficient, and the corresponding zero-crossing field (H_c) and optimum bias field (H_{opt}); (d) For positive grading (g) of q (P: magnitude of q increases away from the PZT-ferrite interface), the peak value of α_{ME} shows a factor of two higher than that of negative grading (N) and homogeneous ME laminates. (e) A significant enhancement of self-biased ME coupling coefficient was attained in symmetric system when operating at the mechanical resonance than that of asymmetric system operating at low frequencies for functionally-graded ME composites. Thus, studies on these compositionally and functionally-graded ME laminates resulted in understanding of the self-biased magnetoelectric coupling and their related electrical response as a function of magnetic field.

Electric-Field-Induced Bending Vibration Mode

According to the above discussion, it can be noticed that the self-biased ME response could be obtained with the presence of the flexural deformation in a ferromagnetic graded/stepped structure. However, this method of generating self-bias depends upon the composition grading which requires a special synthesis process and this creates additional steps in developing functional devices. Moreover, one important question needs to be addressed: whether the self-biased ME effect will be generated or not in ferromagnetic homogenous system with net zero magnetization moment?

In addressing this issue, Yang et al. first proposed an alternative methodology for inducing external bending strain via changing electrical connection to invoke self-biased ME response, as shown in Figure 10 (Yang et al. 2010). In this work, a 2–2 type composite was fabricated by laminating Ni plate in the center of two 3–0 type particulate composite plates (Figure 10(d)). This 3–0 type composites consisted of $0.948Na_{0.5}K_{0.5}NbO_3$–$0.052LiSbO_3$ (NKNLS) matrix and $Ni_{0.8}Zn_{0.2}Fe_2O_4$ (NZF) as dispersant. The differences in the magnitude of susceptibility and coercivity between Ni and NZF particles resulted in a built-in bias field (H_{int}) along the interface. However, it was further noted that the three-phase laminate did not have effective net magnetic gradient due to the balanced symmetry NZF-Ni-NZF (zero net built-in bias) structure. Furthermore, by comparing the laminates under different electrical connection, laminates with induced radial vibration showed zero remnant α_{ME} (α_{ER}), while laminates with induced bending vibration exhibited hysteresis in α_{ME} as a function of DC magnetic field with non-zero α_{ER}. The induced bending mode was considered to be originating

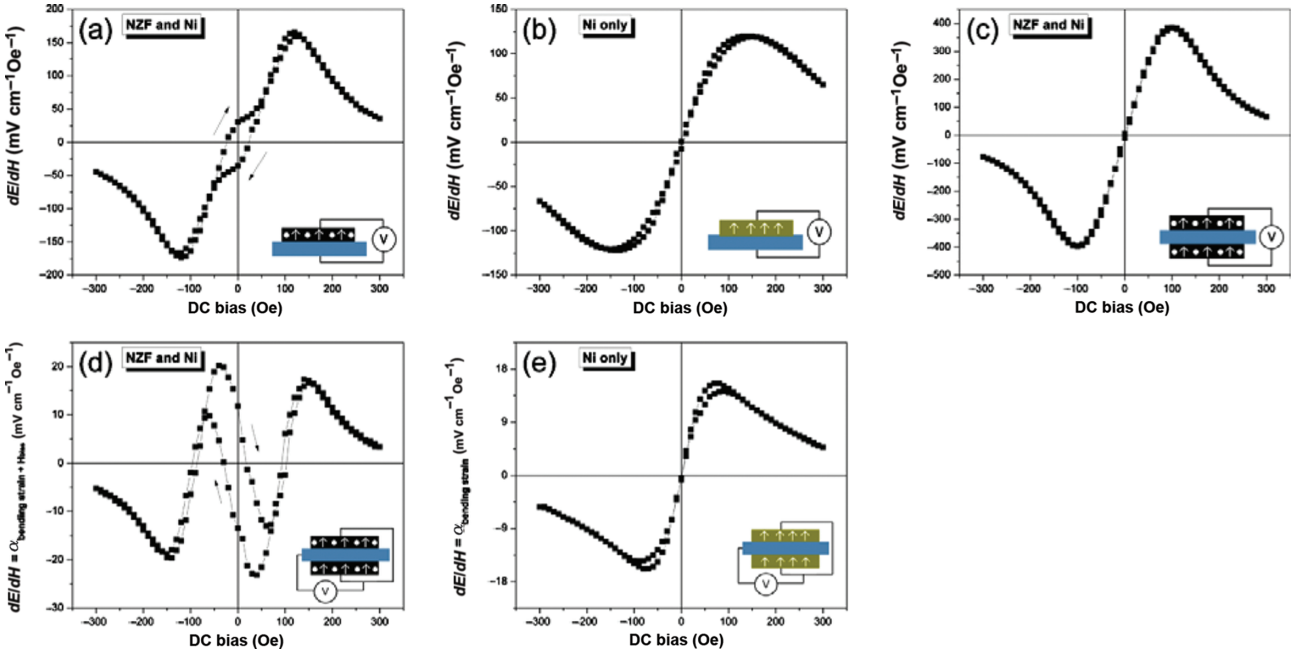

Figure 10: ME voltage coefficient of ME composites in various configuration, (a) NKNLS-NZF/Ni bilayer, (b) NKNLS/Ni bilayer, (c) NKNLS-NZF/Ni/NKNLS-NZF trilayer with series electrical connection, (d) NKNLS-NZF/Ni/NKNLS-NZF trilayer with parallel electrical connection, and (e) NKNLS/Ni/NKNLS trilayer with parallel electrical connection (Yang et al. 2010).

from the electrical connection with 180° voltage phase difference between top and bottom of the poled 3–0 particulate composites. This asymmetry, including bending strain, was found to increase the magnetic interaction variation alternatively along the two interphases. This further resulted in an effective magnetic gradient in the dynamic process. These results demonstrated that the self-biased effect can be realized in a symmetric structure with zero net magnetic gradients by invoking the bending strain through electrical connections.

Since the different ferromagnetic phases have been considered to play an important role in magnetic interaction, the influence of the NZF particles distribution and interaction toward self-biased behavior was further presented (Yang et al. 2011). This was expected since the magnetic interaction between NZF and Ni could be tuned by modifying the anisotropic response of NZF particles with different distribution (θ_{NZF}), size (R_{NZF}) and shape. However, a proper model that associates with all these variables to a ME coupling is yet to be formulated, so that $\Delta a_{ER} = f(H_{bias}, \Delta x_{composition}, \theta_{NZF}, R_{NZF})$ could be predicted and used to control the dependence and magnitude of self-biased magnetoelectric coefficient.

The influence of operation mode in the three-phase lead-free laminates has been investigated, as shown in Figure 11 (Yang et al. 2011). Similar hysteretic α_{ME} behavior was demonstrated between direct-ME (Figure 11(a)) and converse-ME (Figure 11(b)) coupling of the composites. Self-biased effect was further explained by the shift of magnetostriction curve of the two-phase ferromagnetic layer under external magnetic bias, as shown in Figure 11(d). The frequency dependence of CME effect was demonstrated to be identical to that of DME effect in both magnetic bias and zero-biased conditions. These results indicated that magnetic induction switching is possible by applying only AC electric field. This is technically important toward developing core-free magnetic flux density and electrically controlled memory devices. Therefore, the self-biased ME effect could be realized even in graded-ferromagnetic system having net zero magnetization under external bending strain induced built-in bias with specific electrical connections. The symmetric structure with simple and easy fabrication

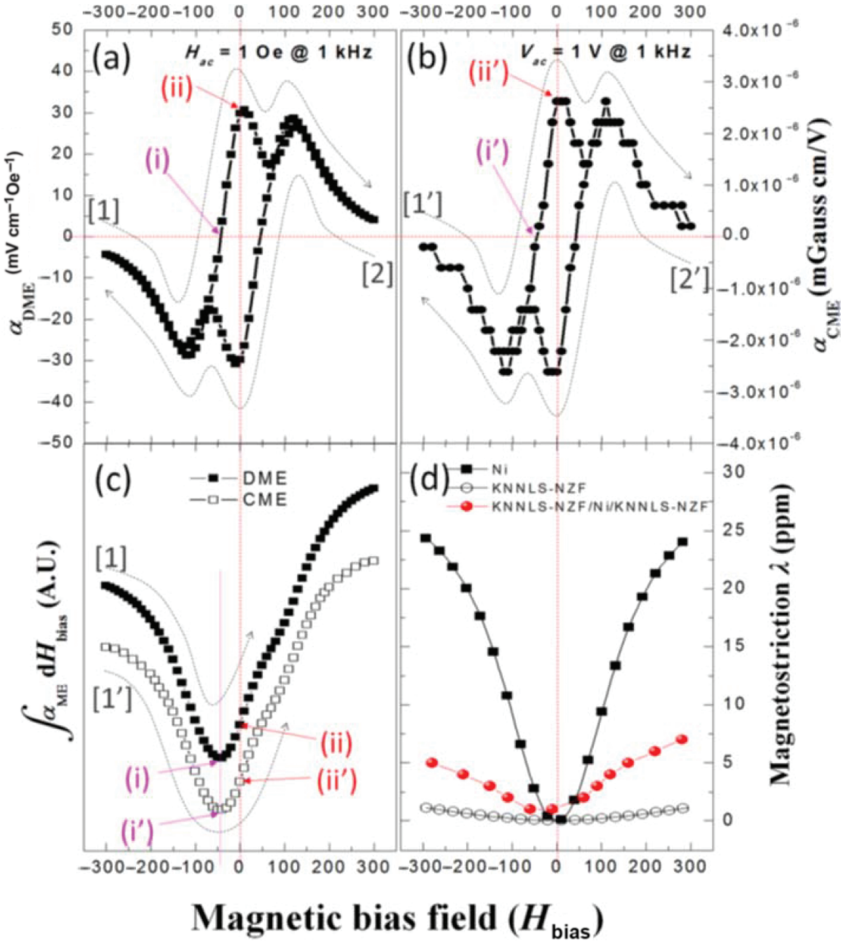

Figure 11: (a) Direct ME coefficient α_{DME} and (b) Converse ME coefficient α_{CME} as a functional of H_{bias}, (c) Integral value of α_{DME} and α_{CME} with respect to the H_{bias}, and (d) magnetostriction variation of Ni, KNNLS-NZF, and bending mode KNNLS-NZF/Ni/KNNLS-NZF as a function of H_{bias} (Yang et al. 2011).

process along with the easy manipulation of the self-biased effect in this three-phase laminates provides attractive advantage in possible ME applications.

In summary, functionally-graded magnetoelectric composites can be realized in various configurations that can be categorized in asymmetric or symmetric configuration, as shown in Figure 12. Taking advantage of the magnetization-graded-induced built-in bias, these functionally graded ME laminates could be used to produce unique phenomena including self-biased magnetoelectric effect, magnetoelectric hysteresis loop and enhanced peak ME coupling coefficient. There are eight typical functionally graded structures: (1) compositionally graded ferromagnetic layer with built-in magnetic potential was first synthesized and analyzed. Asymmetric/symmetric ME laminates based on compositionally-graded-ferromagnetic layer illustrated a new path toward realizing enhanced ME coupling coefficient; (2) Subsequently, for ease of fabrication, two ferromagnetic metal/alloy/ceramic thin plates with different piezomagnetic coefficient were laminated together with different sequence to form the graded magnetization (or built-in bias), namely stepped-ferromagnetic layer. ME laminates based on this concept were well studied with the effect of materials selection, thickness ratio, grading sequence and so on, (3) Discrete graded ME laminates with opposite magnetostrictive layer on either side of piezoelectric and piezoelectric cantilever with graded ferromagnetic tip mass; (4) Three phase ME laminates with 0–3 particulate composites on a homogenous ferromagnetic layer. Even with a net zero magnetization under a P-M-P configuration, the self-biased ME effect can be evoked by the electrical connection induced bending moment. All of these configurations were made possible due to the simple epoxy bonding approach, and this simple approach also opens up the possibility to fabricate more complex composite configurations and/or poling conditions resulting in different operation mode (such as L-T, T-L, L-L or T-T (Zhai et al. 2008)).

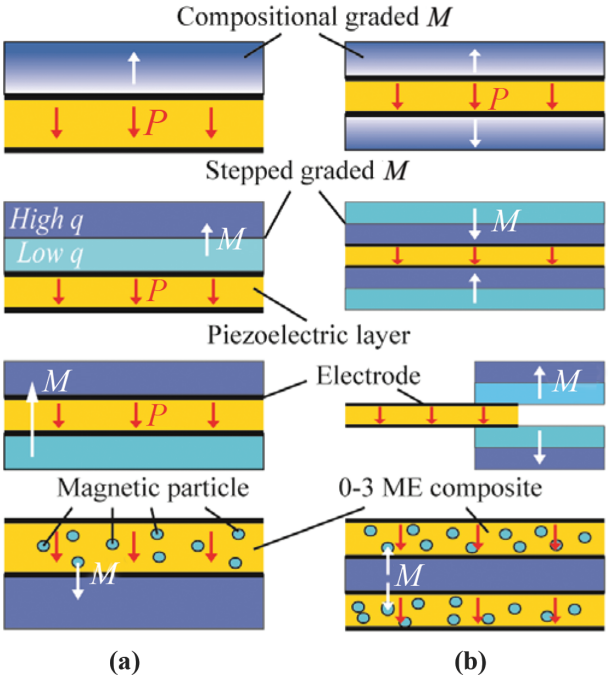

Figure 12: Schematic illustration of various functionally graded magnetoelectric composites configuration: (a) asymmetric structure; (b) symmetric structure.

Exchange Bias Effect

Exchange bias (EB) or exchange anisotropy effect (Meiklejohn and Bean 1957) is one of the most powerful tools for obtaining unique properties of multicomponent magnetic systems for spin valves, magnetic sensors, random access memories, magnetic tunnel junctions and other spintronic devices (Nogués and Schuller 1999; Berkowitz and Takano 1999; Freitas et al. 1994; Dieny et al. 1991). The exchange bias behavior is generally characterized as a horizontal shift of the magnetization-field (*M-H*) hysteresis loop along the magnetic field axis by an specific amount, namely the exchange bias field (H_{EB}), as shown in Figure 13. The physical properties of an EB material that is in the form of fine particles, multilayered films and/or inhomogeneous materials are determined by the properties of the constituents as well as by the interactions between them (Nogués and Schuller 1999; Berkowitz and Takano 1999). There are mainly three different exchange interaction mechanisms for creating the magnetic anisotropy, as shown in Figure 14

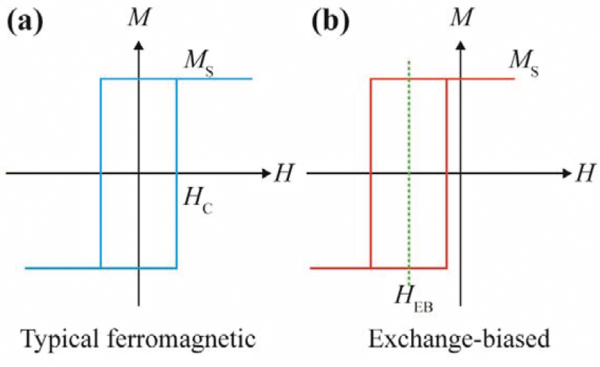

Figure 13: Magnetization hysteresis loop for a (a) typical ferromagnetic material, and (b) a magnetic material with exchange anisotropy.

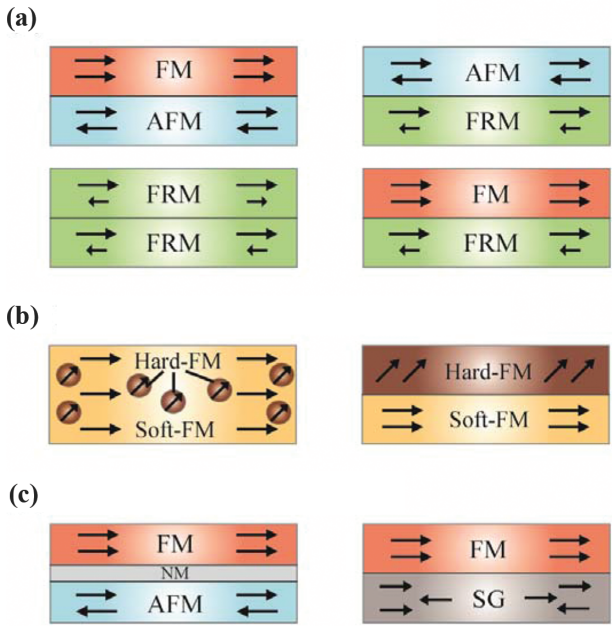

Figure 14: Schematic diagrams of three different exchange interaction mechanisms for creating the magnetic anisotropy, (a) direct exchange coupling, (b) long-range dipolar field interaction, (c) indirect RKKY type coupling.

- *Direct exchange coupling between subsequent phases*: the most general exchange bias structure was achieved in antiferromagnetic (AFM)-ferromagnetic (FM) materials systems (AFM-FM) (Nogués and Schuller 1999; Berkowitz and Takano 1999), where the magnetically hard AFM spin plays an important role in exerting a microscopic torque on the FM spin through interfacial coupling, therefore leading to the EB behavior. Usually, to induce an exchange bias, a field cooling process across the Néel temperature of the AFM material with FM materials in the saturated state is necessary (Meiklejohn and Bean 1957; Nogués and Schuller 1999; Berkowitz and Takano 1999). It can be noted that the EB effect has also been observed in ferrimagnetic (FRM)-AFM (Vanderzaag et al. 1995), FRM-FRM (Tokunaga et al. 1990) and FRM-FM (Cain and Kryder 1990; Freitas et al. 1994) material systems.
- *Long-range dipolar-field interaction*: the EB behavior can be also obtained in a soft-hard biphase magnetic systems consisting of an ultrasoft ferromagnetic core (generally metallic amorphous alloy) surrounded by a crystalline harder magnet outer shell (Giri, Patra, and Majumdar 2011; Gonzalez et al. 2000; Gubbiotti et al. 2002; Rivas et al. 2005), where the low field exchange anisotropy is ascribed to the magnetic dipolar-field interaction. After premagnetizing in a DC saturation field, the low field hysteresis loop shifts are ascribed to the local unidirectional stray field generated by the uncompensated poles at the magnetic harder particles/layer in the soft amorphous matrix/core. Usually, this biphase system can be realized by either partial crystallization of the metallic glass via annealing (Rivas et al. 2005; He et al. 2009; Zhou et al. 2009) or by depositing a hard magnetic outer shell onto the amorphous ribbons (Torrejon et al. 2007).
- *Indirect Ruderman-Kittel-Kasuya-Yosida (RKKY) typed coupling*: the magnetic coupling between AFM and FM through a nonmagnetic (NM) conductive spacer (AFM-NM-FM) (Gokemeijer, Ambrose, and Chien 1997) have been experimentally demonstrated and the EB behavior can be understood within the framework of a model based on long-range oscillatory Ruderman-Kittel-Kasuya-Yosida (RKKY) coupled spins (Bruno and Chappert 1991; 1992). The exchange coupling at interface of the AFM-NM-FM trilayer, different from the AFM-FM bilayer, are dominated by the AFM coupling at low temperature while the long-range RKKY-like coupling may overcome the AFM coupling at high temperature, resulting in an oscillatory H_{EB} (Parkin, Bhadra, and Roche 1991; Mewes et al. 2000; Lin et al. 2001). This oscillatory H_{EB} is also sensitive to the NM layer thickness. It should also be noted that this RKKY-like exchange coupling has also been reported in a spin glass/ferromagnetic (SG-FM) bilayer system (Ali et al. 2007; Gruyters 2005; Yuan et al. 2010).

The EB effect is quite appealing for obtaining unique magnetization behavior from multicomponent magnetic systems. The EB was initially designed and dedicated to stabilize the magnetization of soft FM layers in anisotropic magnetoresistance (AMR) disk drive recording head (Hempstead, Krongelb, and Thompson 1978). During the past two decades, extensive investigations on the EB effect have been undertaken due to its technological importance in spin-electronic devices, such as spin valve sensors for magnetic recording heads (Lin et al. 1995), tunnel valve cells for magnetic memories (Kools 1996) and so on.

Until recently, a number of investigations in terms of magnetoelectronics based on ME materials and EB effect have been proposed (Binek and Doudin 2005; Martin et al. 2008). Taking advantage of the intrinsic magnetoelectric coupling (electric-field-controlled magnetization) and extrinsic exchange bias coupling (AFM-FM spin interaction), researchers were able to utilize the electric field-induced net magnetic moment to manipulate the

ferromagnetism of a neighboring FM layer and create an alternative pathway toward electrical modulation over EB anisotropy in ME nanostructures (Martin et al. 2008; Vaz et al. 2010; Ma et al. 2011). The first electrically controlled EB interaction was demonstrated in Cr_2O_3-[Co/Pt] heterostructures, where the sign of the H_{EB} variation dependent on ME coupling of Cr_2O_3 were explored (Binek et al. 2005; Borisov et al. 2005). Subsequently, multiferroics (e.g. $YMnO_3$ and $BiFeO_3$) with ferromagnetic layer (e.g. NiFe, $SrRuO_3$, FeCo, CoFeB) have also been well explored and the H_{EB} in these nanostructures can be electrically tuned directly (Laukhin et al. 2006; 2007; Marti et al. 2006; Martin et al. 2008; Allibe et al. 2009; Dho et al. 2006; Chu et al. 2008; Martin et al. 2007). Among them, BFO-FM heterostructure offers an opportunity of operating the EB at room temperature, which is technologically required for practical applications.

However, all the previous studies on EB mediated ME composites, were focused on electric field controlled EB anisotropic ferromagnetism, namely CME effect (Martin et al. 2008; Vaz et al. 2010; Ma et al. 2011). Very few studies have investigated the DME effect in EB mediated ME composites even though it has significance for magnetically controlled polarization devices such as sensors, tunable transformers and energy harvesting devices. Specifically, the magnetization shift arising from EB anisotropy coupling may yield a corresponding shift in magnetostriction of the FM layer, leading to a self-biased ME coupling coefficient. This hypothesis originates from the nature of magnetostrictive materials, where the magnetostriction is generated via the variation of magnetization under applied magnetic field due to domain shift and/or rotation. Therefore, the magnetization shift is expected to induce a similar shift of λ and the resultant q as a function of H_{dc}, which is tightly correlated with α_{ME}. However so far to our knowledge, DME effect, particularly self-biased DME effect, based on EB coupling has been only reported in two systems, one in (AFM-FM)-FE nanostructured thin films (Lage et al. 2012) and the other in (Soft-Hard biphase FM)-FE bulk structure (Li et al. 2013). Detailed information regarding these two systems is discussed in the following sections.

(AFM-FM)-FE Exchange Bias Mediated ME Nanostructure

It was not until 2012, Lage and Meyners et al. developed the self-biased ME nanostructured composites based on intrinsic magnetostriction arising from exchange bias coupling (Lage et al. 2012). Figure 15(a) shows the schematic configuration of the EB mediated ME composite, where the multilayers with the sequence of NM-AFM-FM Ta/Cu-$Mn_{70}Ir_{30}$-($Fe_{50}Co_{50}$ or $Fe_{70.2}Co_{7.8}Si_{12}B_{10}$)] serving as the magnetostrictive component, while the AlN was selected as piezoelectric phase. Similar to EB coupling discussed above, the magnetically hard AFM spin plays an

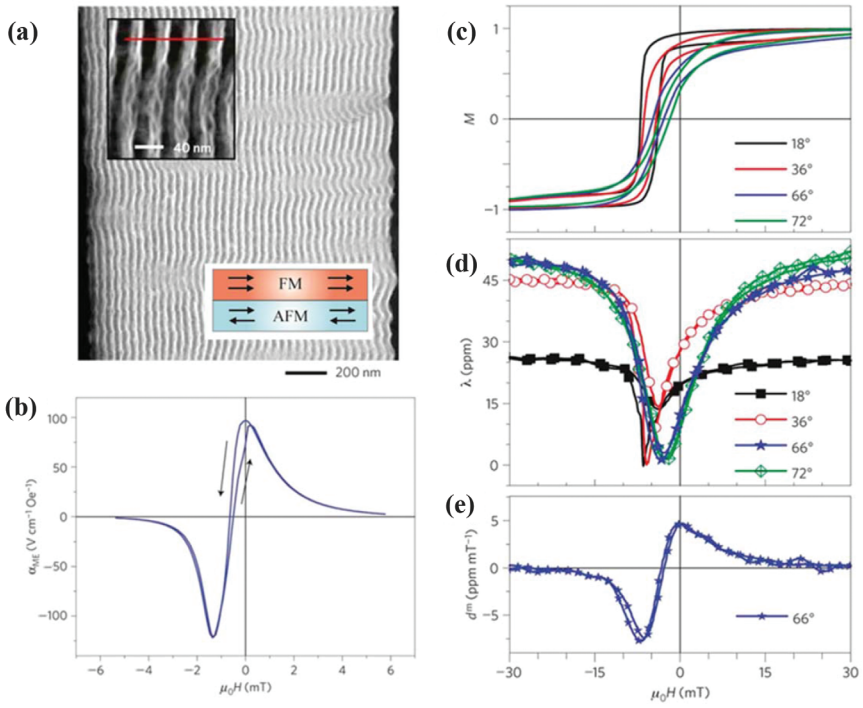

Figure 15: (a) TEM image of the $Fe_{50}Co_{50}$ multilayer system on a AlN substrate and a magnified view (inset), (b) magnetoelectric voltage coefficient for the $Fe_{70.2}Co_{7.8}Si_{12}B_{10}$-based multilayer system with the pinning direction induced at $\varphi = 70°$, (c) normalized magnetization curves, (d) corresponding magnetostriction curves and (e) piezomagnetic coefficient of $Fe_{50}Co_{50}$ multilayer stacks on cantilever samples for selected values of the inclination angle φ (Lage et al. 2012).

important role in exerting a microscopic toque on the FM spin, leading to a shift of H_{EB} (Berkowitz and Takano 1999) and (Nogués and Schuller 1999). The NM Ta/Cu bilayer was used as a buffer layer for texturing AFM ($Mn_{70}Ir_{30}$), which was mandatory for reliable EB. To evoke the H_{EB}, a field cooling process for the multilayered system above the Néel temperature of the AFM material is necessary. Normally, the magnitude of the shift is attributed to the thickness, interface microstructure and roughness of the AFM/FM layer (Berkowitz and Takano 1999; Nogués and Schuller 1999). In the AFM-FM bilayer system, due to the pining effect anisotropy, exchanging bias has always been observed along the pinning longitudinal direction of the thin film. On the contrary, the anisotropic field is approximately reciprocally proportional to the magnetostriction leading to a maximum magnetostriction under a transverse magnetic field. Therefore, in order to adjust the shift of magnetostriction curve for a maximum q and the resultant self-biased ME voltage coefficient, an inclination angle (φ) was induced with respect to the longitudinal direction of the film, as shown in Figure 15(c)–(e). By optimizing the thickness and inclination angle of the system, this EB mediated self-biased ME nanostructures demonstrated a giant ME coefficient of 96.7 V cm^{-1} Oe^{-1} for $\varphi = 70^{o}$ at $fr = 1.19$ kHz at zero-bias field, as shown in Figure 15(b). This concept has now further lead to an maximum coefficient of 430 V cm^{-1} Oe^{-1} by a thickness variation of the ferromagnetic layer (Lage et al. 2014).

Although the first EB mediated self-biased ME composites were reported recently, the development of AFM-FM exchange bias mediated self-biased ME sensor has been rather slow (Lage et al. 2012,2013; Jahns et al. 2013). The lack of immediate progress could be due to the difficulty in synthesizing such system with complex multilayer stacked design, need for field cooling and control of ME coupling by film thickness and EB inclination angle. However, it has been believed that the implementation of such EB mediated ME nanostructure with self-biased effect could be promising toward MEMS-scale on-chip device fabrication (e.g. magnetic field sensor array). What's more important, this work created a new pathway for developing magnetoelectric composites by incorporating the exchange bias coupling.

(Soft-Hard Biphase FM)-FE Exchange Bias Mediated ME Bulk Laminate

Continuing the work on EB mediated self-biased ME composite, it has been noted that although the film thickness, field cooling and incident angle control of the (AFM-FM)-FE multilayer configuration is not the main obstacle to study the EB coupled self-biased coupling, synthesizing the complex multilayer nanostructure is rather challenging and expensive toward practical application. To make it easier and cost effective, bulk ME laminates based on the soft-hard biphase FM exchange bias coupling was demonstrated in 2–2 type multi-push-pull configuration consisting of annealed Metglas, Metglas and PZT. (Li et al. 2013) It is well known that amorphous Metglas foil with a homogenous "soft" ferromagnetic material, usually shows a symmetrical slim M-H hysteresis loops with a biquadratic λ behavior with respect to H_{bias} at zero-bias point. However, under high temperature annealing, transition metal elements (Fe, Co) of the alloy tends to form crystallized hcp-Co, a-Fe and iron oxide phases, which possess "harder" magnetic properties as compared to that of amorphous Metglas (Rivas et al. 2005; He et al. 2009). These partially crystallized particles lead to unidirectional magnetization anisotropy (after premagnetizing) in adjacent amorphous Metglas layers. This reflects in the shift of M-H loop (Giri, Patra, and Majumdar 2011; Gonzalez et al. 2000; Gubbiotti et al. 2002; Rivas et al. 2005). Since the magnetostriction originated from magnetization variation (magnetic domain rotation and domain wall migration), the exchange bias resulted in a same magnitude of shift in the position of $\lambda = 0$ at H_{EB} with non-zero q at zero-bias. Therefore, a giant self-bias ME coefficient was realized with the magnitude of 12 V cm^{-1} Oe^{-1} as shown in Figure 16, which could be further enhanced to 380 V cm^{-1} Oe^{-1} at the EMR frequency of 33.7 kHz (Li et al. 2013).

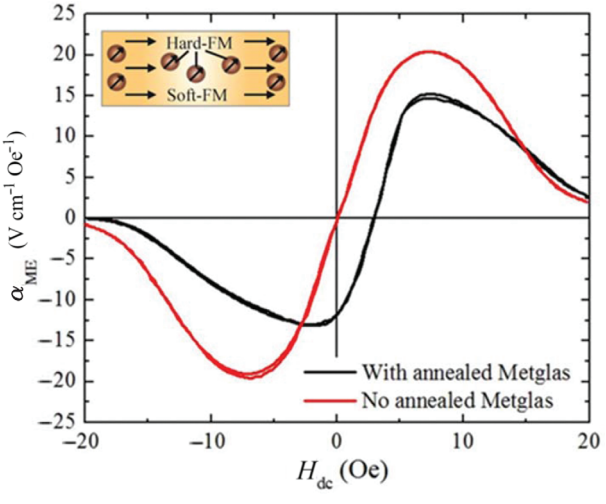

Figure 16: Magnetoelectric voltage coefficient of Metglas/PZT/Metglas laminates measured at $H_{ac} = 0.1$ Oe at a frequency of $f = 1$ kHz (Li et al. 2013).

However, except for the high self-biased response and simple EB coupling mechanism of this laminate composites, the magnitude of maximum α_{ME} was lower than that of conventional push-pull mode ME laminates with same dimension (Li et al. 2012). This difference in α_{ME} was ascribed to the precipitation of magnetically hard particles. These particles not only play an important role in EB coupling, but also dramatically affect the saturate magnetostriction of Metglas. The magnitude of α_{H0} can be manipulated by controlling the thickness of annealed Metglas, however it is rather hard to operate due to the contrary behaviors of H_{EB} and $\alpha_{ME,}$ where the increase of H_{EB} will result in a decrease of α_{ME}.

To summarize this section, a schematic diagram of EB mediated ME composite with various configuration is shown in Figure 17. Although the investigation of exchange bias has been ongoing since its discovery in 1956 (Meiklejohn and Bean 1957), the utilization of exchange bias coupling in magnetoelectric/multiferroic system attracted interest of researchers a decade ago. Among these prior research of EB mediated ME coupling; most of efforts have been focused on electrical control of magnetism in FM films (Martin et al. 2008; Vaz et al. 2010; Ma et al. 2011). The investigation of EB induced self-biased ME effect has just started with two preliminary research in either a (AFM-FM)-FE thin film nanostructure(Lage et al. 2012) or a (Soft-hard biphase FM)-FE bulk laminate(Li et al. 2013), as shown in Figure 17(a) and (b). Despite these efforts, the fundamental understanding of the impact of EB mediated self-biased response and its technological aspects are not well established. In principle, the concept of exchange bias mediated magnetoelectric composites could also be expanded to other EB coupling mechanism including: (1) multiferroic with (FE-AFM)-FE nanostructure Figure 17(c)], (2) soft-hard biphase FM-FE core-shelled bulk structure Figure 17(d)], and (3) RKKY-liked EB coupling such as (AFM-NM-FM)-FE or (SG-FM)-FE nanostructures. In that case, the multicomponent magnetic layers with EB coupling could be used to establish a non-zero piezomagnetic coefficient at zero-bias. This would further lead to a giant self-biased ME coupling. In particular, exchange bias with multiferroic (e.g. $BiFeO_3$ with FE and AFM order) and soft-hard biphase FM multilayer ribbon seems to be most promising candidate, as shown in Figure 17(c) and (d), for aforementioned purpose due to their ease of synthesis and capable of EB coupling at room temperature.

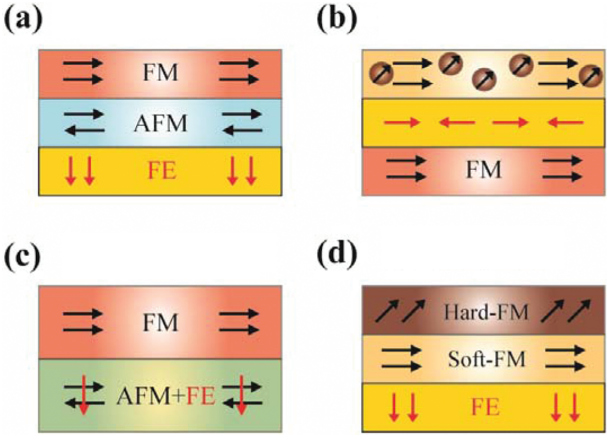

Figure 17: Schematic diagram of four possible EB mediated ME composite configurations. (a) (AFM-FM)-FE; (b) (soft/hard FM)-FE; (c) FM-multiferroic (d) hard-soft-FE.

Low-Field Magnetostriction Hysteresis Effect

The idea of synthesizing a composite with homogenous ferromagnetic phase displaying a self-biased ME effect was firstly demonstrated by Yang et al. in 2011, as discussed above. They suggested an electrical-connection-induced methodology that was able to evoke the self-biased coupling when the external bending strain activates built-in bias. However, this idea was proved to be indispensable with a dispersion of other ferromagnetic particles in the piezoelectric layer and the self-biased coupling was rather low and difficult to control. Thus, it is both scientifically and technically important to demonstrate a self-biased response in homogeneous ferromagnetic system with the feasibility of controllable tunability.

Interestingly, the early observation of self-biased ME coupling in homogenous ferromagnetic system can be traced back to the research published by Srinivasan et al. in 2002. They found hysteresis and remanence in α_{ME} versus H_{bias} plots in co-fired $La_{0.7}Sr_{0.3}MnO_3$ (LSMO)-PZT laminates (Srinivasan et al. 2002). Similar hysteretic behavior has also been found in layered transition metal (TM)-PZT trilayer for Co-PZT-Co and Fe-PZT-Fe (Laletin et al. 2005). They also observed unique characteristics including zero crossing and a switching in the sign of α_{ME} (phase shift of 180^o) at high field range, which was attributed to the variation in piezomagnetic coefficient with H. Alternatively, Pan et al. investigated the geometry effect of Ni electroplated PZT ME composites, in which they presented a non-zero α_{ME} at zero bias field and double peak/linear behavior at high field range in both long-type or cylindrical trilayer laminates (Pan et al. 2009). Similarly, Chen et al. made a quasi-one-dimensional ME sensor consisting of a PZT tube and FeNi (high saturation magnetization, $4\pi M_s = 19$ kG) magnetostrictive wire, which indicated a high zero bias field

sensitivity of 1.65 V cm^{-1} Oe^{-1} (Chen et al. 2011). Despite the above investigations in bulk composite, thin film ME heterostructures with single phase ferromagnetic layer have also been extensively reported with non-zero α_{ME} at zero field (Wan et al. 2005; 2006). More interestingly, not only in layered ME composites, self-biased ME coupling was also acquired in single-phase multiferroics, such as thin film $BiFeO_3$ (Wang et al. 2003) and bulk $Sr_3Co_2Fe_{24}O_{41}$ (Wu et al. 2012).

Although the self-biased ME coupling behavior has been reported in several systems (from bulk to thin film, from multiferroic to composite, from quasi-one-dimension to three dimension), however, a proper understanding about this unique effect was not achieved in almost two decades of research since its first observation. Furthermore, in spite of these observations, majority of the investigations were not able to demonstrate the self-biased effects theoretically and experimentally both. Various reasons identified for this discrepancy can be rationalized as:

Use of static piezomagnetic coefficient for a dynamic phenomenon in conventional theoretical calculation. Although homogeneous ferromagnetic materials are not piezomagnetic, one can achieve a pseudopiezomagnetic effect ($q = d\lambda/dH$) by subjecting the sample in the presence of an applied H_{dc} superimposed with a H_{ac}. Thus, the AC magnetomechanical coupling in the form of $q = (4\pi\lambda'\mu_r/Y)^{1/2}$ should be considered, where λ' is the AC magnetostrictive constant, μ_r is the reversible permeability, and Y is the Young's modulus (Burgt 1953).

- High demagnetization field (H_d) of the magnetostrictive phase. If the demagnetization field is high, the effective magnetic induction becomes small under applied DC bias and therefore leading to a reduced or negligible self-biased ME coefficient (Zhou et al. 2012). This H_d is dependent on the dimension and geometry (Osborn 1945; Soinski 1990; Pan et al. 2008). Therefore divergence in ME behavior of the composite was observed in the samples with same constituent.
- Composition gradient induced along the interfacial region by the chemical reactions and/or inter-diffusion between constituents during co-sintering process. Because of the high sintering temperature, element from the starting materials may inter-diffuse into other phases, therefore creating a composition gradient structure, in which the built-in bias might be induced and played an important role toward self-biased ME effect.
- Residual stress arising from thin film growth or co-sintering process. Due to the lattice mismatch of the starting materials or thermal mismatch during the high-temperature sintering process, a residual stress/strain is always generated along the film/substrate or phase/phase interface. This residual stress will not only limit/enhance the mechanical coupling at the interphase between constituents, but also result in unique behavior like self-biased effect.

These explanations were demonstrated from either intrinsic property (demagnetization field) or extrinsic properties (inter-diffusion or residual stress from thermal treating process). Detailed information regarding the extrinsic effect on self-biased effect will be discussed in the next section. It was not only until 2012, when considering magnetization hysteresis and the demagnetization effect of ferromagnetic layer, Yuan et al. for the first time, demonstrated and systematically explained the self-biased ME effect in homogeneous two-phase magnetostrictive-piezoelectric laminates (Zhou et al. 2012). Ni-PZT bilayer shows a hysteretic α_{ME} behavior with counterclockwise direction during H_{dc} sweep in compared to that of Metglas-PZT with non-hysteretic cyclic response (Figure 18(a)). This phenomenon can be attributed to the magnetization hysteretic behavior (counterclockwise) of Ni and the resultant non-zero λ and/or q in the low field range in compared to that of Metglas, as shown in Figure 18(b)–(d) (Zhou et al. 2012).

Because of the complex nature of the ferromagnetic materials, the relation between the applied magnetic field and the magnetostriction induced in the sample is not simple linear behavior under applied magnetic field. The typical magnetization and strain curves are similar to that of Ni as depicted in Figure 18(b)–(c), where presence of inherent non-linearity and hysteresis were clearly observed. Thus, in principle, a self-biased ME response may arise in homogenous ferromagnetic system with a hysteresis in magnetostriction behavior and the resultant non-zero piezomagnetic coefficient. However, for materials such as amorphous Metglas, the slim hysteresis can originate from the difference in the crystallinity and domain structure. It is generally accepted that the domain rotation and domain wall motion accounts for the hysteresis phenomenon. It should be also noted here that the self-biased ME coefficient is also tightly related with the shape-induced demagnetization effect (Figure 19(c)) and the resultant effective magnetic induction of the ferromagnetic layer (Figure 19(d)) (Zhou et al. 2012). Thus, the self-biased ME effect could be further tuned via geometry of ferromagnetic layer, as shown in Figure 19. By optimizing the geometry and use of a MFC as the piezoelectric layer, the Ni based composite

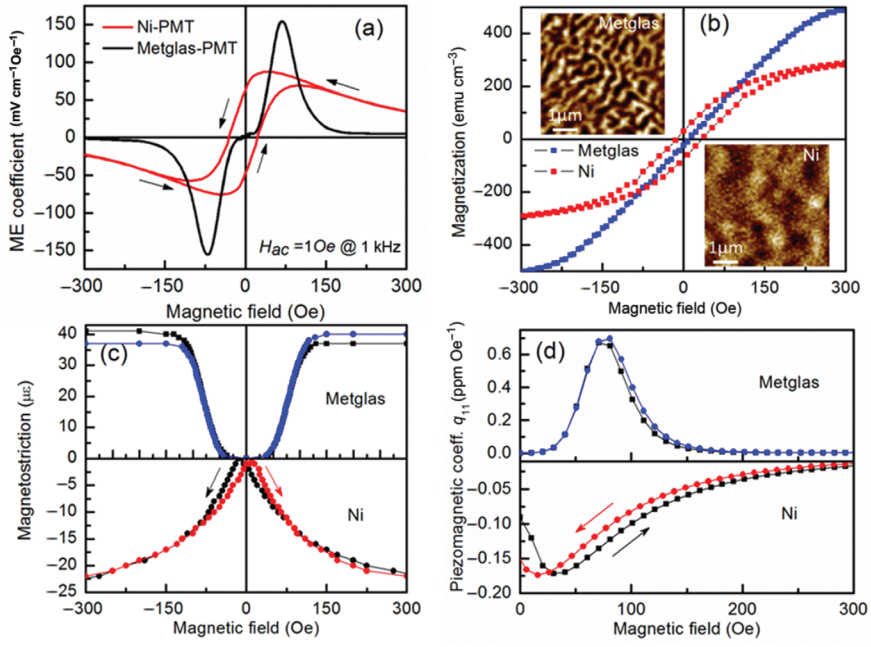

Figure 18: (a) Magnetoelectric voltage coefficients of Ni-PZT and Metglas-PZT bilayer laminates as a function of DC magnetic field, (b) magnetization-magnetic field response of Ni and Metglas, inset shows their magnetic domain images, (c) DC magnetic field dependence of the magnetostriction, and (d) DC magnetic field dependence of piezomagnetic coefficient for Ni and Metglas (Zhou et al. 2012).

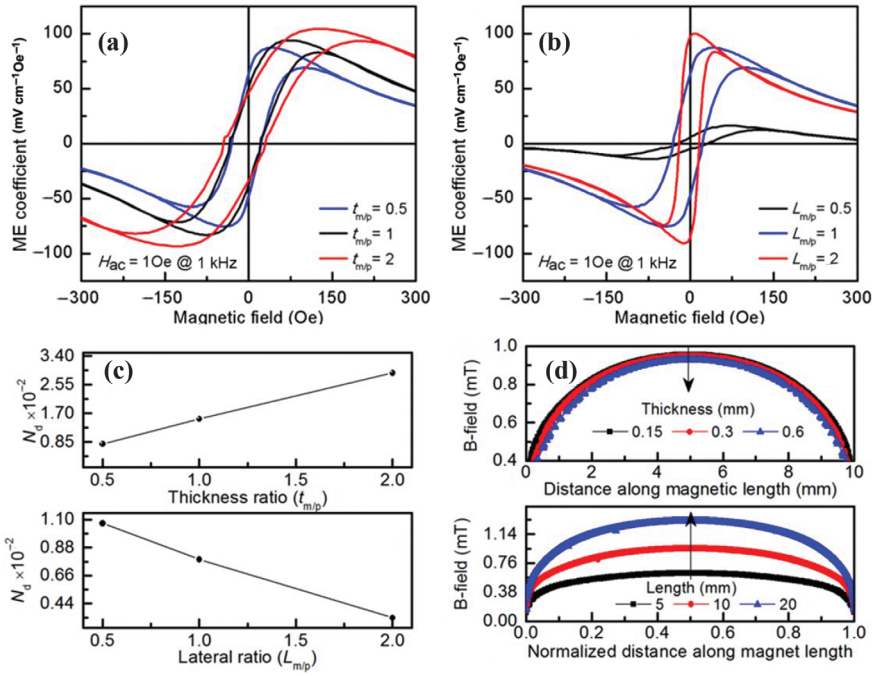

Figure 19: Magnetoelectric voltage coefficient of Ni-PZT laminates with (a) varied thickness ratio, and (b) lateral dimension; (c) demagnetization factor variation and (d) simulated in-plane magnetic field strength along the center plane of Ni sheet as a function of sample thickness/lateral ratio in response to zero DC bias field (Zhou et al. 2012).

operating in L-L mode generated a large response of –1.25 V cm^{-1} Oe^{-1} at zero bias at 1kHz (Zhou et al. 2012).

Following the demonstration of self-biased ME effect from a Ni based composite with magnetostriction hysteresis behavior, Zhang et al. reported a similar self-biased hysteretic behavior in magnetostrictive Samfenol ($SmFe_2$) based laminates, where a giant resonant self-biased ME coefficient of 39.5 V cm^{-1} Oe^{-1} was obtained through intrinsic magnetic anisotropy and the resultant non-zero dynamic piezomagnetic coefficient (Zhang et al. 2013). Alternatively, Yan et al. demonstrated a large self-biased ME response of –1.21 V cm^{-1} Oe^{-1} in a co-fired NCZF/Ag/Textured-PMN-PT/Ag/NCZF multilayer composite, where similar α_{ME} vs H_{dc} hysteretic behavior was observed and further correlated with NCZF magnetostriction hysteresis effect at low field range (Yan, Zhou, and Priya 2013). McDannald et al. reported a remnant magnetoelectricity at zero field in 3–0 type particulate nanocomposite films

with $CoFe_2O_4$ (CFO) nanoparticles (NP) dispersed in $PbZr_{0.52}Ti_{0.48}O_3$ (PZT) matrix (McDannald et al. 2013). In these films, the clustering of the CFO NPs displayed a finite M_r, which lead to a self-biased α_{ME}. Therefore, according to these demonstrations, the explanation of self-biased effect based on the magnetostriction hysteresis effect is expandable to most of the cases in homogeneous ferromagnetic systems. However, it should be further noted here, for a co-fired ME composite and thin film heterostructures, the mechanism of self-biased effect is not only based on the intrinsic magnetostriction hysteresis but also results from the interfacial built-in stress originating during the thermal treating process. These effects will be further discussed in the next section.

To summarize this section, the self-biased ME response can be achieved in homogenous ferromagnetic-piezoelectric two phase systems. The underlying cause of this effect can be attributed to the existence of nature ferromagnetic hysteresis, which results in a nonzero magnetostriction and/or piezomagnetic coefficient at low field range. This mechanism has been effective in both multiferroics and composites in the form of bulk laminates or thin film nanostructures. Table 3 summarized the self-biased effect observed in various homogenous ME system that can be explained using the intrinsic properties of ferromagnetic phase. Some of these systems can also be influenced by the built-in stress. This will be discussed in the next section. From viewpoint of practical applications, self-biased effect of the homogenous ME systems subjected to magnetostriction hysteresis is feasible for subsequent device design and fabrication. Simple structure and geometry controlled tunability not only provides great flexibility in developing functional tunable devices (sensors, transformers, and energy harvesting systems) (Zhou, Apo, and Priya 2013a; Zhou and Priya 2014), but also opens possibility of implementation in MEMS-scale components (Zhou, Bhalla, and Priya 2013). However, the strain effect present here could result in another challenge for on-chip components as synthesis process has to account for the built-in strain during film growth/co-sintering.

Built-in Stress Effect

The quest for magnetoelectric materials displaying the self-biased ME effect was accompanied by utilizing either a multilayer magnetic system with built-in/exchange-bias effect or a single phase FM with magnetostriction hysteresis in a composite structure. These self-biased composites can be realized by using epoxy bonding, co-firing and/or thin film deposition techniques. Most of the efforts on explaining mechanism of the self-biased ME effect in laminates so far were devoted to contribution of the magnetic components. Besides the consideration of the intrinsic properties of magnetic phase, the ME coefficient has been strongly dependent upon the effective strain coupling between phases. Experiments on

Table 3: Characteristics of different type of homogenous self-biased ME composites.

Class	Constitution	Synthesis	α_{H0}	α_{max} ($V\ cm^{-1}\ Oe^{-1}$)	f_{ac} (kHz)	References
Multiferroic	$Sr_3Co_2Fe_{24}O_{41}$	co-fired	33×10^{-3}	42×10^{-3}	1	Wu et al. (2012)
	$BiFeO_3$	film	3	3.5	–	Wang et al. (2003)
0-3 composite	CFO-$Sr_{1.9}Ca_{0.1}NaNb_5O_{15}$	co-fired	5.7×10^{-3}	6.7×10^{-3}	5	Liu et al. (2008)
	NFO-PZT	co-fired	2.6	6.12	430	Zeng et al. (2004)
2-2 composite	CFO-PZT	film	0.4	0.55	1	McDannald et al. (2013)
	Fe-PZT-Fe	epoxy	4.5×10^{-3}	66.7×10^{-3}	1	Laletin et al. (2005)
	Co-PZT-Co	epoxy	0	42.5×10^{-3}	1	Laletin et al. (2005)
	Ni-PZT	epoxy	63.3×10^{-3}	87.3×10^{-3}	1	Zhou et al. (2012)
	Ni-MFC	epoxy	1.25	1.38	1	Zhou et al. (2012)
	$SmFe_2$-PZT	epoxy	39.5	48	119.7	Zhang et al. (2013)
	LSMO-PZT	co-fire	16×10^{-3}	32×10^{-3}	0.1	Srinivasan et al. (2002)
	NCZF-PMNPT-NCZF	co-fire	1.21	1.35	1	Yan, Zhou, and Priya (2013)
	$Fe_{0.7}Ga_{0.3}$-PZT	film	26.9	33.6	3.83	Onuta et al. (2011)
	FeCoSiB-AlN	film	91.4	101	1	Tong et al. (2013)
Quasi 1–3 composite	FeNi-PZT	epoxy	1.65	2.2	0.1	Chen et al. (2011)
	FeNi-PZT	epoxy	0.315	0.536	0.025	Gillette et al. (2014)
	FeGa-PZT	epoxy	0.112	0.689	0.025	Gillette et al. (2014)
	FeCoV-PZT	epoxy	0.084	0.212	0.025	Gillette et al. (2014)

multilayer composites revealed a different behavior of the ME coefficient on the stress-biased coupling, in which the self-biased response is pronounced with an enhanced ME coupling under a suitable mechanically preload (Dong et al. 2007) The basic features of the relation between the ME coupling and the mechanical stress can be understood as follows: under a suitable mechanical preload, the grain oriented Terfenol-D exhibits a higher magnetostriction due to a "Jump effect"(Clark 1980), leading to a higher effective piezomagnetic coefficient with hysteresis behavior. This reminds us that the self-biased coupling may also arise from the built-in stress between the piezoelectric and magnetostrictive phases through direct (co-firing, thin film deposition) or indirect bonding (epoxy). Among them, residual stress induced in the materials interface are widely observed in co-fired ceramic composites and thin film heterostructures since the direct bonding between different phases are realized at elevated temperature. A brief overview of these developments is given in the next sections.

Co-Fired Ceramic Composites

Since the ME effect originates through elastic coupling at the interface, it is important to consider the influence of synthesis method toward optimizing the interface bonding. The direct bonding that completely excludes the utilization of epoxy layer with low mechanical strength is favorable. In bulk system, co-firing techniques at high temperature not only enhances the mechanical coupling between the piezoelectric and magnetostrictive constituent (Srinivasan et al. 2001; Yan, Zhou, and Priya 2013; Yan, Zhou, and Priya 2014a), but also dramatically reduces the cost due to utilization of conventional processes used for multilayer capacitors (Israel, Mathur, and Scott 2008). Different materials combinations, mole ratios, phase connectivity, physical geometries, compacting procedures, sintering procedures and microstructures were therefore examined (Fiebig 2005; Priya et al. 2007; Nan et al. 2008; Zhai et al. 2008; Vaz et al. 2010; Ma et al. 2011). However, in spite of all these efforts, the development of co-fired ME composite has been pretty slow. Several obstacles for the development of co-fired ME composites were identified:

(1) Co-sintering different phases together is extremely challenging through high temperature thermal cycling because of the large difference in shrinkage rates and thermal expansion mismatch among different phases.
(2) The opposing behavior between high concentration of magnetostrictive particles and low resistivity of sintered particulate ME composites, results in either an ineffective magnetic induced interaction or bad poling condition.
(3) Atomic interfacial inter-diffusion and/or chemical reactions between the constituents and/or their starting materials during the high temperature co-sintering process.
(4) Residual strain or stress originated due to mechanical defects, interface diffusion, lattice mismatch and thermal expansion mismatch between different constituents, leading to either a limited mechanical coupling or unexpected magnetic/piezoelectric property anisotropy.

Figure 20 summarizes the development of co-fired ME composites. Particulate ME composites have been widely investigated by using the simple, scalable and cost-effective conventional solid sintering process. Control variables including starting materials, dispersion concentration, particle size, sintering temperature/time/procedures, grain size, annealing/aging process, and other variables were investigated (Priya et al. 2007; Vaz et al. 2010; Ma et al. 2011). The magnetoelectric coupling coefficients of these composites were larger than those of single phase multiferroics at room temperature, having the magnitude of 0.1 V cm^{-1} Oe^{-1} (Ryu et al. 2001) However, the reciprocal behavior of high concentration of ferrite particles for good magnetic induced coupling and low resistivity for poor poling condition hindered their further improvement. An alternative approach was adapted by using the core-shell structure with ferrite core and piezoelectric shell (Islam et al. 2008), in which an effective

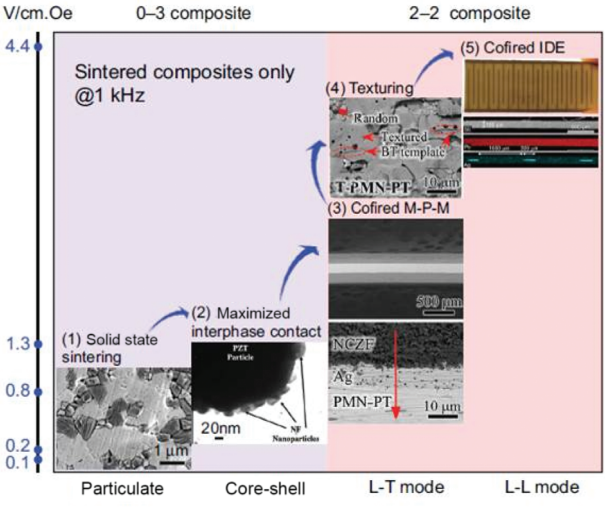

Figure 20: Development of co-fired magnetoelectric composites. It shows ME voltage coefficient (α_{ME}) for different types of sintered ME composites (Yan, Zhou, and Priya 2014b).

enhancement (−0.2 V cm^{-1} Oe^{-1}) was realized due to increasing contact interface and indirect contact of ferrite particles during sintering. Further, 2–2 type layered co-fired laminates were developed. These laminate composites exhibited significantly higher ME coefficient (−0.8 V cm^{-1} Oe^{-1}) than that of multiferroics and particulate composites as a result of elimination of leakage problem (Yan, Zhou, and Priya 2013). By optimizing the piezoelectric materials via texturing and poling condition, ME signal loss from ferrite layer was dramatically decreased. These results lead to a further improvement of α_{ME} to 1.3 V cm^{-1} Oe^{-1} (Yan, Zhou, and Priya 2013). With the utilization of longitudinal poling via co-firing the interdigital electrodes (IDE) inside the piezoelectric ceramic layer, a giant magnetoelectric effect in longitudinal-longitudinal (L-L) mode was found to be 4.4 V cm^{-1} Oe^{-1}.

The co-fired bulk ME ceramic composites exhibited promising larger ME effect. However, the self-biased ME effect was observed in high-temperature co-fired ceramic composites. This effect has been rarely reported and explained, mainly due to their inherent preparation challenges and acquired built-in stress during co-firing process. Islam et al. found that 0.8PZT-0.2NZF particulate composite exhibited a high response of 0.45 V cm^{-1} Oe^{-1} with a non-zero α_{ME} of 0.09 V cm^{-1} Oe^{-1} at the low frequency of 1 kHz. The magnetic particles were well dispersed in the matrix of piezoelectric materials and their effective contact interface can be further controlled by the concentration of induced magnetic particles, leading to a tunable feature. (Islam et al. 2006) With the use of nano-grained $NiFe_{1.98}O_4$ (NFO) in the matrix of $BaTiO_3$ (BTO) powders, Sreenivasulu et al. found a large maximum α_{ME} of 0.252 V cm^{-1} Oe^{-1} in BTO-NFO particulate composite, which was about five times larger than their respective microcomposites (Sreenivasulu et al. 2009). More interestingly, different from conventional microcomposites, all the corresponding nanocomposites illustrate an obvious hysteretic α_{ME} vs H behavior, demonstrating a maximum α_{H0} of 0.15 V cm^{-1} Oe^{-1}. The manipulation of ME and self-biased ME response can be attributed to the difference in lattice strain, interface contacts and their effect on the corresponding magnetic properties.

Alternatively, Srinivasan et al. observed a giant enhancement (0.46 V cm^{-1} Oe^{-1}) and a noticeable non-zero α_{ME} (0.1 V cm^{-1} Oe^{-1}) at zero-bias field in a co-fired PZT/NFO laminates, as shown in Figure 21(a) (Srinivasan et al. 2001). For the first time, they considered the influence of growth-induced stress and its effect on magnetic anisotropy and the interfacial coupling. As expected, differential thermal expansion (2 ppm for PZT vs 10 ppm for most ferrites) and thermal conductivity could result in built-in strain between contacting constituents during the high temperature process. This strain may further couple with the magnetostrictive strain resulting a magnetic anisotropy and/or enhanced ME coupling. Continuing this research, they observed a giant hysteresis and remanence in α_{ME} vs H in the co-fired LSMO/PZT bilayer system (Figure 21(b)) (Srinivasan et al. 2002). With increasing the numbers of co-fired layers, a degradation of α_{ME} was observed and attributed to the element diffusion through enlarged interface area and growth-

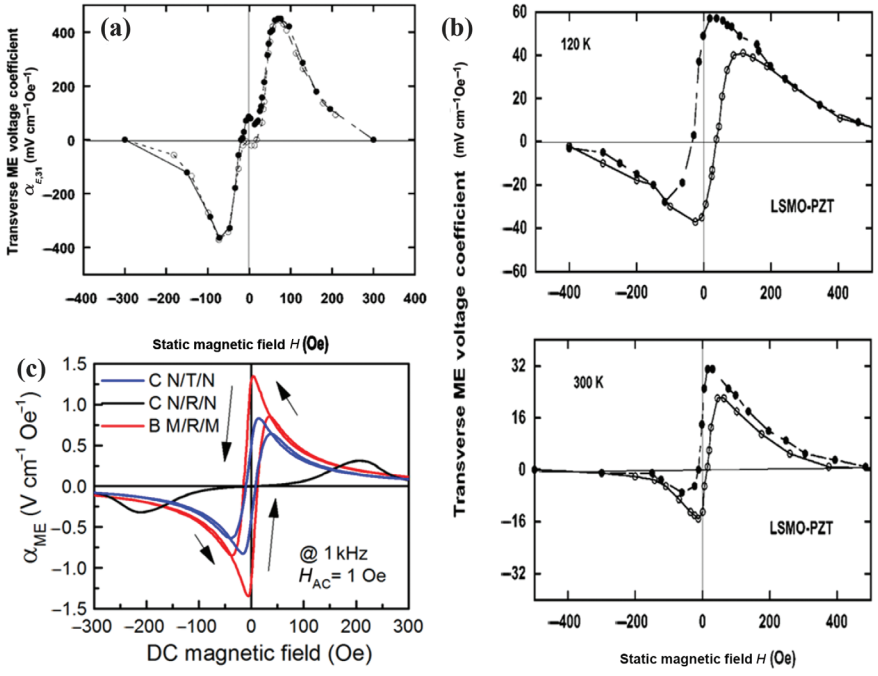

Figure 21: ME voltage coefficient of various co-fired ME composites (a) PZT-NFO bilayer structure (Srinivasan et al. 2001), (b) LSMO-PZT bilayer structure (Srinivasan et al. 2002), (c) NCZF/T-PMN-PT/NCZF (C-N/T/N), NCZF/R-PMN-PT/NCZF (C-N/R/N), and epoxy bonded Metglas/R-PMN-PT/Metglas (B-M/R/M) trilayer structures. R and T stands for random and textured ceramics (Yan, Zhou, and Priya 2013).

induced strain at the interface. Similar behavior was also observed in other co-fired 2–2 laminated systems such as BTO-NCZF and PZT-NCZF multilayers (Islam and Priya 2006; Yan, Zhou, and Priya 2013). Interface homogeneities, microstructure roughness, intrinsic lattice strain, inter-diffusion and chemical reactions between constituents has been hindering their improvement toward higher coupling factor. It was not until recently Yan et al. cofired a NCZF-PMNPT-NCZF trilayer composite utilizing Ag electrode as buffer layer between different constituents (Yan, Zhou, and Priya 2013) With the effective Ag barrier, chemical reaction and/or element migration of the constituents is avoided by macroscopic separation of the magnetostrictive and piezoelectric phases. They obtained a giant ME voltage coefficient of 0.83 V cm^{-1} Oe^{-1} followed with a self-biased $a_{H0} > 0.5$ V cm^{-1} Oe^{-1} (Figure 21(c)). By using the textured piezoelectric layer to form the engineered domain state, they were able to further enhanced the self-biased ME voltage coefficient up to 1.21 V cm^{-1} Oe^{-1}, which exceeds the highest value gained from any co-fired ME composites by a factor of 10!

Although it has been discussed that the magnetostriction hysteresis of the ferromagnetic layer in low field range plays an important role toward self-biased ME effect (Yan, Zhou, and Priya 2013), we can speculate one more possible reason for a unique and favorable interface bonding in which the growth induced built-in stress cannot be neglected. For co-firing laminates without barrier layer, except for thermal expansion and conductivity mismatch between constituents, the rough interface contact and inter-diffusion may also bring extra stress during co-sintering process. For co-firing laminates using Ag as an effective barrier layer, the silver itself has even much larger thermal expansion coefficient (–18 ppm) than that of piezoelectric (– 2 ppm) and ferrites (–10 ppm) phase, and its thermal conductivity is much higher than that of piezoelectric and ferrite. Difference in thermal expansion and thermal conductivity could result in built-in interface strain which is comparable to magnetostrictive strain. However, none of these hypotheses have been demonstrated experimentally. As an extension to Yan's work (Yan, Zhou, and Priya 2013), we co-fired the NCZF-PMNPT-NCZF composite with and without the Ag electrode. As shown in Figure 22, the hysteresis in the ME response was dramatically reduced without Ag inner electrode. This result clearly demonstrated the relationship between the hysteretic behavior and internal stress arising due to the thermal mismatch between metallic and ceramic layers.

In summary, the development of the co-fired self-biased magnetoelectric composites can be categorized into three

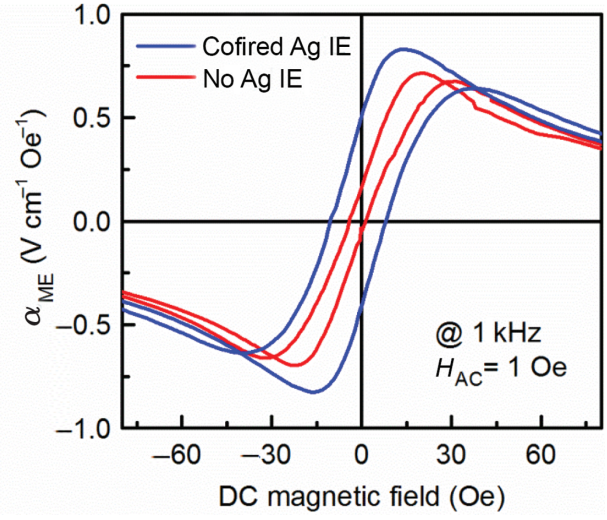

Figure 22: Magnetoelectric voltage coefficient as a function of DC magnetic field for co-fired ME laminates with and without Ag inner electrode (IE).

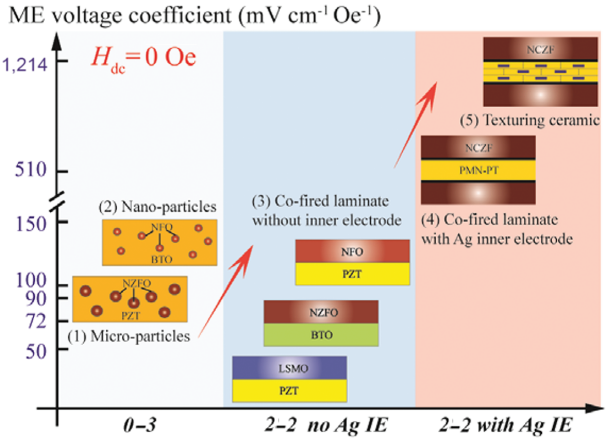

Figure 23: Development of co-fired self-biased ME composites.

groups, as shown in Figure 23. The self-biased ME response of the co-fired composites is determined by two major aspects: (1) low field magnetostrictive hysteresis; (2) built-in stress arising from thermal mismatch, lattice mismatch, chemical reaction, inter-diffusion, and so on. This phenomenon can be further controlled by several impact factors including: (1) selected constituents' composition, (2) magnetic particle size and distribution, (3) sintering process, (4) buffer layer between constituents and so on.

Thin Film Residual Stress

The thin film deposition is another widely accepted direct bonding method for ME composites with unique

advantages over co-fired bulk composite. Thin film deposited heterostructures, with less possibility of inter-diffusion during low temperature (600°C–800°C) growth process, provide strong bonding at coherent interface. This method further provides opportunity for manipulating composition and connectivity of thin film composites at nanoscale, which is advantageous for their implementation in on-chip scalable MEMS functional devices. Nanostructured thin film ME composites has been investigated in various phase connectivity (0–3 type particular films, 2–2 type layered heterostructures, 1–3 type vertical heterostructures) using either physical vapor deposition (PVD) methods (pulsed laser deposition, sputtering, molecular beam epitaxial) or chemical vapor deposition (CVD) methods (sol-gel spin coating, metal-organic chemical vapor deposition) (Ma et al. 2011; Ramesh and Spaldin 2007; Wang et al. 2010; Martin et al. 2008, Jahns et al. 2013). By optimizing the materials selection and deposition parameters, ME composite thin films with coherent interface were developed by precise control of the lattice mismatching and thickness of constituent components.

The coupling interaction, between piezoelectric and magnetostrictive phases, in the nanostructured films has been attributed to the elastic coupling as in bulk composites. However, in thin films, the mechanical constrain arising from the substrate (Nan et al. 2005) and built-in stress (Ibach 1997), could significantly affect the ME interactions. Furthermore, prior studies of stress effect indicated that the magnetoelastic coupling of strained ferromagnetic films deviated sharply from the respective bulk behavior due to strain (Sander et al. 2003). These factors result in remarkable variations of spontaneous polarization and magnetization in the ME films, thereby a dramatically different magnetoelectric behavior than that of bulk system (Table 4).

The non-zero α_{ME} at zero bias has been commonly found in thin film ME nanostructures. In some cases, at zero-bias the film (CFO-PZT particulate) exhibited an initial high α_{ME} value of 0.22 V cm^{-1} Oe^{-1} at H_{ac} = 10 Oe at1 kHz (Figure 24(a)), which was much larger than that of biased condition, indicating an easy-magnetization characteristic of the film (Wan et al. 2005). However, considering the magnetically "hard" bulk CFO material with large coercivity beyond –2 kOe, the ease of domain rotation was attributed to the residual stress arising along the film-on-substrate interface. Since the residual stress from the film-on-substrate structure has been considered sensitive to the thickness, subsequent study performed on the CFO-PZT system with higher thickness – 1 μm, as shown in Figure 24(b) (Wan et al. 2006). The variation in the magnitude of stress not only resulted in the sharp reduction of the self-biased α_{ME} to 0.005 V cm^{-1} Oe^{-1}, but also shifted the optimum H_{bias} to a higher value of 4.5 kOe. Moreover, similar to the bulk samples, the magnetic particle size/concentration in the ferroelectric matrix was found to significantly affect the self-biased ME response of the composites films (Zeng et al. 2004; McDannald et al. 2013). Figure 24(c) illustrates a series of ME voltage coefficient as a function of magnetostrictive phase (CFO) concentration for 0–3 type PZT-CFO nanocomposite films (McDannald et al. 2013). This tunable self-biased behavior was explained by assuming a finite remnant

Table 4: List of self-biased ME thin films with various phase connectivity.

Class	Constitution	Thickness (μm)	α_{H0}	α_{max}	H_{bias} (Oe)	f_{ac} (kHz)	References
			(V cm^{-1} Oe^{-1})				
Multiferroic	$0.1NdFeO_3$-$0.9PbTiO_3$	0.2	0.4×10^{-3}	0.9×10^{-3}	500	1	Zhao et al. (2013)
	BFO	0.2	3.0	3.5	500	–	Wang et al. (2003)
0-3	CFO-PZT	0.4	0.22	0.22	0	1	Wan et al. (2005)
	CFO-PZT	0.4	0.31	0.31	0	50	Wan et al. (2005)
	CFO-PZT	1	0.005	0.03	4.5×10^3	10	Wan et al. (2006)
	NFO-PZT	–	0.005	0.016	3×10^3	0.19	Ryu et al. (2006)
	CFO-BNT	0.22	0.005	0.035	6.5×10^3	20	Zhong et al. (2007)
	Co-BTO	0.5	0.17	0.17	0	50	Park et al. (2008)
	CFO-PZT	0.23	0.4	0.55	453	1	McDannald et al. (2013)
2-2	$TbCo_2$-FeCo-AlN	5.5	2.0	5.0	100	2	Tiercelin et al. (2008)
	CFO-PZT	1	0.20	0.23	460	–	Shi et al. (2011)
	CFO-PZT	0.34	0.075	0.29	900	0.6	Tahmasebi et al. (2011)
	BTO-BFO	0.5	20.67	20.75	2.5×10^3	1	Michael et al. (2014)
	FeCoSiB-AlN	–	72	79.64	11	1	Tong et al. (2014)
	FeCoSiB-Terfenol-AlN	–	76.3	78.1	11	1	Tong et al. (2014)

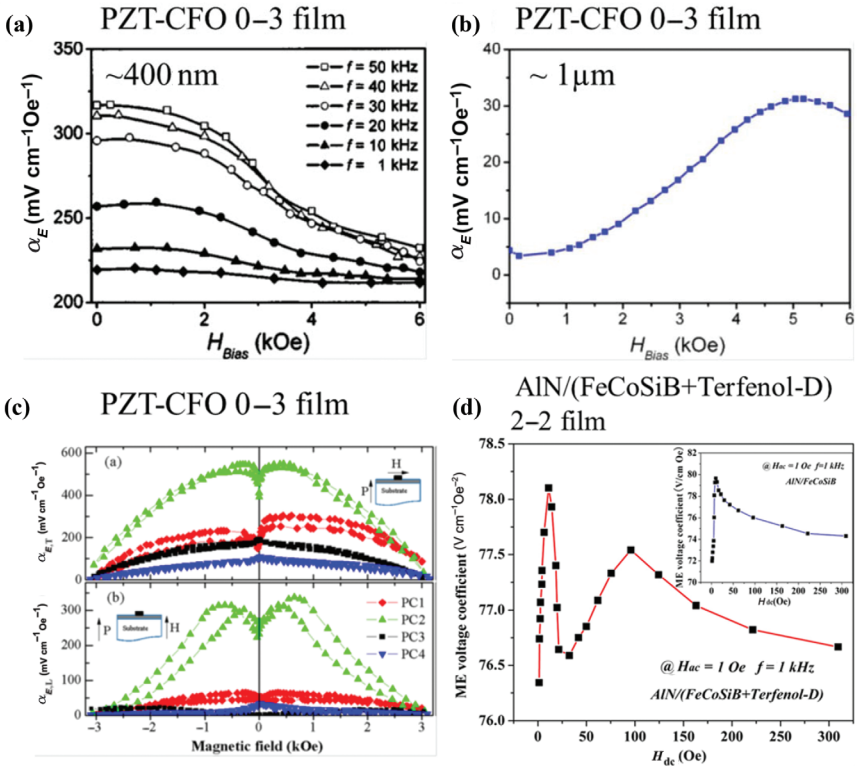

Figure 24: ME voltage coefficient as a function of DC magnetic field for (a) PZT-CFO 0–3 type nanocomposite films with thickness of –400 nm (Wan et al. 2005), (b) PZT-CFO 0–3 type nanocomposite films with thickness of –1 μm (Wan et al. 2006), (c) PZT-CFO 0–3 type nanocomposites films with various magnetic concentration. PC1, PC2, PC3 and PC4 are stands for films with, 0.065%, 0.10%, 0.14% and 0.46% molar concentration of CFO, respectively (McDannald et al. 2013); (d) 2–2 type AlN/[FeCoSiB + Terfenol-D] composite films, inset is the ME coefficient of AlN/FeCoSiB composite film (Tiercelin et al. 2008; Tong et al. 2014).

magnetization of the magnetic nanoparticle upon clustering (McDannald et al. 2013; Tahmasebi et al. 2011). Alternatively, 2–2 type layered heterostructures (Figure 24(d)) exhibited significant larger self-biased α_{ME} than that of 0–3 type particulate film and single phase multiferroic films (Tiercelin et al. 2008; Tong et al. 2014).

Non-linear ME Effect

So far, we discussed studies on self-biased ME effect primarily devoted to the investigation of the ferromagnetic phase or the interfacial coupling, where either the selected composition and/or functional graded structure was needed or a giant built-in stress along the constituents interface was required. Interestingly, it was found that a non-zero peak ME voltage coefficient could be obtained at f_r and $f_r/2$ without applied bias (H_{dc} = 0 Oe) in a conventional epoxy bonded Terfenol-D/PZT laminates (Wan et al. 2003). Once a nonzero magnetic bias was applied, the peak at $f_r/2$ gradually suppressed, and the consequent ME effect became weaker. While the origin of the peak behavior at f_r could be understood to be originating from the fundamental longitudinal vibration of the sample, the details of the $f_r/2$ peak behavior were not well understood.

The conventional ME characterization involves the measurement of ME voltage output across the sample by locating the sample under a DC magnetic bias ($H_{dc} = 5$ Oe– 5 kOe) with a small oscillation field ($H_{ac} = 0.01$–1 Oe). Generally, the measured ME voltage is linearly proportional to the applied AC magnetic field, following the relationship $\alpha_{ME} = \delta E_{ac}/\delta H_{ac}$. The calculated coupling coefficient was the field conversion ratio between applied AC magnetic field and induced AC electric field, which was directly related to the effectiveness of elastic coupling between two phases and the magnetostriction/piezomagnetic coefficient of ferromagnetic phase. It was however known that both the magnetostriction of ferromagnetic and the polarization of piezoelectric material depend nonlinearly on magnetic field or electric field, respectively. Therefore, considering

the constituent's material nonlinearity, a rich variety of nonlinear ME phenomena were observed, including frequency multiplication and generation of harmonics. These phenomena will be discussed in detail in the following sections.

Nonlinear Magnetoelectric Effect Characterization

Demonstration of the nonlinear magnetoelectric effect controlled by the amplitude and frequency of applied AC magnetic field was reported in a ceramic NZFO/PZT laminated structure, where frequency doubling and generation of harmonics were explored at very low frequencies (1 mHz to 1 Hz) and high field amplitudes (200 Oe–1000 Oe) (Kamentsev, Fetisov, and Srinivasana 2006). Inspired by this work, Ma et al proposed a frequency multiplier based on an epoxy bonded FeBSiC/PZT laminate and demonstrated its capability of doubling frequency in a broad range (20 Hz to 2 kHz) without additional adjustment (Ma et al. 2011b). Thereafter, Zhang et al. expanded the study of the frequency multiplying behavior using fast Fourier transform (FFT) frequency spectral patterns of the ME voltage in a Metglas/PZT unimorph structure (Zhang et al. 2012). Both even and odd harmonic signals were found with applied H_{dc}, whereas only even harmonic signals were observed in the absence of H_{dc}. This behavior was attributed to the combination of a mechanical resonance phenomenon and the nonlinear character of the magnetostriction. Furthermore, Wang et al. systematically investigated the ME voltage (V_{ME}) for various amplitudes of H_{ac} up to 9 Oe over a frequency range of 0.1–40 kHz with zero-bias DC magnetic field (Wang et al. 2013). The anomalous responses of V_{ME} were suggested to be associated with the eddy-current loss in the magnetostrictive layers. Theoretical calculation conducted for the nonlinear magnetoelectric coupling shows its potential for applications such as tunable magnetic field sensors and frequency multipliers (Fetisov et al. 2013).

Nonlinear behavior of the magnetoelectric coupling observed under the varying amplitude or frequency of applied magnetic field arises mainly due to the influence of the nonlinearities in magnetic and magnetostrictive phase. Four aspects of this nonlinear ME effects has been rationalized as:

- Frequency doubling: The frequency doubling was characterized as an output V_{ME} with a frequency of $2f$ was generated from the sample by applying a bipolar H_{ac} with frequency f in the absence of H_{dc} (0 Oe), as shown in Figure 25 (Ma et al. 2011; Kamentsev, Fetisov, and Srinivasana 2006). This effect was found to rely on the fact that the magnetostriction was independent of the sign of applied magnetic field, but the amplitude (Wang et al. 2013). Therefore, the generation of an unipolar strain under bipolar magnetic field gave rise to the double frequency $2f$ of the generated signal V_{ME}. Additionally, this double frequency behavior could be used under a broad frequency and amplitude range, and could be further switched by a low DC magnetic field (Kamentsev, Fetisov, and Srinivasana 2006; Ma et al. 2011; Zhang et al. 2012).
- High-order harmonics: By investigating the FFT frequency spectral pattern of V_{ME}, it was found that higher-order harmonic signals were present (Kamentsev, Fetisov, and Srinivasana 2006). The number of harmonics seen in the spectra were found to decrease with an increase in the applied f_{ac} (Zhang et al. 2012), whereas the relative amplitude of the harmonic peaks increased at high magnitude of H_{ac} (Wang et al. 2013). More interestingly, both odd and even harmonics were found with applied H_{dc}, while only even harmonics for zero-biased condition were observed (Zhang et al. 2012). On tuning the input H_{ac} with frequency of fr/n, the nonlinear ME coupling was dramatically enhanced (Fetisov et al. 2013). Thus, this phenomenon offers an effective way for achieving a high ME coefficient with lower input frequency, which breaks the geometrical limitation of sample resonance frequency.
- DC Magnetic field effect: Depending on the amplitude of applied H_{ac}, the H_{dc} was found to play an important role toward switching the frequency

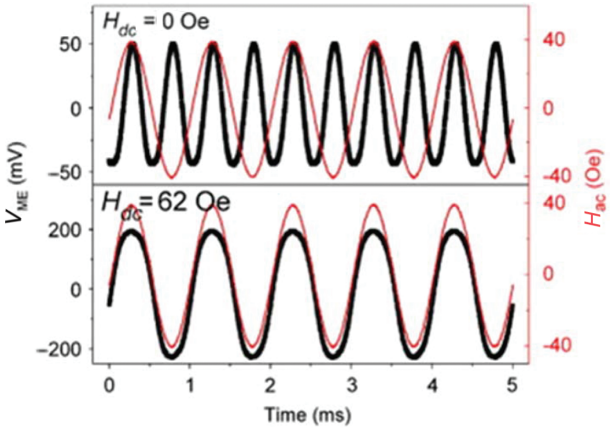

Figure 25: Waveform of ME voltage output without (a) and with (b) DC magnetic field. The thin red lines correspond to the input signal while the thick dark dot curves correspond to the output signals (Ma et al. 2011).

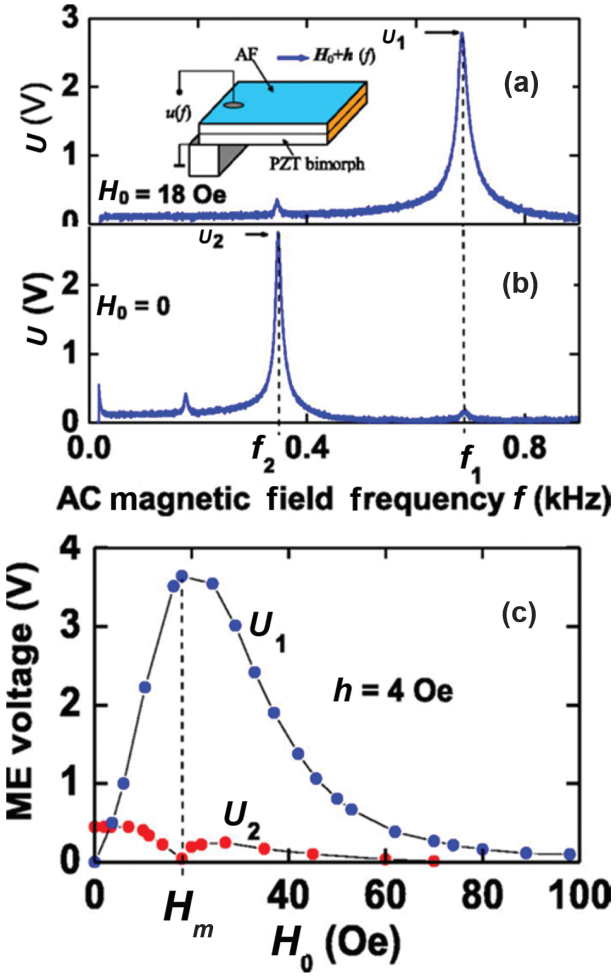

Figure 26: Dependence of the ME voltage u generated by the FeBSiC-PZT bimorph structure as a function of the frequency f of ac magnetic field h. (a) u_1 is the voltage under linear ME excitation regime with the DC bias $H_0 = 18$ Oe, (b) u_2 is the voltage under nonlinear excitation regime with the bias field $H_0 = 0$ Oe, (c) the linear ME voltage u_1 and nonlinear ME voltage u_2 as a function of applied DC bias field H_0 (Zhang et al. 2012).

multiplier behavior of nonlinear ME coupling, as shown in Figure 26(a) and (b) (Ma et al. 2011; Zhang et al. 2012). When $H_{dc} = 0$ Oe, the ME response V_{ME} was found to double the frequency of applied H_{ac} due to magnetostriction nonlinearity as discussed before. However, on applying a H_{dc} with amplitude larger than H_{ac}, this double frequency behavior was found to disappear. This DC field effect was attributed to the extrinsic relations of the applied magnetic field and V_{ME} (Ma et al. 2011):

$$V_{ME} \propto H^2 = H_{dc}H_{ac}\sin(2\pi ft) + H_{ac}{}^2\cos(4\pi ft) \quad [6]$$

It is obvious that the $\sin(2\pi ft)$ term becomes dominant when $H_{dc} > H_{ac}$, leading to a trace of the waveform of the magnetic excitation signal. Additionally, different from the linear V_{ME} response, the nonlinear V_{ME} (V_{NLME}) at $2f$ can be expressed as (Fetisov et al. 2013):

$$V_{NLME} \propto \mathrm{A}pH_{ac}{}^2 \quad [7]$$

where A is a constant independent of applied magnetic field and depends only on the compliance of the constituents in the composite, the $p = \partial^2\lambda/\partial H^2$ is the second derivative of magnetostriction over the field. Hence, the nonlinear ME coefficient $[a_{NLME} = V_{NLME}/(t_p H_{ac}{}^2)]$ was found to follow p, (Figure 26(c)) and reached a maximum near zero bias field. It further vanished at H_{bias} illustrating another peak value and then gradually reduced to zero at higher field.

– AC Magnetic field effect: Both amplitude and frequency of H_{ac} was found to play an important role toward nonlinear ME interactions through a combination of various phenomena including eddy-current loss and nonlinearity of the magnetostrictive phase. In the absence of H_{dc}, the magnetostriction can be expressed as (Wang et al. 2013):

$$\lambda(H_{ac}) = \mathrm{A}_0 + \mathrm{A}_1\cos(\omega t) + \mathrm{A}_2\cos(2\omega t) + \mathrm{A}_3\cos(3\omega t) + \mathrm{A}_4\cos(4\omega t) + \mathrm{A}_5\cos(5\omega t) \quad [8]$$

where $\mathrm{A}_0 = a_0 + \frac{1}{2}a_2H_{ac}{}^2 + \frac{3}{8}a_4H_{ac}{}^2$, $\mathrm{A}_1 = a_1H_{ac} + \frac{3}{4}a_3H_{ac}{}^3 + \frac{5}{8}a_5H_{ac}{}^5$, $\mathrm{A}_2 = \frac{1}{2}a_2H_{ac}{}^2 + \frac{1}{2}a_4H_{ac}{}^4$, $\mathrm{A}_3 = \frac{1}{4}a_3H_{ac}{}^3 + \frac{5}{16}a_5H_{ac}{}^5$, and $\mathrm{A}_5 = \frac{5}{16}a_5H_{ac}{}^5$ and $\mathrm{A}_5 = \frac{5}{16}a_5H_{ac}{}^5$, where a_i are the ith Fourier coefficient. Considering equation 5, the variation of H_{ac} gives rise to the change in the relative amplitude of the harmonic signals as discussed before. The eddy-current induced losses in soft magnetic materials can be given as (Kendall and Piercy 1993; Wang et al. 2013):

$$W_{ec} = \frac{\pi s(\mu_0\mu^{zero}H_{pk})^2 f}{4\rho} \quad [9]$$

where s and ρ are the cross-sectional area and resistivity of the magnetic material, μ^{zero} is the dynamic permeability extrapolated to zero frequency, and H_{pk} is the peak value of the applied bipolar magnetic field. The eddy-current induced energy loss becomes larger, leading to a reduced dynamic magnetostriction and therefore a decrease in V_{ME} with increasing f, as shown in Figure 27 (Wang et al. 2013).

According to the above discussion, it can be concluded that the self-biased response can be also realized by relying on the magnetostrictive nonlinearity. Therefore, in the absence of H_{dc}, a giant nonlinear ME voltage coupling coefficient could be obtained in ME laminates, which could be further controlled using the amplitude and frequency of applied AC magnetic field.

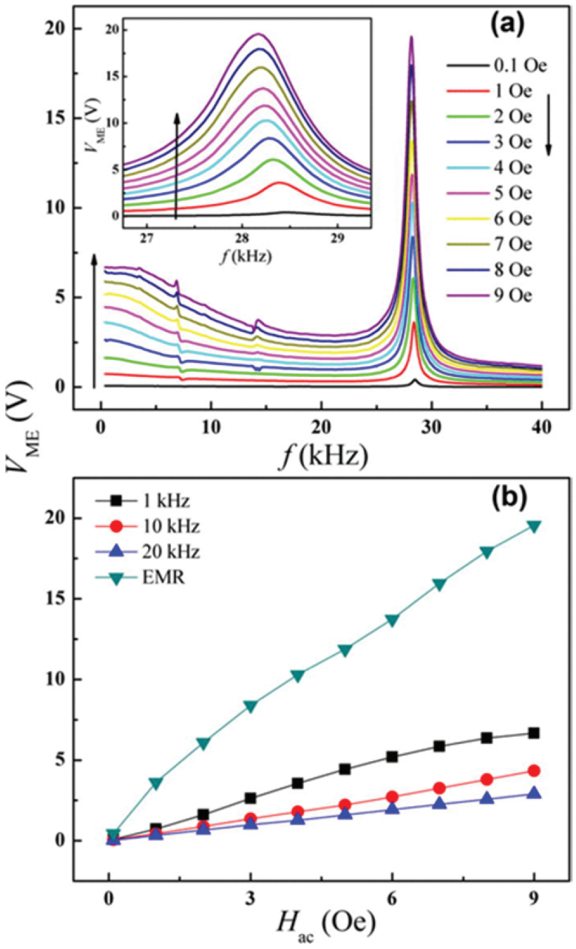

Figure 27: (a) ME voltage variation as a function of frequency under various amplitudes of H_{ac}, inset shows an enlarged view near the resonance frequency, (b) ME voltage output as a function of H_{ac} at resonance frequency of 1, 10, 20kHz and the EMR condition (Wang et al. 2013).

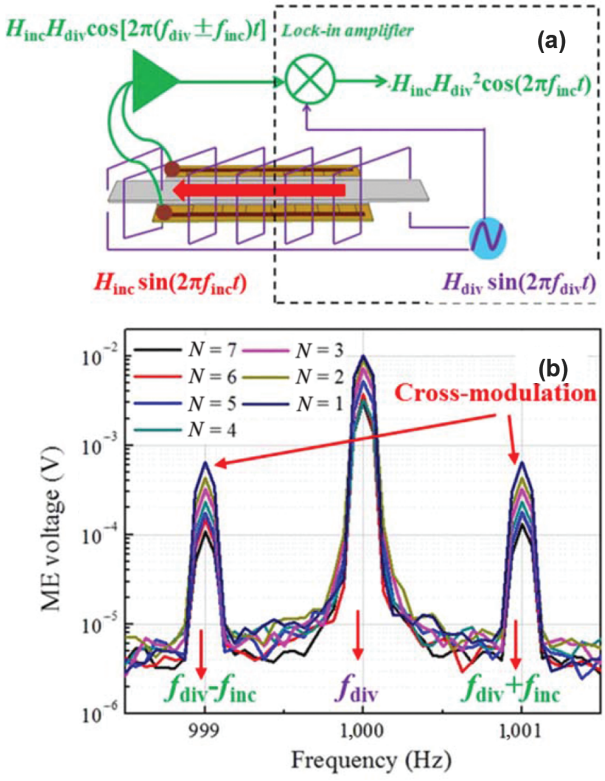

Figure 28: (a) Schematic illustration of the cross-modulation based ME composite, (b) measured modulation spectrum taken at $f_{div} = 1$ kHz, $f_{inc} = 1$ Hz from PZT-Metglas laminate with different numbers N of Metglas layers (Shen et al. 2011).

What's more important, the unique frequency multiplying behavior provides great potential of using such nonlinear ME effect towards applications including high sensitivity sensors and frequency multiplier devices.

Cross-Modulation Techniques

Furthermore, by utilizing the nonlinear magnetoelectric coupling, cross-modulation (or frequency conversion) technique was proposed (Zhuang et al. 2011; Shen et al. 2011). In particular, in order to detect an incident AC field $H_{inc}\sin(2\pi f_{inc}t)$ with low frequency f_{inc} (0.1 Hz–1 Hz), a drive field $H_{div}\sin(2\pi f_{div}t)$ with higher frequency f_{div} (1 kHz or higher) was applied, as shown in the schematic (Figure 28(a)). In the presence of two AC magnetic field, the nonlinear ME interaction resulted in generation of the cross-modulated voltage with frequency of $(f_{div} \pm f_{inc})$, as shown in Figure 28(b). Therefore, the low frequency signals were modulated to a higher frequency in which lower noise floor were present. The effective magnetic field and generated V_{ME} could be expressed as (Zhuang et al. 2011):

$$H(t) = H_{dc} + H_{inc}\sin(2\pi f_{inc}t) + H_{div}\sin(2\pi f_{div}t), \quad [10]$$

$$V_{ME}(t) = a_0 + a_1H(t) + a_2H^2(t) + a_3H^3(t) + \ldots, \quad [11]$$

without applying DC bias, the induced nonlinear ME output could be measured by considering the 2nd order cross-term, given as (Shen et al. 2013):

$$V_{NLME} \propto a_2H_{inc}H_{div}\cos[2\pi(f_{div} \pm f_{inc})t], \quad [12]$$

where the 2nd order coefficient could be expressed as the nonlinear ME coefficient (a_{NLME}) (Shen et al. 2011), (Shen et al. 2013):

$$a_{NLME} = \frac{dV^2}{d^2H} = \frac{E}{H_{inc} \times H_{div}}\left[\mathrm{Vcm^{-1}Oe^{-2}}\right] \quad [13]$$

Shen et al. investigated the cross-modulation techniques with Metglas/piezoelectric laminates and found that an optimum α_{NLME} could be obtained near $H_{dc} = 0$ Oe for Metglas/PMN-PT (Shen et al. 2011). The lack of requirement for the DC bias makes the modulation approach promising. The nonlinear ME coefficient was found to be highly dependent on the magnetic flux concentration. A giant $\alpha_{NLME} = 7.5$ V cm^{-1} Oe^{-2} at $H_{dc} = 0$ Oe was obtained by optimizing the Metglas configuration (Shen et al. 2013). The behavior of α_{NLME} follows well with the second derivative of the magnetostriction as a function of DC bias, as shown in Figure 29. The results demonstrated high sensitivity of 200 pT at 10 mHz and 20 pT at 1 Hz by effectively reducing the vibration noise through the frequency modulation (Liu et al. 2013). Theoretical investigation regarding the nonlinear ME interaction and its applications in frequency modulation have been conducted and compared with the experimental data (Burdin et al. 2014). Different from linear ME interaction, the nonlinear magnetostriction at the cross-modulation frequency $f_{div} \pm f_{inc}$ was given as $\lambda = \frac{3\lambda_s \chi^2}{2M_s^2} H_{div} H_{inc}$, where thinner magnetostrictive materials with higher magnitude of χ were desired (Gillette et al. 2011; Li et al. 2013). Hence, the magnitude of α_{NLME} was further improved to 100 V cm^{-1} Oe^{-2} at $H_{dc} = 0$ Oe at f_r in Metglas/PMN-PT based laminates with thin Metglas (Shen et al. 2014).

In summary, the self-biased magnetoelectric response can also be observed in conventional laminated composites due to the nonlinear magnetoelectric interaction effect. The ME nonlinearity of the composites could be determined by several major factors including: (1) the absence of DC magnetic bias $H_{dc} = 0$ Oe; (2) proportionality to the second derivative of the magnetostriction $p = \partial^2\lambda/\partial H^2$; (3) sensitivity to the amplitude and frequency of the applied AC magnetic field; (4) dependence on the magnetic susceptibility and flux density of the magnetic layer in the composites.

Identification of Self-Biased Magnetoelectric Response

The ME response is related to the effectiveness of the elastic coupling between the consecutive phases. Generally, considering the intrinsic factors of the composite structure, the magnetoelectric coupling coefficient can be written as (Yan, Zhou, and Priya 2013):

$$\alpha_{DME} = \frac{\partial E}{\partial H} = \frac{\partial S}{\partial H} \times \left| \frac{\partial T}{\partial S} \times \frac{\partial D}{\partial T} \times \frac{\partial E}{\partial D} \right| = q \times \left| \frac{d}{\varepsilon \times s} \right| \quad [14]$$

where E is the output electric field, H is the applied magnetic field, S is the mechanical strain, T is the mechanical stress, D is the electric displacement, d is the piezoelectric constant, ε is the dielectric constant, s is the elastic compliance of piezoelectric layer, and $q = \frac{d\lambda}{dH}$ is piezomagnetic coefficient of magnetostrictive layer. Since the parameters of piezoelectric materials are independent of the applied magnetic field, the ME coefficient under applied magnetic field is directly related to the nature of ferromagnetic phase $\alpha_{DME} \propto q = \frac{d\lambda}{dH}$ and the

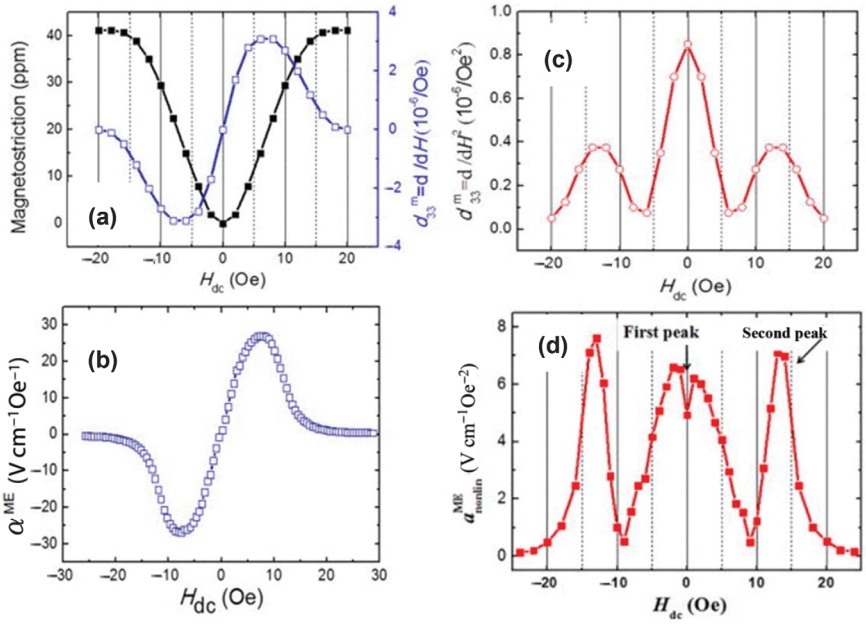

Figure 29: (a) Magnetostriction and piezoelectric coefficient of 8 cm-long Metglas as a function of H_{dc}, (b) The corresponding ME coefficient curve which is shown to be highly dependent on the piezomagnetic coefficient, (c) Derivative strength of piezomagnetic coefficient as a function of $H_{dc,}$ (d). The corresponding nonlinear ME coefficient curve which is shown to be highly dependent on the derivative of piezomagnetic coefficient (Shen et al. 2013).

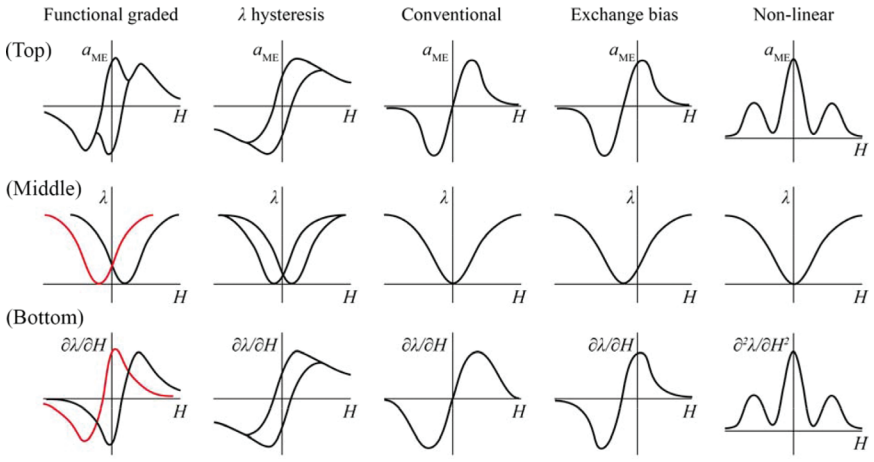

Figure 30: Schematic diagram of five types of self-biased ME composites with different α_{ME}-H (top row), λ-H (middle row), and q-H curves (bottom row).

effectiveness of elastic coupling between the two phases. Therefore, according to the classification of ME working mechanism, the α_{ME}-H curves can be categorized into five groups with corresponding λ, q-H curves, as shown in Figure 30.

(1) In conventional magnetoelectric composites, the most common α_{ME}-H curve possesses the feature as shown in the center of Figure 30. The trends of variations in ME voltage coefficient was found to follow q, resulting in increased value with increasing H_{dc}, with a maximum at an optimized DC bias H_{opt}. On further increasing H_{dc}, ME voltage coefficient was found to decrease. From the α_{ME}-H curve, the maximum ME coefficient α_{max} at optimized DC bias H_{opt} could be easily achieved. For different ferromagnetic materials, the slope of magnetostriction was found to vary significantly, which can be devoted to the domain wall migration and domain rotations under the magnetic field. On applying magnetic field, first, the domain walls of ferromagnetic materials started to migrate followed by domain rotation to align themselves in the direction of magnetic field, which resulted in a saturated magnetization/magnetostriction state. Most of the ferromagnetic materials exhibited zero piezomagnetic coefficient when $H_{dc} = 0$ Oe and consequently negligible α_{ME} near zero bias. By optimizing the composition and configuration of the ferromagnetic phase, one can tune the magnitude of H_{opt} ranging from 5 Oe to 6.8 kOe (Nan et al. 2008; Srinivasan 2010b; Dong et al. 2006).

(2) In functional graded ME composites, their α_{ME}-H curve illustrated an unusual trend/shape of hysteretic loop with a giant remanent magnetoelectric coupling. The loop was found to be counterclockwise under low field region with the positive grading (the magnitude of q increases away from the interface) in the ferromagnetic layer sequence; however, the loop was clockwise with negative grading in the ferromagnetic layer sequence. Moreover, the shape of the hysteresis loop was found to be tightly related with the graded ferromagnetic layers thickness ratio. These behaviors were attributed to the torque and/or domain rearrangement resulting from the interaction of built-in bias and the applied AC magnetic field. Therefore, considering the induced torque, the λ-H curve was represented as a combination of two ferromagnetic materials with different magnetic behavior. Once the net magnetization was induced, the q-H curves exhibited a double peak feature.

(3) In magnetoelectric composites with selected homogeneous ferromagnetic material, the bipolar λ-H curves show symmetric "butterfly" curve due to the nature of ferromagnetic hysteresis. This behavior resulted in to a large non-zero magnetostriction and/or piezomagnetic coefficient in the low field range. Correspondingly, the composite was found to show a hysteretic α_{ME} behavior with counterclockwise direction during H_{dc} sweep as compared to that of the ferromagnetic magnetization hysteretic behavior (counterclockwise). Generally, it has been accepted that the domain wall motion accounts for the hysteresis phenomena. In ferromagnetic materials possessing macrosized domains with long range ordering, once the domains are oriented with respect to external magnetic field, the randomization of domains would require higher field resulting in a hysteresis loop. It should also be noted here that this hysteretic behavior is tightly related with the shape-induced demagnetization factor and the resultant effective magnetic induction of the ferromagnetic layer.

(4) In exchange bias mediated ME composites, the corresponding λ-H curve possess similar slim loop as that of conventional ferromagnetic materials. However, exchange coupling induced large nonzero magnetostriction and corresponding piezomagnetic coefficient at zero bias was found to shift the loop horizontally. In above mentioned three kinds of α_{ME}-H curves, the common feature is that all of them exhibit a symmetric shape with respect to the zero-biased point. However, for exchange bias mediated composites, the α_{ME}-H curve was always found to exhibit an asymmetric feature with respect to the horizontal axis at a certain H_{EB}. Normally, the magnitude of this shift has been attributed to the thickness, interface microstructure of the multicomponent magnetic system, and the inclination angle of the measurement.

(5) Finally, for conventional ME composites measured in nonlinear region, the λ-H curve was found to be similar to that of conventional ferromagnetic materials, while the ME voltage coefficient followed well the trend of variations of the second derivative of λ, as shown in Figure 30. This behavior was attributed to the nonlinear dependence of magnetostriction under magnetic field in ferromagnetic materials. Consequently, the nonlinear coefficient p presented a unique feature of three ME voltage coefficient peaks during H_{dc} sweep, leading to a curve that shows the occurrence of maximum coupling near the zero bias. This nonlinear behavior of magnetoelectric coupling was further controlled by varying the amplitude and/or frequency of applied magnetic field.

In summary, it is clear that every self-biased magnetoelectric composite system has its own characteristic α_{ME}-H curves containing information related to its properties and structure. Irrespective of the nature of mechanism that causes the self-biased ME effect, the α_{ME}-H curves can always be related to the corresponding magnetostriction/piezomagnetic coefficient versus magnetic field characteristics. Classification and understanding the characteristics of self-biased ME response provides great potential towards predicting and designing of subsequent ME devices.

Application of Self-Biased ME Composites

Promising applications of self-biased ME composites have been developed including magnetic field sensors, energy harvesters, tunable devices, filters, phase shifters and so on. Comprehensive reviews on conventional ME device applications have been presented by Nan (Nan et al. 2008) and Scott (Scott 2012), therefore, next we will provide progress on the self-biased ME composites based devices, especially emphasizing energy harvesters, magnetic sensors and four state memories.

Energy Harvesting

For energy harvesting applications, the ME composite could be used to generate the electricity from stray AC magnetic field present in the surrounding and additionally from converting the mechanical vibrations into electricity with higher efficiency. The scavenging mechanism could be described as follows: when the ME composite was placed in an AC magnetic field, the magnetostrictive layer responded by elongating or contracting, thereby, straining the piezoelectric layer that resulted in output voltage across the electrical load through direct piezoelectric effect. Due to the existence of piezoelectric phase in the composite, mechanical oscillation applied on to the composite could directly create electrical voltage. Thus, a ME energy harvester could be used to harness energy from both vibrations and AC magnetic field at the same time. This combination is expected to enhance the power output and conversion efficiency.

In the past decade, ME composites with varying connectivity and structures were developed in order to scavenge the ambient magnetic (Li, Wen, and Bian 2007; Gao et al. 2012), mechanical energy (Dai et al. 2009; 2011) or both of them simultaneously (Dong et al. 2008; Kambale et al. 2013; Zhou, Apo, and Priya 2013b). Recently, Gao et al. designed an unsymmetrical bilayered Metglas/Pb(Zr, Ti)O_3 laminate in push-pull configuration with tunable resonance frequency for a 60 Hz magnetic field energy harvester and experimentally reported a power output of 16 μW/Oe with the power density of $\geq$ 200 μW cm^{-3} (Gao et al. 2012). Dai et al. demonstrated a series of vibration energy harvester based on combining the cantilever structure with a single or multiple ME transducers at the free end placed in the air gap between magnets (Dai et al. 2009; 2011; Yang et al. 2011; Bai et al. 2012). The ME transducer moves through a concentrated magnetic flux variation and was able to provide a maximum power of –7.13 mW (1.1 mW cm^{-3}) under acceleration of 2.5 g at 35 Hz (Dai et al. 2011). Since the ME effect in composites is a product property of magnetostrictive and piezoelectric mechanism, the induced strain from different phases can be expected to be combined together. Based on this

hypothesis, Dong et al. reported an multimodal magnetoelectric cantilever based on the push-pull type Metglas/PZT laminate, and demonstrated a sum effect from ME and piezoelectric contribution with an open circuit output voltage of 8 $V_{p\text{-}p}$ at $H_{ac} = 2$ Oe and $a = 50$ mg at 20 Hz (Dong et al. 2008). However, despite of these intriguing design or performance, the need of DC bias source presented a great challenge in device miniaturization and correspondingly limitation in the power density.

Utilizing the self-biased magnetoelectric response, Yuan et al. reported the first dual-phase ME energy harvesting system that can simultaneously scavenge magnetic and vibration energy in the absence of DC magnetic field, namely Dual-phase self-biased ME energy harvester (Zhou, Apo, and Priya 2013b). The device was designed by combining magnetoelectric laminate (Ni/PZT micro-fiber composite) and piezoelectric unimorph in a cantilever configuration, as illustrated in Figure 31(a)–(c). Large magnetoelectric coefficient 50 V cm^{-1} Oe ($H_{dc} = 0$ Oe) and power density 4.5 mW cm^{-3} (1 g acceleration) was obtained at their resonant mode. Under dual-phase mode, an additive effect in voltage output was realized under zero-biased condition in comparison to that of vibration or magnetic field only mode, as shown in Figure 31(d). This implied the enhancement in both power density and scavenging efficiency. These results presented significant advancement toward MEMS-scalable high energy density multimode energy harvesting system.

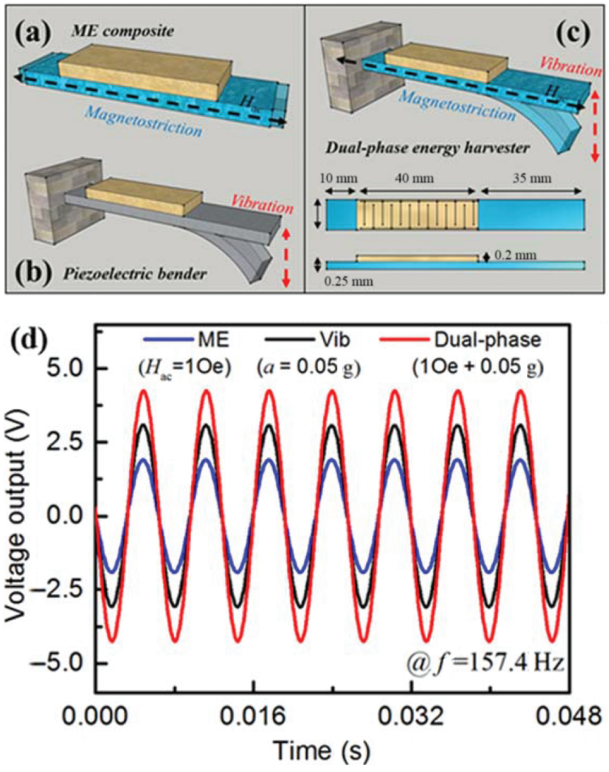

Figure 31: (a)–(c) Schematic diagram of self-biased dual-phase energy harvester consisting of magnetostrictive bender and ME composites. (d) Performance of the energy harvester working under only magnetic field active condition ($H_{ac} = 1$ Oe), only vibration active condition ($a = 0.05$ g) and the dual-phase mode (1 Oe + 0.05 g) at 157.4 Hz (Zhou, Apo, and Priya 2013b).

Magnetic Field Sensor

Motivated by the linear response of ME composites in response to a weak AC magnetic field or the DC bias dependence of the ME voltage coefficient, the ME composites could be used to sense either AC or DC magnetic field by monitoring the electrical signals, acting as a passive magnetic field sensor. A high field sensitivity could be obtained from a ME composite with high ME voltage coefficient and low noise ratio. The sensitivity could be further increased by a factor of 10 at their mechanical resonance frequency. By optimizing materials combination and composite geometry, one can obtain detection sensitivity on the order of pT $Hz^{-1/2}$. A push-pull mode Metglas/PMN-PT fibers/Metglas sensor reported by Wang et al. was able to detect AC magnetic field on the order of 10 pico-Tesla (PT) with magnetic floor noise of 5 pT $Hz^{-1/2}$ at a frequency of 1 Hz ambient conditions (Wang et al. 2011). Similar to that of conventional ME composites, self-biased ME composites could be also used as magnetic field sensors. More interestingly, the unique self-biased response provides great potential toward sensor implementations. New functionalities with the self-biased magnetic field sensors could be rationalized as:

(1) Devices miniaturization: For conventional ME composites, long type laminates with high magnetic flux concentration and low electromechanical resonance have been favorable toward high sensitive ME sensors. However, the large size of such composites was found to hinder their way toward practical application. For self-biased ME composites, a giant ME voltage coefficient could be obtained at zero-bias, which eliminates the need of permanent magnets or coils required for DC bias. The absence of DC bias source could not only dramatically decrease the devices size, but also keep the sensor with an optimized ME coefficient for high sensitivity detection.

(2) Limited electromagnetic noise: From the practical application point of view, fabrication of the magnetic field sensor arrays composed of multiple ME sensors could be of great importance toward increasing the signal-to-noise ratio (SNR) and

mapping the field comprehensively (Xing et al. 2009). By optimizing the geometrical arrangement of sensors in arrays, one is able to further enhance the field detectivity (Li et al. 2012). However, the requirement for optimized DC bias for each sensor puts limit on the implementation. Specifically, for vector field sensor arrays, each component needed an individual bias, which would not only make the device size bulky, but also induce electromagnetic interference between neighboring bias sources. However, for sensor arrays made of self-biased composites, the interference of individual bias field could be avoided due to the absence of the DC bias requirement. Accordingly, based on exchange bias mediated self-biased ME composites, two dimensional vector magnetometer was fabricated (Lage et al. 2013). Figure 32 shows the schematic of this sensor array consisting of two detection component used as 2D ME vector sensor. When the test field was under different orientation with respect to the sensor arrangement, the response of the two composites was found to differ. Therefore, one was able to determine the angle αbetween test field and x axis by monitoring the response of both the sensors. These results indicated a new path for integrating sensor arrays in ultrahigh-sensitivity detection components.

(3) Reduced noise: Another advantage of the self-biased ME composites has been the use of frequency modulation to reduce the environmental vibrational noise and $1/f$ noise by shifting low frequency signals to higher frequency (Petrie et al. 2011; Zhuang et al. 2011). This method was based on the nonlinear ME effect as discussed in Section 3.5.2. In the presence of two AC magnetic field, the nonlinear ME interaction resulted in generation of cross-modulated voltage with frequency of $(f_{div} \pm f_{inc})$, as shown in Figure 28(b). This nonlinear ME coupling was strong near zero-biased field. For example, in Figure 33(a), the non-linear ME coefficient of a Metglas/PMN-PT laminate was found to show a giant value of 100 V cm^{-1} Oe^{-2} at $H_{dc} = 0$ Oe under the $f_{div} = 24.2$ kHz (EMR of the laminate) (Shen et al. 2014).

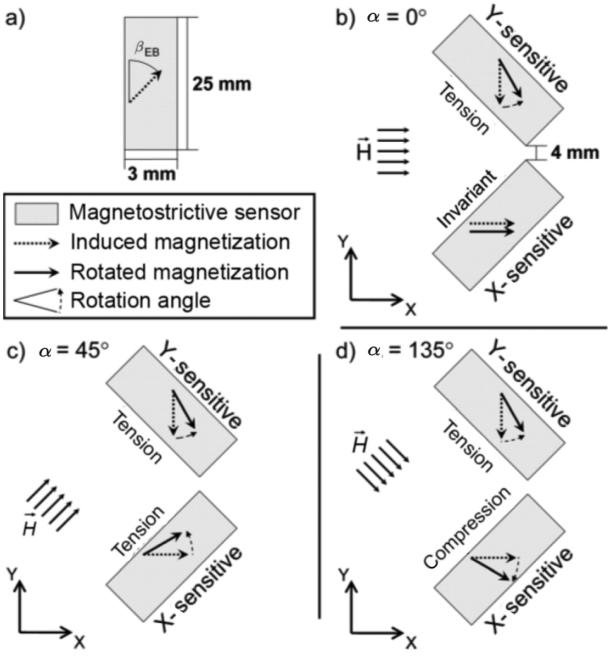

Figure 32: Exchange biased magnetostrictive layers with aligned magnetization. (a) The induced anisotropy inclined with respect to the long cantilever axis. (b)–(d) Illustration that external magnetic fields rotate the magnetization resulting in magnetostrictive deformation (Lage et al. 2013).

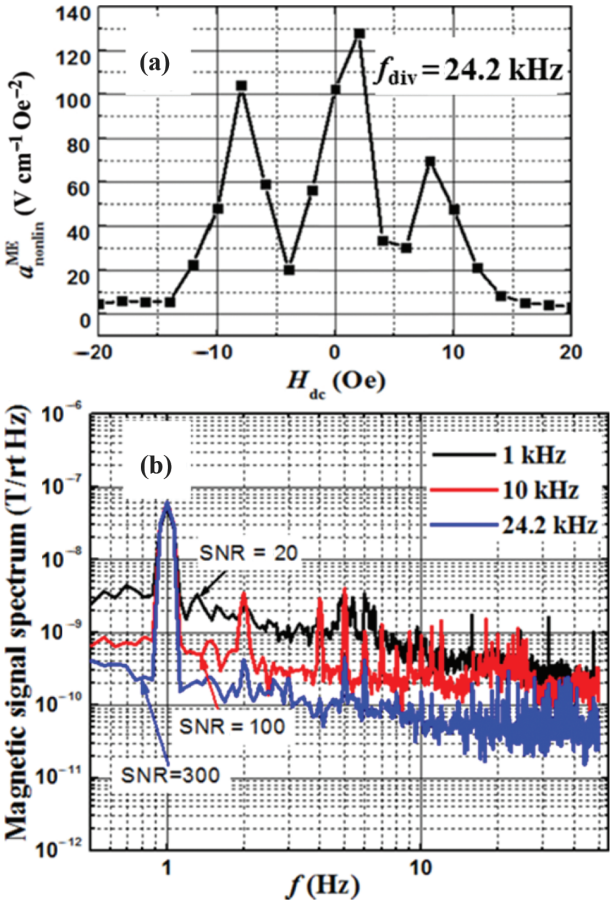

Figure 33: (a) Non-linear ME coefficient as a function of H_{dc} for Metglas/PMN-PT laminate composites with $f = 24.2$ kHz (EMR of the laminate), (b) Equivalent magnetic noise spectrum for a magnetic signal at 1Hz, after applying modulation transfer functions at various driving frequencies at 1, 10 and 24.2 kHz (Shen et al. 2014).

Accordingly, when low frequency signals ($H_{inc} = 18$ nT at $f_{inc} = 1$ Hz) were modulated to higher frequency ($H_{div} = 70$ nT at $f_{div} = 1$, 10 or 24.2 kHz), one was able to lower the detection limit by increasing the SNR, as shown in Figure 33(b). The noise floor was seen to be about 0.2 nT $Hz^{-1/2}$ for $f_{div} = 24.2$ kHz, which was much lower than that of 3 nT $Hz^{-1/2}$ for $f_{div} = 1$ kHz. Other studies have also reported high sensitivity magnetic field sensor based on frequency modulation technique. The best sensitivity of 4 pT $Hz^{-1/2}$ at 1 Hz were reported for a Metglas/PZT fiber/Metglas long type laminate in a magnetically unshielded environment (Petrie et al. 2012).

(4) Angular dependence: For exchange bias mediated self-biased ME composites, the dependence of q at zero bias as a function of induced anisotropy (H_{EB}) was determined by the inclination angle (φ: angle between the induced field and the longitudinal direction of the sample), which provides another potential for vector sensor application. In particular, the exchange bias mediated ME composite response could be used to detect field direction with respect to the sensor position in the absence of DC bias. Figure 34(a) illustrates the schematic of EB mediated self-biased ME cantilever sensor and Figure 34(b) shows its corresponding angular response with respect to an AC magnetic field of 100μT near resonance frequency (Jahns et al. 2013). The sensor output voltage was found to dependent on the inclination angle, with maximum signal at $\varphi = \pm 90^{o}$, while minimum signal at $\varphi = 0^{o}$ and $\pm 180^{o}$. As a consequence, one is able to use the angular dependence of EB mediated composite as a two dimensional vector magnetometer.

(5) Enhanced stability: For AC field sensor, the sensing is based on monitoring the induced ME voltage output due to its linear response with respect to applied AC magnetic field under certain H_{dc}. The field sensitivity can be dramatically enhanced under application of optimum DC bias to achieve the maximum α_{ME}. However, the α_{ME} peak behavior in response to H_{dc} presented a challenge as slight variations in H_{dc} could result in a dramatic decrease in AC sensitivity due to the modulation of α_{ME}. To address this issue, a tunable Ni/PZT self-biased system with a geometry gradient ME composite and a separate magnetic flux concentration was proposed (Zhou and Priya 2014) as shown in Figure 35(a). Through combination of the output from separate sections of the composite, a near flat ME response over a wide range of magnetic DC bias was realized in the range of 0–260 Oe, as shown in Figure 35(b). Thus, the geometry gradient self-biased ME composite was found to exhibit significant enhancement in the AC field detection stability regardless of the variation in DC bias.

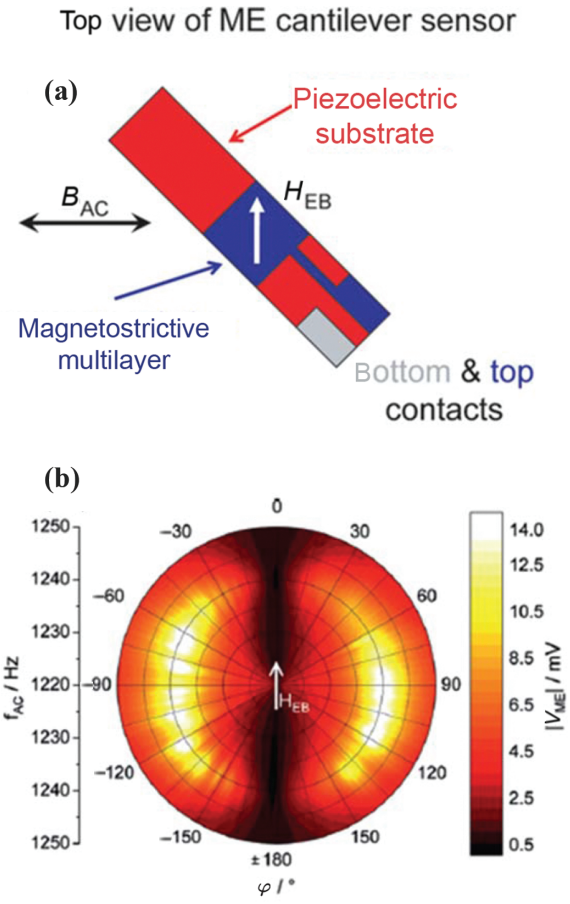

Figure 34: (a) Schematic of an exchange bias mediated self-biased ME composite in a cantilever configuration, (b) corresponding ME voltage response of the self-biased sensor as a function of inclination angle and frequency in the absence of DC bias (Jahns et al. 2013).

Four-state Memory Devices

Due to the magnetoelectric coupling, multiferroics could be also used as memory devices which can be electrically written and magnetically read (Scott 2007; Kimura et al. 2003). The coexistence of electrical polarization ($\pm P$) and magnetization ($\pm M$) provides a great potential toward multiple-state magnetoelectric memory devices (Chun et al. 2012; Fang et al. 2011; Shi et al. 2008). One of the significant breakthrough in this field was the

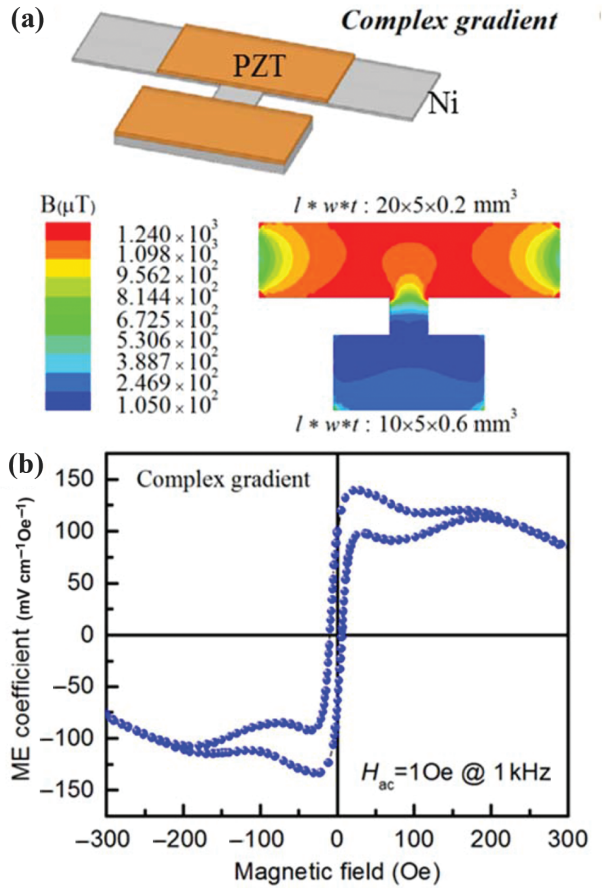

Figure 35: (a) Schematic diagram and the simulated magnetic flux density distribution of geometry gradient Ni/PZT magnetoelectric composite. (b) ME voltage coefficient of the gradient composite under DC field sweep at $H_{ac} = 1$ Oe at 1 kHz (Zhou and Priya 2014).

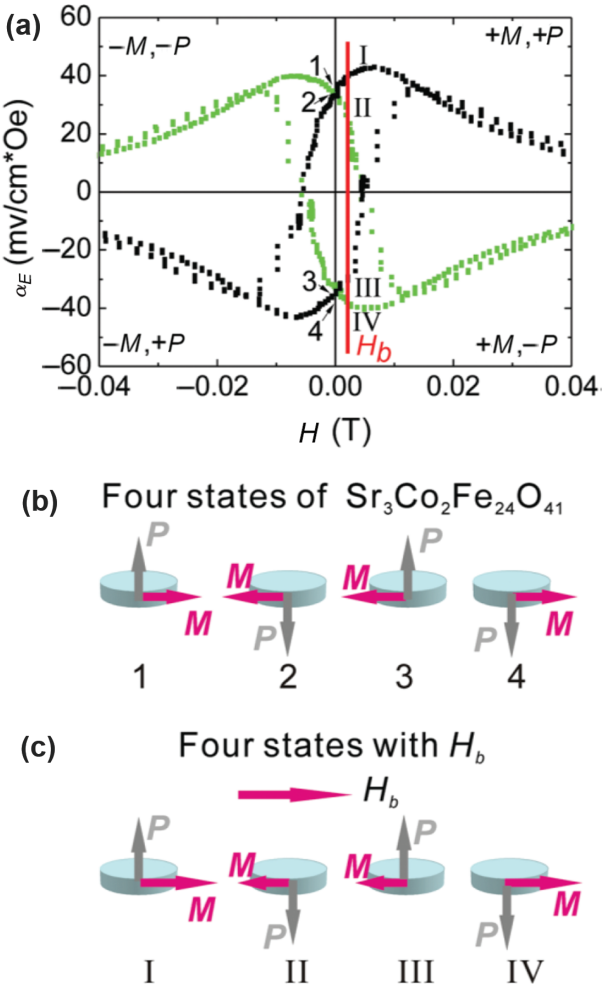

Figure 36: (a) ME voltage coefficient as a function of DC bias for a $Sr_3Co_2Fe_{24}O_4$ multiferroic. Black line indicates measurement after positive electrical polarization, whereas green line represents measurement after negative polarization. (b) Schematic diagram of four physical state of the multiferroic. (c) Schematic diagram of four physical states of the FSM prototype under bias condition. M represents the magnetic polarization and P represent electrical polarization (Wu et al. 2012).

demonstration of four-state resistive memory element based on multiferroic lanthanum bismuth manganite (LBMO) thin film as barrier in a tunnel junction (Gajek et al. 2007). However, the need for liquid nitrogen cooling toward significant memory effect hindered their potential practical applications. Therefore, considering from application point of view, research on room temperature multiferroics or magnetoelectric composites is highly desired.

By utilizing the unique ME coefficient hysteresis behavior in a self-biased multiferroic, a nonvolatile four-state memory device was presented (Wu et al. 2012). In this study, $Sr_3Co_2Fe_{24}O_{41}$ multiferroic ceramic exhibited a strong self-biased magnetoelectric effect at room temperature and the ME coupling coefficient also changed its sign after reversal of electric polarization, leading to four physical states including (+P, +M), (−P, −M), (+P, −M), (−P, +M) represented as 1, 2, 3, 4 as shown in Figure 36. However, the symmetry α_{ME} vs H hysteresis curve under reversed polarization resulted in similar magnitude of α_{ME} at different state (1 and 2, 3 and 4) due to the correlated polarization-magnetization coupling. In addressing this issue, an external bias field (H_b) was used to make each physical state more distinguishable with respect to their magnitude of ME coefficient. Thus, by monitoring the variation of α_{ME} under a small bias, one could identify the information of each state written by magnetic and electric field in a self-biased ME composites, acting as memory devices.

In summary, the performance of functional ME devices such as magnetic field sensors, energy harvesters and memory devices can be further enhanced or extended by using self-biased ME composites due to their unique

characteristics. Besides these promising applications mentioned above, there are other possibilities, including current sensor (Lu et al. 2014), frequency multiplier (Ma et al. 2011), tunable magnetic field generator (Yang et al. 2011), magnetoelectronics (Martin et al. 2008) and so on. The development of self-biased functional ME devices has just started and there is tremendous potential towards fundamental understanding of self-biased ME coupling and manipulating them with magnetic/electric field.

Conclusion and Future Perspective

In conclusion, self-biased magnetoelectric materials characterized as materials which possess large magnetoelectric voltage coefficient in the absence of DC magnetic field, have become an important topic of ever-increasing interest in the past decade. The self-biased ME composites could be divided into five groups according to their working principles as: functional graded ferromagnetic based SME, exchange bias mediated SME, magnetostriction hysteresis based SME, built-in stress based SME, and nonlinear effect based SME. To understand the mechanism of the self-biased ME interaction, we discussed the working principles, background, characterization response, impact factors, advantages and limits of each type self-biased ME composites. By considering the intrinsic properties of each constituent and their elastic coupling in the composites, the general rules of the evolution of the α_{ME} vs H curve were summarized. Finally, potential applications taking advantage of the self-biased ME effect were discussed.

Although tremendous progress has been achieved in the past few years, efforts on self-biased ME composites are likely to continue with several open questions regarding the working mechanism of different types of self-biased coupling and their manipulation for technological applications. For these materials, the future research will likely address the following topics:

(1) Materials: For single phase homogenous ferromagnetic based SME, it remains to be seen whether there exists more ferromagnetic materials in which the magnetostriction would show large hysteresis in the low field region at room temperature and result in a large piezomagnetic coefficient in the absence of DC bias. For multi-component magnetic system, specifically for exchange bias mediated SME, only two preliminary research [(AFM-FM)-FE thin film nanostructure and a (Soft-hard biphase FM)-FE bulk laminate] have been reported. Other EB coupling mechanism, in principle, could be also expanded to the realization of self-biased coupling. In particular, exchange bias mediated composite with multiferroic (e.g. $BiFeO_3$ with FE and AFM order) and/or soft-hard functional graded FM multilayer ribbon seems to be most promising candidate, as shown in Figure 17(c) and (d).

(2) Theoretical analysis: There have been lot of theoretical calculations devoted to the conventional ME composite in determining ME coupling coefficient with respect to impact factors including materials properties, interfacial coupling and so on. For self-biased ME composites, although some theoretical calculation have been reported to understand the coupling in functional graded ME composites and non-linear ME effect, more analysis on the figure of merit for self-biased composite based applications is needed.

(3) Scaling consideration: Most of the self-biased composites discussed in this review were bulky in size. Only very few applications have been demonstrated in form of nanostructured thin films. Growth of thick-film, epitaxial heterostructures and studies on ME interactions are critically important in particular for sensors and high-frequency device applications. Especially, for eliminating use of DC bias field, self-biased ME composites provide great potential of device miniaturization and implementation for on-chip components.

(4) Converse self-biased ME effect: Most of the self-biased effects discussed in this review are direct ME effect, which reflects the polarization variation as a function of magnetic field. However, the effects of electric field E control of magnetization M on the nature of the ME coupling has been rarely investigated so far, which is also technologically important toward microelectronics applications.

(5) Interfacial coupling: A deeper understanding of the built-in stress effect arising from synthesis processing (co-firing or thin film deposition) would be helpful toward enhancing the self-biased coupling in co-fired or thin film based ME composites.

(6) Applications: Although some potential applications and prototypes devices have been suggested and demonstrated by taking advantage of self-biased coupling, there are still lots of work needed to be performed for realization of practical devices.

Acknowledgments: The authors gratefully acknowledge the financial support from the Office of Basic Energy Science, Department of Energy (DE-FG02-06ER46290). The authors also thank the Office of Naval Research for supporting the research (Y. Zhou) through Center for

Energy Harvesting Materials and Systems. S.P. acknowledges the support from Air Force Office of Scientific Research (AFOSR). EQ gratefully acknowledges funding by the German Science Foundation (DFG).

Funding: This work was financially supported by the German Science Foundation (DFG), U.S. Department of Energy (grant/award no.: DE-FG02-06ER46290), Office of Naval Research, Air Force Office of Scientific Research (AFOSR).

References

Ali, M., P. Adie, C. H. Marrows, D. Greig, B. J. Hickey, and R. L. Stamps. 2007. "Exchange Bias Using a Spin Glass." *Nature Materials* 6 (1):70–5.

Allibe, J., I. C. Infante, S. Fusil, K. Bouzehouane, E. Jacquet, C. Deranlot, M. Bibes, and A. Barthelemy. 2009. "Coengineering of Ferroelectric and Exchange Bias Properties in $BiFeO_3$ Based Heterostructures." *Applied Physics Letters* 95 (18):182503.

Bai, X., Y. Wen, J. Yang, P. Li, J. Qiu, and Y. Zhu. 2012. "A Magnetoelectric Energy Harvester with the Magnetic Coupling to Enhance the Output Performance." *Journal of Applied Physics* 111 (7):07A938–3.

Ban, Z. G., S. P. Alpay, and J. V. Mantese. 2003. "Fundamentals of Graded Ferroic Materials and Devices." *Physical Review B* 67 (18):184104.

Berkowitz, A. E., and K. Takano. 1999. "Exchange Anisotropy – A Review." *Journal of Magnetism and Magnetic Materials* 200 (1–3):552–70. doi:http://dx.doi.org/10.1016/S0304-8853(99)00453-9.

Binek, C., and B. Doudin. 2005. "Magnetoelectronics with Magnetoelectrics." *Journal of Physics: Condensed Matter* 17 (2): L39–44.

Binek, C., A. Hochstrat, X. Chen, P. Borisov, W. Kleemann, and B. Doudin. 2005. "Electrically Controlled Exchange Bias for Spintronic Applications." *Journal of Applied Physics* 97:10C514. doi: 10.1063/1.1853836.

Borisov, P., A. Hochstrat, X. Chen, W. Kleemann, and C. Binek. 2005. "Magnetoelectric Switching of Exchange Bias." *Physical Review Letters* 94:117203. doi: 10.1103/PhysRevLett.94.117203.

Brown, W. F., R. M. Hornreich, and S. Shtrikman. 1968. "Upper Bound on the Magnetoelectric Susceptibility." *Physical Review* 168 (2):574–7.

Bruno, P., and C. Chappert. 1991. "Oscillatory Coupling between Ferromagnetic Layers Separated by a Nonmagnetic Metal Spacer." *Physical Review Letters* 67 (12):1602–5. doi: 10.1103/PhysRevLett.67.1602.

Bruno, P., and C. Chappert. 1992. "Ruderman-Kittel Theory of Oscillatory Interlayer Exchange Coupling." *Physical Review B* 46 (1):261–70. doi: 10.1103/PhysRevB.46.261.

Buchel'nikov, V. D., V. S. Romanov, and V. G. Shavrov. 1998. "Oscillating Polaritons in Antiferromagnetics with the Magnetoelectric Effect." *Journal of Communications Technology and Electronics* 43 (1):80–4.

Burdin, D. A., D. V. Chashin, N. A. Ekonomov, L. Y. Fetisov, Y. K. Fetisov, G. Sreenivasulu, and G. Srinivasan. 2014. "Nonlinear Magneto-electric Effects in Ferromagnetic-Piezoelectric Composites." *Journal of Magnetism and Magnetic Materials* 358–359:98–104. doi: 10.1016/j.jmmm.2014.01.062.

Burgt, C. M. van der. 1953. "Dynamical Physical Parameters of the Magnetostrictive Excitation of Extensional and Torsional Vibrations in Ferrites." *Philips Research Reports* 8:91–132.

Cain, W. C., and M. H. Kryder. 1990. "Investigation of the Exchange Mechanism in NiFe-TbCo Bilayers." *Journal of Applied Physics* 67 (9):5722–4. doi: http://dx.doi.org/10.1063/1.346107.

Chen, Y. J., S. M. Gillette, T. Fitchorov, L. P. Jiang, H. B. Hao, J. H. Li, X. X. Gao, A. Geiler, C. Vittoria, and V. G. Harris. 2011. "Quasi-One-Dimensional Miniature Multiferroic Magnetic Field Sensor with High Sensitivity at Zero Bias Field." *Applied Physics Letters* 99:042505.

Chen, L., P. Li, Y. Wen, and P. Wang. 2012. "Highly Zero-Biased Magnetoelectric Response in Magnetostrictive/Piezoelectric Composite." *Journal of Applied Physics* 112 (2):024504. doi: 10.1063/1.4737404.

Chen, L., P. Li, Y. Wen, and Y. Zhu. 2013. "Note: High Sensitivity Self-Bias Magnetoelectric Sensor with Two Different Magnetostrictive Materials." *Review of Scientific Instruments* 84 (6):066101. doi: 10.1063/1.4808322.

Chu, Y. H., L. W. Martin, M. B. Holcomb, M. Gajek, S. J. Han, Q. He, N. Balke, C. H. Yang, D. Lee, W. Hu, et al. 2008. "Electric-Field Control of Local Ferromagnetism Using a Magnetoelectric Multiferroic." *Nature Materials* 7 (6):478–82.

Chun, S. H., Yi S. Chai, B. G. Jeon, H. J. Kim, Y. S. Oh, I. Kim, H. Kim, B. Jo. Jeon, So. Y. Haam, J.-Y. Park, et al. 2012. "Electric Field Control of Nonvolatile Four-State Magnetization at Room Temperature." *Physical Review Letters* 108:177201. doi: 10.1103/PhysRevLett.108.177201.

Clark, A. E. 1980. *Ferromagnetic Materials*, Vol. 1. Amsterdam: North-Holland.

Dai, X., Y. Wen, P. Li, J. Yang, and M. Li. 2011. "Energy Harvesting from Mechanical Vibrations Using Multiple Magnetostrictive/Piezoelectric Composite Transducers." *Sensors and Actuators A: Physical* 166 (1):94–101. doi: 10.1016/j.sna.2010.12.025.

Dai, X., Y. Wen, P. Li, J. Yang, and G. Zhang. 2009. "Modeling, Characterization and Fabrication of Vibration Energy Harvester Using Terfenol-D/PZT/Terfenol-D Composite Transducer." *Sensors and Actuators A: Physical* 156 (2):350–8. doi: 10.1016/j.sna.2009.10.002.

Dho, J., X. Qi, H. Kim, J. L. MacManus-Driscoll, and M. G. Blamire. 2006. "Large Electric Polarization and Exchange Bias in Multiferroic $BiFeO_3$." *Advanced Materials* 18 (11):1445–8. doi: 10.1002/adma.200502622.

Dieny, B., V. S. Speriosu, S. S. P. Parkin, B. A. Gurney, D. R. Wilhoit, and D. Mauri. 1991. "Giant Magnetoresistance in Soft Ferromagnetic Multilayers." *Physical Review B* 43 (1):1297–300. doi: 10.1103/PhysRevB.43.1297.

Dong, S., J. Zhai, J. Li, and D. Viehland. 2006. "Near-Ideal Magnetoelectricity in High-Permeability Magnetostrictive/Piezofiber Laminates with a (2–1) Connectivity." *Applied Physics Letters* 89 (25):252904. doi: 10.1063/1.2420772.

Dong, S. X., J. Y. Zhai, J. F. Li, D. Viehland, and S. Priya. 2008. "Multimodal System for Harvesting Magnetic and Mechanical Energy." *Applied Physics Letters* 93:103511. doi: 10.1063/1.2982099.

Dong, S., J. Zhai, J.-F. Li, D. Viehland, and E. Summers. 2007. "Strong Magnetoelectric Charge Coupling in Stress-Biased Multilayer-Piezoelectric/Magnetostrictive Composites." *Journal of Applied Physics* 101 (12):124102. doi: 10.1063/1.2748712.

Eerenstein, W., N. D. Mathur, and J. F. Scott. 2006. "Multiferroic and Magnetoelectric Materials." *Nature* 442 (7104):759–65. doi: 10.1038/nature05023.

Fang, F., Y. T. Xu, W. P. Zhu, and W. Yang. 2011. "A Four-State Magnetoelectric Coupling for Embedded Piezoelectric/Magnetic Composites." *Journal of Applied Physics* 110:084109. doi: 10.1063/1.3653293.

Fetisov, L. Y., Y. K. Fetisov, G. Sreenivasulu, and G. Srinivasan. 2013. "Nonlinear Resonant Magnetoelectric Interactions and Efficient Frequency Doubling in a Ferromagnetic-Ferroelectric Layered Structure." *Journal of Applied Physics* 113 (11):116101.

Fiebig, M. 2005. "Revival of the Magnetoelectric Effect." *Journal of Physics D: Applied Physics* 38 (8):R123–52. doi: 10.1088/0022-3727/38/8/r01.

Folen, V. J., G. T. Rado, and E. W. Stalder. 1961. "Anisotropy of the Magnetoelectric Effect in Cr2O3." *Physical Review Letters* 6 (11):607–8.

Freitas, P. P., J. L. Leal, L. V. Melo, N. J. Oliveira, L. Rodrigues, and A. T. Sousa. 1994. "Spin-Valve Sensors Exchange-Biased by Ultrathin TbCo Films." *Applied Physics Letters* 65 (4):493–5. doi: 10.1063/1.112304.

Gajek, M., M. Bibes, S. Fusil, K. Bouzehouane, J. Fontcuberta, A. Barthelemy, and A. Fert. 2007. "Tunnel Junctions with Multiferroic Barriers." *Nature Materials* 6 (4):296–302.

Gao, J. Q., D. Hasanyan, Y. Shen, Y. J. Wang, J. F. Li, and D. Viehland. 2012. "Giant Resonant Magnetoelectric Effect in Bi-layered Metglas/Pb(Zr,Ti)O-3 Composites." *Journal of Applied Physics* 112 (10):104101.

Gillette, S. M., T. Fitchorov, O. Obi, L. Jiang, H. Hao, S. Wu, Y. Chen, and V. G. Harris. 2014. "Effects of Intrinsic Magnetostriction on Tube-Topology Magnetoelectric Sensors with High Magnetic Field Sensitivity." *Journal of Applied Physics* 115 (17):17C734. doi: 10.1063/1.4868326.

Gillette, S. M., A. L. Geiler, D. Gray, D. Viehland, C. Vittoria, and V. G. Harris. 2011. "Improved Sensitivity and Noise in Magneto-Electric Magnetic Field Sensors by Use of Modulated AC Magnetostriction." *Magnetics Letters, IEEE* 2:2500104–2500104. doi: 10.1109/LMAG.2011.2151178.

Giri, S., M. Patra, and S. Majumdar. 2011. "Exchange Bias Effect in Alloys and Compounds." *Journal of Physics: Condensed Matter* 23 (7):073201.

Gokemeijer, N. J., T. Ambrose, and C. L. Chien. 1997. "Long-Range Exchange Bias across a Spacer Layer." *Physical Review Letters* 79 (21):4270–3. doi: 10.1103/PhysRevLett.79.4270.

Gonzalez, J. M., M. I. Montero, V. Raposo, and A. Hernando. 2000. "On the Relationship between the Hysteresis Loop Shift and the Dipolar Interactions in Hard-Soft Nanocomposite Samples." *Journal of Magnetism and Magnetic Materials* 221 (1–2): 187–95. doi: 10.1016/s0304-8853(00)00526-6.

Greve, H., E. Woltermann, H.-J. Quenzer, B. Wagner, and E. Quandt. 2010. "Giant Magnetoelectric Coefficients in (Fe[Sub 90]Co[Sub 10])[Sub 78]Si[Sub 12]B[Sub 10]-AlN Thin Film Composites." *Applied Physics Letters* 96 (18):182501. doi: 10.1063/1.3377908.

Gruyters, M. 2005. "Spin-Glass-Like Behavior in COO Nanoparticles and the Origin of Exchange Bias in Layered COO/Ferromagnet Structures." *Physical Review Letters* 95 (7):077204.

Gubbiotti, G., G. Carlotti, M. Madami, J. Weston, P. Vavassori, and G. Zangari. 2002. "Exchange Coupling in FeTaN-FeSM-FeTaN Multilayers: A Kerr Effect Study." *IEEE Transactions on Magnetics* 38 (5):2779–81. doi: 10.1109/tmag.2002.803238.

He, J., L. Zhou, D. L. Zhao, and X. L. Wang. 2009. "Hysteresis Loop Shift Behavior of CoFeSiB Amorphous Ribbons." *Journal of Materials Research* 24 (4):1607–10.

Hempstead, R. D., S. Krongelb, and D. A. Thompson. 1978. "Unidirectional Anisotropy in Nickel-Iron Films by Exchange Coupling with Anti-Ferromagnetic Films." *IEEE Transactions on Magnetics* 14 (5):521–3. doi: 10.1109/tmag.1978.1059838.

Hill, N. A. 2000. "Why Are There so Few Magnetic Ferroelectrics?." *Journal of Physical Chemistry B* 104 (29):6694–709. doi: 10.1021/jp000114x.

Hong, H., Y. G. Wang, K. Bi, and F. G. Chen. 2013. "Resonant Magnetoelectric Effects in Ni/Pb(Zr, Ti)O_3/FeCo Trilayered Semicircular Composites." *Surface Review and Letters* 20 (01):1350004. doi: 10.1142/s0218625x13500042.

Ibach, H. 1997. "The Role of Surface Stress in Reconstruction, Epitaxial Growth and Stabilization of Mesoscopic Structures." *Surface Science Reports* 29 (5–6):195–263. doi: http://dx.doi.org/10.1016/S0167-5729(97)00010-1.

Islam, R. A., V. Bedekar, N. Poudyal, J. P. Liu, and S. Priya. 2008. "Magnetoelectric Properties of Core-Shell Particulate Nanocomposites." *Journal of Applied Physics* 104 (10):104111.

Islam, R. A., H. Kim, S. Priya, and H. Stephanou. 2006. "Piezoelectric Transformer Based Ultrahigh Sensitivity Magnetic Field Sensor." *Applied Physics Letters* 89 (15):152908.

Islam, R. A., and S. Priya. 2006. "Magnetoelectric Properties of the Lead-Free Cofired $BaTiO_3$-(Ni0.8zn0.2)Fe_2O_4 Bilayer Composite." *Applied Physics Letters* 89 (15):152911.

Israel, C., N. D. Mathur, and J. F. Scott. 2008. "A One-Cent Room-Temperature Magnetoelectric Sensor." *Nature Materials* 7 (2):93–4. doi: 10.1038/nmat2106.

Jahns, R., A. Piorra, E. Lage, C. Kirchhof, D. Meyners, J. L. Gugat, M. Krantz, M. Gerken, R. Knöchel, E. Quandt, et al. 2013. "Giant Magnetoelectric Effect in Thin-Film Composites." *Journal of the American Ceramic Society* 96 (6):1673–81. doi: 10.1111/jace.12400.

Jungho, R., A. V. Carazo, K. Uchino, and H.-E. Kim. 2001. "Magnetoelectric Properties in Piezoelectric and Magnetostrictive Laminate Composites." *Japanese Journal of Applied Physics* 40:4948–51.

Kambale, R. C., W.-Ha. Yoon, D.-S. Park, J.-J. Choi, C. -W. Ahn, J.-W. Kim, B.-D. Hahn, D.-Y. Jeong, B. C. Lee, G.-S. Chung, et al. 2013. "Magnetoelectric Properties and Magnetomechanical Energy Harvesting From Stray Vibration and Electromagnetic Wave by Pb(Mg1/3nb2/3)O3-Pb(Zr,Ti)O_3 Single Crystal/Ni Cantilever." *Journal of Applied Physics* 113 (20):204108. doi: 10.1063/1.4804959.

Kamentsev, K. E., Y. K. Fetisov, and G. Srinivasana. 2006. "Low-Frequency Nonlinear Magnetoelectric Effects in a Ferrite-Piezoelectric Multilayer." *Applied Physics Letters* 89 (14):142510.

Kendall, D., and A. R. Piercy. 1993. "The Frequency Dependence of Eddy Current Losses in Terfenol-D." *Journal of Applied Physics* 73 (10):6174–6. doi: http://dx.doi.org/10.1063/1.352686.

Kimura, T., T. Goto, H. Shintani, K. Ishizaka, T. Arima, and Y. Tokura. 2003. "Magnetic Control of Ferroelectric Polarization." *Nature* 426 (6962):55–8. doi: 10.1038/nature02018.

Kirchhof, C., M. Krantz, I. Teliban, R. Jahns, S. Marauska, B. Wagner, R. Knöchel, M. Gerken, D. Meyners, and E. Quandt. 2013. "Giant Magnetoelectric Effect in Vacuum." *Applied Physics Letters* 102 (23):232905. doi: http://dx.doi.org/10.1063/1.4810750.

Kools, J. C. S. 1996. "Exchange-Biased Spin-Valves for Magnetic Storage." *IEEE Transactions on Magnetics* 32 (4):3165–84. doi: 10.1109/20.508381.

Lage, E., C. Kirchhof, V. Hrkac, L. Kienle, R. Jahns, R. Knochel, E. Quandt, and D. Meyners. 2012. "Exchange Biasing of Magnetoelectric Composites." *Nature Materials* 11 (6):523–9.

Lage, E., N. O. Urs, V. Röbisch, I. Teliban, R. Knöchel, D. Meyners, J. McCord, and E. Quandt. 2014. "Magnetic Domain Control and Voltage Response of Exchange Biased Magnetoelectric Composites." *Applied Physics Letters* 104 (13):132405. doi: http://dx.doi.org/10.1063/1.4870511.

Lage, E., F. Woltering, E. Quandt, and D. Meyners. 2013. "Exchange Biased Magnetoelectric Composites for Vector Field Magnetometers." *Journal of Applied Physics* 113 (17):17C725. doi: 10.1063/1.4798791.

Laletin, V. M., N. Paddubnaya, G. Srinivasan, C. P. De Vreugd, M. I. Bichurin, V. M. Petrov, and D. A. Filippov. 2005. "Frequency and Field Dependence of Magnetoelectric Interactions in Layered Ferromagnetic Transition Metal-Piezoelectric Lead Zirconate Titanate." *Applied Physics Letters* 87 (22):222507. doi: 10.1063/1.2137450.

Laletin, U., G. Sreenivasulu, V. M. Petrov, T. Garg, A. R. Kulkarni, N. Venkataramani, and G. Srinivasan. 2012. "Hysteresis and Remanence in Magnetoelectric Effects in Functionally Graded Magnetostrictive-Piezoelectric Layered Composites." *Physical Review B* 85 (10):104404.

Laukhin, V., X. Marti, V. Skumryev, D. Hrabovsky, F. Sanchez, M. V. Garcia-Cuenca, C. Ferrater, M. Varela, U. Lueders, J. F. Bobo, et al. 2007. "Electric Field Effects on Magnetotransport Properties of Multiferroic Py/$YMnO_3$/Pt Heterostructures." *Philosophical Magazine Letters* 87 (3–4):183–91. doi: 10.1080/09500830701210011.

Laukhin, V., V. Skumryev, X. Marti, D. Hrabovsky, F. Sanchez, M. V. Garcia-Cuenca, C. Ferrater, M. Varela, U. Lueders, J. F. Bobo, et al. 2006. "Electric-Field Control of Exchange Bias in Multiferroic Epitaxial Heterostructures." *Physical Review Letters* 97 (22):227201. doi: 10.1103/PhysRevLett.97.227201.

Li, M. H., Y. J. Wang, J. Q. Gao, D. Gray, J. F. Li, and D. Viehland. 2012. "Dependence of Magnetic Field Sensitivity of a Magnetoelectric Laminate Sensor Pair on Separation Distance: Effect of Mutual Inductance." *Journal of Applied Physics* 111 (3):033923.

Li, M., Y. Wang, J. Gao, J. Li, and D. Viehland. 2012. "Enhanced Magnetoelectric Effect in Self-Stressed Multi-Push-Pull Mode Metglas/Pb(Zr,Ti)O_3/Metglas Laminates." *Applied Physics Letters* 101 (2):022908. doi: http://dx.doi.org/10.1063/1.4737179.

Li, M. H., Y. J. Wang, Y. Shen, J. Q. Gao, J. F. Li, and D. Viehland. 2013. "Structural Dependence of Nonlinear Magnetoelectric Effect for Magnetic Field Detection by Frequency Modulation." *Journal of Applied Physics* 114 (14):144501.

Li, M., Z. Wang, Y. Wang, J. Li, and D. Viehland. 2013. "Giant Magnetoelectric Effect in Self-Biased Laminates under Zero Magnetic Field." *Applied Physics Letters* 102 (8):082404. doi: 10.1063/1.4794056.

Li, P., Y. M. Wen, and L. X. Bian. 2007. "Enhanced Magnetoelectric Effects in Composite of Piezoelectric Ceramics, Rare-Earth Iron Alloys, and Ultrasonic Horn." *Applied Physics Letters* 90 (2):022503.

Lin, M. T., C. H. Ho, C. R. Chang, and Y. D. Yao. 2001. "Temperature-Dependence of Interlayer Exchange Bias Coupling in NiO/Cu/NiFe." *Journal of Applied Physics* 89 (11):7540–2.

Lin, T., C. Tsang, R. E. Fontana, and J. K. Howard. 1995. "Exchange-Coupled Ni-Fe/Fe-Mn, Ni-Fe/Ni-Mn and NiO/Ni-Fe Films for Stabilization of Magnetoresistive Sensors." *IEEE Transactions on Magnetics* 31 (6):2585–90.

Liu, Y. T., J. Jiao, J. S. Ma, B. Ren, L. Y. Li, X. Y. Zhao, H. S. Luo, and L. Shi. 2013. "Frequency Conversion in Magnetoelectric Composites for Quasi-Static Magnetic Field Detection." *Applied Physics Letters* 103 (21):212902.

Liu, W. C., C. L. Mak, K. H. Wong, C. Y. Lo, S. W. Or, W. Zhou, A. Hauser, F. Y. Yang, and R. Sooryakumar. 2008. "Magnetoelectric and Dielectric Relaxation Properties of the High Curie Temperature Composite Sr(1.9)Ca(0.1)NaNb(5)O(15)-CoFe(2)O(4)." *Journal of Physics D: Applied Physics* 41 (12):125402.

Lu, C., P. Li, Y. Wen, A. Yang, W. He, J. Zhang, J. Yang, J. Wen, Y. Zhu, and M. Yu. 2013. "Investigation of Magnetostrictive/Piezoelectric Multilayer Composite with a Giant Zero-Biased Magnetoelectric Effect." *Applied Physics A* 113 (2):413–21. doi: 10.1007/s00339-013-7557-y.

Lu, C. J., P. Li, Y. M. Wen, A. C. Yang, C. Yang, D. C. Wang, W. He, and J. T. Zhang. 2014. "Zero-Biased Magnetoelectric Composite Fe73.5cu1nb3si13.5B9/Ni/Pb(Zr1-x,Tix)O-3 for Current Sensing." *Journal of Alloys and Compounds* 589:498–501. doi: 10.1016/j.jallcom.2013.12.038.

Lu, C., P. Li, Y. Wen, A. Yang, C. Yang, J. Yang, W. He, J. Zhang, and W. Li. 2014. "Dynamic Magnetostrictive Properties of Magnetization-Graded Ferromagnetic Material and Application in Magnetoelectric Composite." *Journal of Applied Physics* 115 (17):17C726. doi: 10.1063/1.4866089.

Ma, J., J. Hu, Z. Li, and C. W. Nan. 2011a. "Recent Progress in Multiferroic Magnetoelectric Composites: From Bulk to Thin Films." *Advanced Materials* 23 (9):1062–87. doi: 10.1002/adma.201003636.

Ma, J., Z. Li, Y. H. Lin, and C. W. Nan. 2011b. "A Novel Frequency Multiplier Based on Magneto Electric Laminate." *Journal of Magnetism and Magnetic Materials* 323 (1):101–3.

Mandal, S. K., G. Sreenivasulu, V. M. Petrov, S. Bandekar, and G. Srinivasan. 2011. "Functionally Graded Piezomagnetic and Piezoelectric Bilayer for Magnetic Field Sensors-Magnetoelectric Interactions at Low Frequency at Bending Modes." *Advances and Applications in Electroceramics* 226:223–30.

Mandal, S. K., G. Sreenivasulu, V. M. Petrov, and G. Srinivasan. 2010. "Flexural Deformation in a Compositionally Stepped Ferrite and Magnetoelectric Effects in a Composite with Piezoelectrics." *Applied Physics Letters* 96 (19):192502.

Mandal, S. K., G. Sreenivasulu, V. M. Petrov, and G. Srinivasan. 2011. "Magnetization-Graded Multiferroic Composite and Magnetoelectric Effects at Zero Bias." *Physical Review B* 84 (1):014432.

Mantese, J. V., A. L. Micheli, N. W. Schubring, R. W. Hayes, G. Srinivasan, and S. P. Alpay. 2005. "Magnetization-Graded Ferromagnets: The Magnetic Analogs of Semiconductor Junction Elements." *Applied Physics Letters* 87 (8):082503.

Marti, X., F. Sanchez, J. Fontcuberta, M. V. Garcia-Cuenca, C. Ferrater, and M. Varela. 2006. "Exchange Bias between Magnetoelectric YMnO3 and Ferromagnetic SrRuO3 Epitaxial Films." *Journal of Applied Physics* 99 (8):08P302. doi: 10.1063/1.2167333.

Martin, L. W., Y.-H. Chu, M. B. Holcomb, M. Huijben, Pu. Yu, S.-J. Han, D. Lee, S. X. Wang, and R. Ramesh. 2008. "Nanoscale Control of Exchange Bias with $BiFeO_3$ Thin Films." *Nano Letters* 8 (7):2050–5. doi: 10.1021/nl801391m.

Martin, L. W., Y. H. Chu, Q. Zhan, R. Ramesh, S. J. Han, S. X. Wang, M. Warusawithana, and D. G. Schlom. 2007. "Room Temperature Exchange Bias and Spin Valves Based on $BiFeO_3$/$SrRuO_3$/$SrTiO_3$/Si (001) Heterostructures." *Applied Physics Letters* 91 (17):172513.

Martin, L., S. P. Crane, Y. H. Chu, M. B. Holcomb, M. Gajek, M. Huijben, C. H. Yang, N. Balke, and R. Ramesh. 2008. "Multiferroics and Magnetoelectrics: Thin Films and Nanostructures." *Journal of Physics: Condensed Matter* 20 (43):434220. doi: 10.1088/0953-8984/20/43/434220.

McDannald, A., M. Staruch, G. Sreenivasulu, C. Cantoni, G. Srinivasan, and M. Jain. 2013. "Magnetoelectric Coupling in Solution Derived 3–0 Type PbZr0.52ti0.48O_3:X$CoFe_2O_4$ Nanocomposite Films." *Applied Physics Letters* 102 (12):122905. doi: 10.1063/1.4799174.

Meiklejohn, W. H., and C. P. Bean. 1957. "New Magnetic Anisotropy." *Physical Review* 105 (3):904–13.

Mewes, T., B. F. P. Roos, S. O. Demokritov, and B. Hillebrands. 2000. "Oscillatory Exchange Bias Effect in FeNi/Cu/FeMn and FeNi/Cr/FeMn Trilayer Systems." *Journal of Applied Physics* 87 (9):5064–6. doi: 10.1063/1.373249.

Michael, L., L. Vera, S. Peter, B. Francis, Z. Michael, M. Hiwa, V. Alexander, J. Van Bael Margriet, T. Kristiaan, V. André, et al. 2014. "Multiferroic $BaTiO_3$–$BiFeO_3$ Composite Thin Films and Multilayers: Strain Engineering and Magnetoelectric Coupling." *Journal of Physics D: Applied Physics* 47 (13):135303.

Nan, C. W. 1993. "Physics of Inhomogeneous Inorganic Materials." *Progress in Materials Science* 37 (1):1–116. doi: 10.1016/0079-6425(93)90004-5.

Nan, C. W., M. I. Bichurin, S. X. Dong, D. Viehland, and G. Srinivasan. 2008. "Multiferroic Magnetoelectric Composites: Historical Perspective, Status, and Future Directions." *Journal of Applied Physics* 103 (3):031101. doi: 10.1063/1.2836410.

Nan, C. W., G. Liu, Y. H. Lin, and H. D. Chen. 2005. "Magnetic-Field-Induced Electric Polarization in Multiferroic Nanostructures." *Physical Review Letters* 94 (19):197203.

Nogués, J., and I. K. Schuller. 1999. "Exchange Bias." *Journal of Magnetism and Magnetic Materials* 192 (2):203–32. doi: http://dx.doi.org/10.1016/S0304-8853(98)00266-2.

Onuta, T. -D., Yi. Wang, C. J. Long, and I. Takeuchi. 2011. "Energy Harvesting Properties of All-Thin-Film Multiferroic Cantilevers." *Applied Physics Letters* 99 (20):203506. doi: 10.1063/1.3662037.

Osborn, J. A. 1945. "Demagnetizing Factors of the General Ellipsoid." *Physical Review* 67 (11):351.

Pan, D., J. Lu, Y. Bai, W. Chu, and L. J. Qiao. 2008. "Shape Demagnetization Effect on Layered Magnetoelectric Composites." *Chinese Science Bulletin* 53 (14):2124–8.

Pan, D. A., J. J. Tian, S. G. Zhang, J. S. Sun, A. A. Volinsky, and L. J. Qiao. 2009. "Geometry Effects on Magnetoelectric Performance of Layered Ni/PZT Composites." *Materials Science and Engineering B-Advanced Functional Solid-State Materials* 163 (2):114–19.

Park, J. H., H. M. Jang, H. S. Kim, C. G. Park, and S. G. Lee. 2008. "Strain-Mediated Magnetoelectric Coupling in BaTiO3-Co Nanocomposite Thin Films." *Applied Physics Letters* 92 (6):062908.

Parkin, S. S. P., R. Bhadra, and K. P. Roche. 1991. "Oscillatory Magnetic Exchange Coupling through Thin Copper Layers." *Physical Review Letters* 66 (16):2152–5. doi: 10.1103/PhysRevLett.66.2152.

Petrie, J., D. Gray, D. Viehland, G. Sreenivasulu, G. Srinivasan, S. Mandal, and A. S. Edelstein. 2012. "Shifting the Operating Frequency of Magnetoelectric Sensors." *Journal of Applied Physics* 111 (7):07C714.

Petrie, J., D. Viehland, D. Gray, S. Mandal, G. Sreenivasulu, G. Srinivasan, and A. S. Edelstein. 2011. "Enhancing the Sensitivity of Magnetoelectric Sensors by Increasing the Operating Frequency." *Journal of Applied Physics* 110 (12):124506. doi: 10.1063/1.3668752.

Petrov, V. M., and G. Srinivasan. 2008. "Enhancement of Magnetoelectric Coupling in Functionally Graded Ferroelectric and Ferromagnetic Bilayers." *Physical Review B* 78 (18):184421.

Prellier, W., M. P. Singh, and P. Murugavel. 2005. "The Single-Phase Multiferroic Oxides: From Bulk to Thin Film." *Journal of Physics: Condensed Matter* 17 (30):R803–R832. doi: 10.1088/0953-8984/17/30/r01.

Priya, S., R. Islam, S. Dong, and D. Viehland. 2007. "Recent Advancements in Magnetoelectric Particulate and Laminate Composites." *Journal of Electroceramics* 19 (1):149–66. doi: 10.1007/s10832-007-9042-5.

Ramesh, R., and N. A. Spaldin. 2007. "Multiferroics: Progress and Prospects in Thin Films." *Nature Materials* 6 (1):21–9. doi: 10.1038/nmat1805.

Rivas, M., J. A. Garcia, M. Tejedor, E. Bertran, and J. G. Cespedes. 2005. "Influence of the Dipolar Interactions in the Magnetization Reversal Asymmetry of Hard-Soft Magnetic Ribbons." *Journal of Applied Physics* 97 (2):023903.

Ryu, J., A. V. Carazo, K. Uchino, and H. E. Kim. 2001. "Piezoelectric and Magnetoelectric Properties of Lead Zirconate Titanate/Ni-Ferrite Particulate Composites." *Journal of Electroceramics* 7 (1):17–24.

Ryu, H., P. Murugavel, J. H. Lee, S. C. Chae, T. W. Noh, Y. S. Oh, H. J. Kim, K. H. Kim, J. H. Jang, M. Kim, et al. 2006. "Magnetoelectric Effects of Nanoparticulate Pb(Zr0.52ti0.48)O-3-$NiFe_2O_4$ Composite Films." *Applied Physics Letters* 89 (10):102907.

Sander, D., H. Meyerheim, S. Ferrer, and J. Kirschner. 2003. "Stress, Strain and Magnetic Anisotropy: All Is Different in Nanometer Thin Films." In *Advances in Solid State Physics*, edited by B. Kramer, 547–62. Berlin Heidelberg: Springer.

Schmid, H. 1994. *Ferroelectrics* 162:317.

Schubring, N. W., J. V. Mantese, A. L. Micheli, A. B. Catalan, and R. J. Lopez. 1992. "Charge Pumping and Pseudopyroelectric Effect in Active Ferroelectric Relaxor-Type Films." *Physical Review Letters* 68 (11):1778–81.

Scott, J. F. 2007. "Data Storage – Multiferroic Memories." *Nature Materials* 6 (4):256–7.

Scott, J. F. 2012. "Applications of Magnetoelectrics." *Journal of Materials Chemistry* 22 (11):4567. doi: 10.1039/c2jm16137k.

Shen, Y., J. Gao, Y. Wang, P. Finkel, J. Li, and D. Viehland. 2013. "Piezomagnetic Strain-Dependent Non-linear Magnetoelectric Response Enhancement by Flux Concentration Effect." *Applied Physics Letters* 102 (17):172904. doi: 10.1063/1.4803660.

Shen, Y., J. Gao, Y. Wang, J. Li, and D. Viehland. 2014. "High Non-Linear Magnetoelectric Coefficient in Metglas/PMN-PT Laminate Composites under Zero Direct Current Magnetic Bias." *Journal of Applied Physics* 115 (9):094102. doi: dx.doi.org/10.1063/1.4867516.

Shen, L. G., M. H. Li, J. Q. Gao, Y. Shen, J. F. Li, D. Viehland, X. Zhuang, M. L. C. Sing, C. Cordier, S. Saez, et al. 2011. "Magnetoelectric Nonlinearity in Magnetoelectric Laminate Sensors." *Journal of Applied Physics* 110 (11):114510.

Shi, Z., C. P. Wang, X. J. Liu, and C. W. Nan. 2008. "A Four-State Memory Cell Based on Magnetoelectric Composite." *Chinese Science Bulletin* 53 (14):2135–8. doi: 10.1007/s11434-008-0275-8.

Shi, M., G. Y. Yu, H. L. Su, R. Z. Zuo, Y. D. Xu, G. Wu, and L. Wang. 2011. "Magnetoelectric Properties of $CoFe_2O_4$-Pb(Zr0.52ti0.48) O-3 Multilayered Composite Film via Sol-Gel Method." *Journal of Materials Science* 46 (13):4710–14.

Soinski, M. 1990. "Demagnetization Effect of Rectangular and Ring-Shaped Samples Made of Electric Sheets Placed in a Stationary Magnetic Field." *IEEE Transactions on Instrumentation and Measurement* 39 (5):704–10.

Spaldin, N. A., and M. Fiebig. 2005. "The Renaissance of Magnetoelectric Multiferroics." *Science* 309 (5733):391–2. doi: 10.1126/science.1113357.

Sreenivasulu, G., V. Hari Babu, G. Markandeyulu, and B. S. Murty. 2009. "Magnetoelectric Effect of (100–x)BaTiO3–(x)NiFe1.98O4 ($X = 20–80$ Wt %) Particulate Nanocomposites." *Applied Physics Letters* 94 (11):112902. doi: http://dx.doi.org/10.1063/1.3095600.

Sreenivasulu, G., S. K. Mandal, S. Bandekar, V. M. Petrov, and G. Srinivasan. 2011. "Low-Frequency and Resonance Magnetoelectric Effects in Piezoelectric and Functionally Stepped Ferromagnetic Layered Composites." *Physical Review B* 84 (14):144426.

Srinivasan, G. 2010. "Magnetoelectric Composites." In Annual Review ofMaterials Research, Vol. 40, 153–78. Palo Alto, CA: Annual Reviews.

Srinivasan, G., E. T. Rasmussen, J. Gallegos, R. Srinivasan, Y. I. Bokhan, and V. M. Laletin. 2001. "Magnetoelectric Bilayer and Multilayer Structuresof Magnetostrictive and Piezoelectric Oxides." *Physical Review B* 64 (21). Art. no. 214408, 1–6.

Srinivasan, G., E. T. Rasmussen, B. J. Levin, and R. Hayes. 2002. "Magnetoelectric Effects in Bilayers and Multilayers of Magnetostrictive and Piezoelectric Perovskite Oxides." *Physical Review B* 65:134402.

Suchtelen, V. J. 1972. "Product Properties: A New Application of Composite Materials." *Philips Research Reports* 27 (1):28–37.

Sudakar, C., R. Naik, G. Lawes, J. V. Mantese, A. L. Micheli, G. Srinivasan, and S. P. Alpay. 2007. "Internal Magnetostatic Potentials of Magnetization-Graded Ferromagnetic Materials." *Applied Physics Letters* 90 (6):062502.

Tahmasebi, K., A. Barzegar, J. Ding, T. S. Herng, A. Huang, and S. Shannigrahi. 2011. "Magnetoelectric Effect in Pb (Zr0.95Ti0.05)O-3 and $CoFe_2O_4$ Heteroepitaxial Thin Film Composite." *Materials and Design* 32 (4):2370–3.

Tiercelin, N., A. Talbi, V. Preobrazhensky, P. Pernod, V. Mortet, K. Haenen, and A. Soltani. 2008. "Magnetoelectric Effect Near Spin Reorientation Transition in Giant Magnetostrictive-Aluminum Nitride Thin Film Structure." *Applied Physics Letters* 93 (16):162902.

Tokunaga, T., M. Taguchi, T. Fukami, Y. Nakaki, and K. Tsutsumi. 1990. "Study of Interface Wall Energy in Exchange-Coupled Double-Layer Film." *Journal of Applied Physics* 67 (9):4417–19. doi: 10.1063/1.344917.

Tong, B., X. Yang, Z. Guo, K. Li, J. Ouyang, G. Lin, and S. Chen. 2013. "Preparation and Characterization of AlN/FeCoSiB Magnetoelectric Thin Film Composites." *Ceramics International* 39 (6):6853–9. doi: http://dx.doi.org/10.1016/j.ceramint.2013.02.019.

Tong, B., X. Yang, J. Ouyang, G. Lin, Y. Zhang, and S. Chen. 2014. "Magnetoelectric Response of AlN/[(Fe90co10)78Si12B10 + Terfenol-D] Composite Films." *Journal of Applied Physics* 115 (17):17D904. doi: http://dx.doi.org/10.1063/1.4863487.

Torrejon, J., L. Kraus, K. R. Pirota, G. Badini, and M. Vazquez. 2007. "Magnetostatic Coupling in Soft/Hard Biphase Magnetic Systems Based on Amorphous Alloys." *Journal of Applied Physics* 101 (9):09N105.

Vandenbo, J., D. R. Terrell, R. A. J. Born, and H. Giller. 1974. "In Situ Grown Eutectic Magnetoelectric Composite-Material.1. Composition and Unidirectional Solidification." *Journal of Materials Science* 9 (10):1705–9.

Vandenboomgaard, J., and R. A. J. Born. 1978. "Sintered Magnetoelectric Composite-Material $BaTiO_3$-Ni(Co, Mn)Fe_2O_4." *Journal of Materials Science* 13 (7):1538–48.

Vandenboomgaard, J., A. Vanrun, and J. Vansuchtelen. 1976. "Magnetoelectricity in Piezoelectric-Magnetostrictive Composites." *Ferroelectrics* 10 (1–4):295–8.

Vanderzaag, P. J., R. M. Wolf, A. R. Ball, C. Bordel, L. F. Feiner, and R. Jungblut. 1995. "A Study of the Magnitude of Exchange Biasing in [111] Fe_3O_4/COO Bilayers." *Journal of Magnetism and Magnetic Materials* 148 (1–2):346–8.

Vaz, C. A. F., J. Hoffman, C. H. Anh, and R. Ramesh. 2010. "Magnetoelectric Coupling Effects in Multiferroic Complex Oxide Composite Structures." *Advanced Materials* 22 (26–27):2900–18.

Wan, J. G., J. M. Liu, H. L. W. Chand, C. L. Choy, G. H. Wang, and C. W. Nan. 2003. "Giant Magnetoelectric Effect of a Hybrid of Magnetostrictive and Piezoelectric Composites." *Journal of Applied Physics* 93 (12):9916–19.

Wan, J. G., X. W. Wang, Y. J. Wu, M. Zeng, Y. Wang, H. Jiang, W. Q. Zhou, G. H. Wang, and J. M. Liu. 2005. "Magnetoelectric $CoFe_2O_4$–Pb(Zr,Ti)O_3 Composite Thin Films Derived by a Sol-Gel Process." *Applied Physics Letters* 86 (12):122501. doi: 10.1063/1.1889237.

Wan, J.–G., H. Zhang, X. Wang, D. Pan, J.–M. Liu, and G. Wang. 2006. "Magnetoelectric CoFe[Sub 2]O[Sub 4]-Lead Zirconate Titanate Thick Films Prepared by a Polyvinylpyrrolidone-Assisted Sol-Gel Method." *Applied Physics Letters* 89 (12):122914. doi: 10.1063/1.2357589.

Wang, Y., D. Gray, D. Berry, J. Gao, M. Li, J. Li, and D. Viehland. 2011. "An Extremely Low Equivalent Magnetic Noise Magnetoelectric Sensor." *Advanced Materials* 23 (35):4111–14. doi: 10.1002/adma.201100773.

Wang, Y., J. M. Hu, Y. H. Lin, and C. W. Nan. 2010. "Multiferroic Magnetoelectric Composite Nanostructures." *NPG Asia Materials* 2 (2):61–8.

Wang, K. F., J. M. Liu, and Z. F. Ren. 2009. "Multiferroicity: The Coupling between Magnetic and Polarization Orders." *Advances in Physics* 58 (4):321–448. doi: 10.1080/00018730902920554.

Wang, J., J. B. Neaton, H. Zheng, V. Nagarajan, S. B. Ogale, B. Liu, D. Viehland, V. Vaithyanathan, D. G. Schlom, U. V. Waghmare, et al. 2003. "Epitaxial $BiFeO_3$ Multiferroic Thin Film Heterostructures." *Science* 299 (5613):1719–22.

Wang, Y., Y. Shen, J. Gao, M. Li, J. Li, and D. Viehland. 2013. "Nonlinear Magnetoelectric Response of a Metglas/Piezofiber Laminate to a High-Frequency Bipolar AC Magnetic Field." *Applied Physics Letters* 102 (10):102905. doi: 10.1063/1.4795307.

Wu, J., Z. Shi, J. Xu, N. Li, Z. Zheng, H. Geng, Z. Xie, and L. Zheng. 2012. "Synthesis and Room Temperature Four-State Memory Prototype of $Sr_3Co_2Fe_{24}O_{41}$ Multiferroics." *Applied Physics Letters* 101 (12):122903. doi: 10.1063/1.4753973.

Xing, Z. P., J. Y. Zhai, J. Q. Gao, J. F. Li, and D. Viehland. 2009. "Magnetic-Field Sensitivity Enhancement by Magnetoelectric Sensor Arrays." *IEEE Electron Device Letters* 30 (5):445–7.

Yan, Y. K., Y. Zhou, and S. Priya. 2013. "Giant Self-Biased Magnetoelectric Coupling in Co-fired Textured Layered Composites." *Applied Physics Letters* 102 (5):052907. doi: 10.1063/1.4791685.

Yan, Y. K., Y. Zhou, and S. Priya. 2014a. "Enhanced Magnetoelectric Effect in Longitudinal-Longitudinal Mode Laminate with Cofired Interdigitated Electrodes." *Applied Physics Letters* 104 (3):032911.

Yan, Y., Y. Zhou, and S. Priya. 2014b. "Enhanced Magnetoelectric Effect in Longitudinal-Longitudinal Mode Laminate with Cofired Interdigitated Electrodes." *Applied Physics Letters* 104 (3):032911. doi: http://dx.doi.org/10.1063/1.4862183.

Yang, S. C., C. W. Ahn, K. H. Cho, and S. Priya. 2011. "Self-Bias Response of Lead-Free (1-x)[0.948 K0.5Na0.5NbO3-0.052 LiSbO3]-xNi(0.8)Zn(0.2)Fe(2)O(4)-Nickel Magnetoelectric Laminate Composites." *Journal of the American Ceramic Society* 94 (11):3889–99.

Yang, S. C., K. H. Cho, C. S. Park, and S. Priya. 2011. "Self-Biased Converse Magnetoelectric Effect." *Applied Physics Letters* 99 (20):202904.

Yang, S. C., C. S. Park, K. H. Cho, and S. Priya. 2010. "Self-Biased Magnetoelectric Response in Three-Phase Laminates." *Journal of Applied Physics* 108 (9):093706.

Yang, J., Yu. Me. i Wen, P. Li, and X. L. Bai. 2011. "A Magnetoelectric-Based Broadband Vibration Energy Harvester for Powering Wireless Sensors." *Science China-Technological Sciences* 54 (6):1419–27. doi: 10.1007/s11431-011-4367-3.

Yuan, F. T., J. K. Lin, Y. D. Yao, and S. F. Lee. 2010. "Exchange Bias in Spin Glass (FeAu)/NiFe Thin Films." *Applied Physics Letters* 96 (16):162502.

Zeng, M., J. G. Wan, Y. Wang, H. Yu, J. M. Liu, X. P. Jiang, and C. W. Nan. 2004. "Resonance Magnetoelectric Effect in Bulk Composites of Lead Zirconate Titanate and Nickel Ferrite." *Journal of Applied Physics* 95 (12):8069–73.

Zhai, J., Z. Xing, S. Dong, J. Li, and D. Viehland. 2008. "Magnetoelectric Laminate Composites: An Overview." *Journal of the American Ceramic Society* 91 (2):351–8. doi: 10.1111/j.1551-2916.2008.02259.x.

Zhang, J., P. Li, Y. Wen, W. He, J. Yang, M. Li, A. Yang, C. Lu, and W. Li. 2014. "High-Sensitivity Laminated Magnetoelectric Sensors Without Bias in Composite of Positive/Negative Giant Magnetostrictive Materials and Piezoelectric Single Crystals." *Journal of Applied Physics* 115 (17):17E517. doi: 10.1063/1.4865973.

Zhang, J., P. Li, Y. Wen, W. He, A. Yang, and C. Lu. 2013. "Giant Self-Biased Magnetoelectric Response with Obvious Hysteresis in Layered Homogeneous Composites of Negative Magnetostrictive Material Samfenol and Piezoelectric Ceramics." *Applied Physics Letters* 103 (20):202902. doi: 10.1063/1.4829634.

Zhang, T., X. Yang, J. Ouyang, S. Chen, B. Tong, Y. Zhu, and Y. Zhang. 2013. "A New Magnetoelectric Composite with Enhanced Magnetoelectric Coefficient and Lower Resonance Frequency." *Applied Composite Materials* 21:579–90. doi: 10.1007/s10443-013-9344-5.

Zhang, W. H., G. Yin, J. W. Cao, J. M. Bai, and F. L. Wei. 2012. "Frequency Multiplying Behavior in a Magnetoelectric Unimorph." *Applied Physics Letters* 100 (3):032903. doi: 10.1063/1.3678635.

Zhao, H. Q., X. Peng, L. X. Zhang, J. Chen, W. S. Yan, and X. R. Xing. 2013. "Large Remanent Polarization in Multiferroic $NdFeO_3$-$PbTiO_3$ Thin Film." *Applied Physics Letters* 103 (8):082904.

Zheng, H., J. Wang, S. E. Lofland, Z. Ma, L. Mohaddes-Ardabili, T. Zhao, L. Salamanca-Riba, S. R. Shinde, S. B. Ogale, F. Bai, et al. 2004. "Multiferroic $BaTiO_3$-$CoFe_2O_4$ Nanostructures." *Science* 303 (5658):661–3.

Zhong, X. L., J. B. Wang, M. Liao, G. J. Huang, S. H. Xie, Y. C. Zhou, Y. Qiao, and J. P. He. 2007. "Multiferroic Nanoparticulate $Bi3.15Nd0.85Ti_3O_{12}$-$CoFe_2O_4$ Composite Thin Films Prepared by a Chemical Solution Deposition Technique." *Applied Physics Letters* 90 (15):152903.

Zhou, Y., D. J. Apo, and S. Priya. 2013a. "Dual-Phase Self-Biased Magnetoelectric Energy Harvester." *Applied Physics Letters* 103 (19):192909.

Zhou, Y., D. J. Apo, and S. Priya. 2013b. "Dual-Phase Self-Biased Magnetoelectric Energy Harvester." *Applied Physics Letters* 103 (19):192909. doi: 10.1063/1.4829151.

Zhou, Y., A. Bhalla, and S. Priya. 2013. "Self-Biased Dual-Phase Energy Harvesting System." *MRS Proceedings* 1556. San Francisco, California.

Zhou, L., J. He, X. Li, B. Li, D. L. Zhao, and X. L. Wang. 2009. "Exchange Bias Behaviour of Amorphous CoFeNiSiB Ribbons." *Journal of Physics D: Applied Physics* 42 (19): 195001.

Zhou, Y., and S. Priya. 2014. "Near-Flat Self-Biased Magnetoelectric Response in Geometry Gradient Composite." *Journal of Applied Physics* 115 (10):104107. doi: 10.1063/1.4868340.

Zhou, Y., S. C. Yang, D. J. Apo, D. Maurya, and S. Priya. 2012. "Tunable Self-Biased Magnetoelectric Response in Homogenous Laminates." *Applied Physics Letters* 101 (23):232905.

Zhuang, X., M. L. C. Sing, C. Cordier, S. Saez, C. Dolabdjian, L. G. Shen, J. F. Li, M. H. Li, and D. Viehland. 2011. "Evaluation of Applied Axial Field Modulation Technique on ME Sensor Input Equivalent Magnetic Noise Rejection." *IEEE Sensors Journal* 11 (10):2266–72.